Genetic tug-of-war analysis of the robustness of cell cycle regulation in fission yeast

March 2013

Ayako Chino

Graduate School of Natural Science and Technology
Doctor's Course
OKAYAMA UNIVERSITY

Table of Contents

Abbreviations

CDK : cyclin-dependent kinase

DSB : DNA double-strand break

GRC : gap-repair cloning

gTOW : genetic tug-of-war

TAP-tag : tandem affinity purification tag

Chapter 1

Introduction

In recent years, dramatic advance in the field of biochemistry and molecular biology has provided us an enormous amount of information about cellular systems, such as genome sequence, regulation of gene expression, protein-protein and protein-DNA interactions, and so on. Rapid accumulation of these "-omics" data directed our attention to how to handle, analyze, and interpret these data comprehensively. Kitano (2004) proposed a new perspective on biology, called "systems biology".

System-level understanding, an approach advocated in systems biology, requires a shift in our notion of "what to look for" in biology. While understanding of genes and proteins continues to be important, the focus is on understanding system's structure and dynamics. Because system is not just an assembly of genes and proteins, its properties cannot be fully understood merely by drawing diagrams of their inter-connections. For example, all of the genes and proteins in an organism are likened to all the parts of an airplane. We need to know how these parts are assembled to form the structure of an airplane. However we are not satisfied to understand the complexity underlying the engineered object only by a catalog of the individual components. This is similar to drawing a diagram of gene-regulatory networks and their biochemical reactions. Such diagrams provide limited knowledge of how changes to one part of a system may affect other parts. To understand how a particular system functions, we must first examine how the individual components dynamically interact during the operation. We must seek answers to questions such as what the voltage is on each signal line, how the signals are encoded, how we can stabilize the voltage against noise and external fluctuations, and how the circuits reacts when a malfunction occurs in the system, what the design principles and possible circuit patterns are, and how we can modify them to improve system performance.

In systems biology, the discovery of fundamental, systems-level principles that underlie complex biological systems is a prime scientific goal (Kitano, 2002). Robustness is one of the fundamental characteristics of biological systems**,** which has emerged during their long evolutional histories (Barkai and Leibler, 1997; Kitano, 2004). Robustness is a property that allows a system to maintain its functions against internal and external perturbations. Robustness cannot be understood by looking at the individual components (Kitano, 2004). To discuss robustness, one must identify the target system, function, and perturbations. It is important to realize that robustness is concerned with maintaining function of a system rather than the system's state, which distinguishes robustness from stability or homeostasis. Homeostasis is clearly a property that maintains the state of a system rather than its functions (Kitano, 2002). Homeostasis, stability, and robustness will be identical if the function to be preserved is the one that maintains the state of the system. In addition, the robustness of a subsystem often contributes to homeostasis of the system at the higher level. Intracellular biochemical parameters, such as gene expression level and enzyme activities are considered to have become optimized through the long history of evolution so that cells can precisely perform their biological activity (Barkai and Leibler, 1997; von Dassow *et al.*, 2000; Kitano, 2002; Meir *et al.*, 2002; Li *et al.*, 2004). Fluctuations in these parameters against internal perturbation, such as noise and mutations, and external perturbation, such as temperature variations, affect cellular systems. However, it has been reported that most cellular systems are robust against such fluctuations in biochemical parameters, suggesting that the cellular systems have mechanisms to be robust. For example, a mechanism for a robust adaptation in signal transduction networks of bacterial chemotaxis was proposed (Barkai and Leibler, 1997; Alon *et al.*, 1999; Yi *et al.*, 2000). von Dassow (2000) showed that the segment polarity network in *Drosophila* is a robust developmental module.

Another well-studied robust cellular subsystem is the cell cycle regulation. The cell cycle is the process of DNA replication, mitosis, and cytokinesis that leads to the production of daughter cells from a mother cell. This cycle is typically divided into four phases. The events of DNA replication (S

phase) and mitosis (M phase) are separated by gaps of varying length called G_1 and G_2. All cell types undergo some variations of this basic cycle, in details of the regulation and the size of the phases. The eukaryotic cell cycle is achieved through the regulation of the activity of cyclin-dependent kinase (CDK). Cyclins and CDKs form the regulatory subunits and the catalytic subunits of an activated heterodimer, respectively; cyclins have no catalytic activity and CDKs are inactive in the absence of their cognate partner cyclins. When activated by a bound cyclin, CDKs perform a common biochemical reaction called phosphorylation that activates or inactivates target proteins to orchestrate coordinated entry into the next phase of the cell cycle. Different cyclin-CDK combinations determine the downstream proteins targets. CDKs are constitutively expressed in cells, whereas cyclins are synthesized at specific stages of the cell cycle in response to various molecular signals. The eukaryotic cell cycle has been extensively studied using budding and fission yeasts as simple models.

Computational analyses using mathematical models based on molecular biological knowledge of the yeast cell cycle predicted robustness of the system against parameter perturbations (Morohashi *et al.*, 2002; Li *et al.*, 2004). However, robustness is less understood due to the absence of effective methods to quantify robustness *in vivo*. Namely, little is known about the permissive ranges of intracellular parameters in real cells. How are cellular systems robust? To answer this question, Moriya *et al.* (*2006*) focused on the cell cycle system of budding yeast and developed a novel method called “genetic tug-of-war” (gTOW) (Moriya *et al.*, 2006). gTOW is a genetic method, which provides an upper limit of gene copy number to maintain the cellular function against gene overexpression in budding yeast. In gTOW, each target gene with its native regulatory DNA elements (promoter and terminator) is used as a unit so that the increased copy number of the gene can be determined quantitatively, and the gene expression level is expected to increase according to the copy number. In the experiment, the properties of 2-micron-based plasmid with the *leu2d* marker gene were used to increase the copy number <100 under selectable conditions. If the target gene cloned into the plasmid has the upper limit of <100, the plasmid copy number

under the selectable condition is expected to become close to the upper limit of the target gene. Moriya *et al.* (2006) measured the copy number limits of 30 cell-cycle regulator genes using gTOW. The data were used to reveal the "robustness profile" against overexpression of elements (genes) in the cell-cycle regulatory system and to evaluate and refine the integrative mathematical model of the budding yeast cell cycle (Moriya *et al.*, 2006; Kaizu *et al.*, 2010).

The fission yeast *Schizosaccharomyces pombe* is a single-celled and free-living archiascomycete fungus sharing many features with cells of more complicated eukaryotes (Wood *et al.*, 2002). Based on gene sequence comparisons and phylogenetic analysis, it has been suggested that fission yeast diverged from the budding yeast *Saccharomyces cerevisiae* around 330-420 million years ago and from Metazoa around 1 billion years ago (Sipiczki, 2000). The genome sequence of *Sc. pombe* was published in 2002 by a consortium led by the Sanger Institute. The 13.8 Mb genome of *Sc. pombe* is distributed in chromosome I (5.7 Mb), II (4.6 Mb), and III (3.5 Mb) with 4,824 genes (Wood *et al.*, 2002). Some gene sequences are as equally diverged between the two yeasts as they are from their human homologues, probably reflecting a more rapid evolution within fungal lineages than in the Metazoan (Wood *et al.*, 2002). *Sc. pombe* was first described in 1890s by Linder. He isolated the yeast from East African beer and chose as its epithet the Swahili word for beer, pombe. *Sc. pombe* has been extensively studied since the 1950's (Leupold, 1950; Mitchison, 1957). The ease with which it can be genetically manipulated is second only to *Sa. cerevisiae* among eukaryotes and it has served as an excellent model organism for the study of cell-cycle control (Baum *et al.*, 1997), mitosis and meiosis (Fantes and Beggs, 2000), DNA repair and recombination (Davis and Smith, 2001), and checkpoint controls important for genome stability (Humphrey, 2000).

The factors and their molecular interaction networks consisting the cell-cycle of both *Sc. pombe* and *Sa. cerevisiae* are highly conserved, although their styles of cellular growth and division are quite different (i.e. fission and budding). The factors and the networks are also conserved up to higher eukaryotes, such as plants and mammals (Csikasz-Nagy *et al*., 2006). As

described above, properties of robustness of the cell cycle have been already studied in *Sa. cerevisiae* using the gTOW method. With this background, I decided to develop the gTOW method in *Sc. pombe* to measure the robustness of the cell cycle regulation. Using the data, I expected to reveal the conserved and cell-type specific features of robustness among eukaryotes. I also expected to evaluate and refine an integrative mathematical model of the cell cycle using the gTOW data, in order to find uncovered regulations. For these purposes, I performed my thesis study as described below.

First, I established a method that quickly and concisely constructs plasmids using the gap-repair cloning (GRC) in *Sc. pombe.* GRC makes use of the homologous recombination activity and is commonly used in the budding yeast (Oldenburg *et al.*, 1997). Due to its flexible design and efficiency, GRC has been frequently used for constructing plasmids with complex structures as well as genome-wide plasmid collections (Zhu *et al.*, 2000; Moriya *et al.*, 2006; Ho *et al.*, 2009). Although there have been reports indicating GRC feasibility in the fission yeast, GRC is not commonly used in this species, because no systematic study to examine the efficiency of GRC in *Sc. pombe* has been performed. I thus investigated the GRC efficiency with different lengths of homologous sequences and the efficiency to combine three DNA fragments. As a result, it was shown that GRC in *Sc. pombe* was sufficiently feasible for regular plasmid constructions as well as for genome-wide analyses of gene functions (Chapter 2).

Next, using GRC that I had established, I constructed plasmids to apply the genetic method gTOW in *Sc. pombe*. To measure the upper limit copy number of a gene to halt cellular functions, I constructed plasmids with autonomously replicating sequences (ARS) to develop three independent gTOW vector plasmids (pTOWsp-L, pTOWsp-M and pTOWsp-H). They have different biases to increase the plasmid copy numbers in *leu1*Δ *Sc. pombe* cells cultured in –leucine conditions. Using these plasmids, I measured the limit copy numbers of 31 cell division cycle regulator genes. As a result, the upper limit of copy number of these genes was various from 1 to > 100. The result suggests that robustness against the overexpression of certain gene varies as was found in *Sa. cerevisiae*

(Moriya *et al.*, 2006). I next compared the robustness profiles of cell cycle regulation between *Sa. cerevisiae* and *Sc. pombe* and found the similarities and differences between the two. One of the similarities was the fragility in the regulation of B-type cyclin. In contrast, the orthologous components in the mitotic exit network (MEN) in *Sa. cerevisiae* showed very different limits from those in the septation-initiation network (SIN) in *Sc. pombe*, though both networks have a conserved architecture. These results suggest that comparison of robustness profiles is a useful way to reveal the conserved/non-conserved properties of cellular systems (Chapter 3).

Finally, I tried to measure the protein amount increase when the copy number increase in gTOW. For this purpose, I investigated the 20 cell division cycle regulator genes. I found that the protein amount increase is proportional to the copy number increase in most cases. I also found some potential feedback regulations in the expression system of cell-cycle regulators (Chapter 4).

Chapter 2

Plasmid construction using recombination activity in fission yeast

2.1 Background

Construction of plasmids is crucial in modern molecular biology. In many cases, plasmids are constructed *in vitro* by digesting DNA fragments with restriction enzymes at specific sites (restriction sites) and then ligating the resulting fragments. The constructed DNA is usually amplified in *E. coli* to analyze its structure. However, a second cloning method using homologous recombination activity (often designated gap-repair cloning or GRC) allows more design flexibility, because restriction sites are not used. The basic GRC procedure is shown in Figure 2.5-1. In the budding yeast *Saccharomyces cerevisiae*, efficient GRC is observed due to its high homologous recombination activity (Ma *et al.*, 1987; Oldenburg *et al.*, 1997). Therefore, this method has been used to construct large-scale systematic plasmid collections (Zhu *et al.*, 2001; Moriya *et al.*, 2006; Ho *et al.*, 2009). In these cases, the target genes are directly cloned into *Sa. cerevisiae* cells to study their function.

The fission yeast *Schizosaccharomyces pombe* is also widely recognized as a model eukaryote (Egel, 2004). Although a previous study has reported GRC feasibility in *Sc. pombe* (Wang *et al.*, 2004), it has not been commonly used because there have been no systematic studies reporting its efficiency in this yeast. Because the gTOW analysis of *Sc. pombe* cell cycle genes, the primary aim of this thesis, requires a large set of plasmids, GRC will be very useful for my work if it is highly efficient. I thus tried to evaluate the applicability of GRC in *Sc. pombe* and establish the protocol.

2.2 Materials and Methods

2.2.1 Strains

Sp286h+ (*h+ ade6 ura4-D18 leu1-32*), a haploid progeny of Sp286 (Bioneer), was used as the host strain for the GRC experiments. FY4012 (*h- ura4-D18 leu1-32 ade6-210 lig4*::*Kan*^{R}) was used as the host strain for GRC without non-homologous end joining.

2.2.2 Plasmids

pDblet (Brun *et al.*, 1995) was used as a plasmid vector in the GRC experiment. pRS315 (Sikorski and Hieter, 1989) was used as the PCR template for the *Sa. cerevisiae LEU2* gene. pHM004_*nmt1-1*, a plasmid containing the *nmt1* promoter (from our laboratory stock), was used as the PCR template for the *nmt1* promoter. pKT128 (Sheff and Thorn, 2004) was used as the PCR template for *EGFP*.

2.2.3 Growth media and conditions

Sc. pombe cells were cultured at 30˚C in a manner similar to that described previously (Moreno *et al.*, 1991). EMM medium and plates were prepared using EMM broth powder (MP Biomedicals).

2.2.4 DNA methods

High-efficiency transformation and plasmid DNA isolation in yeast were performed in a manner similar to by replacing the culture medium with one more appropriate for *Sc. pombe* (Amberg *et al.*, 2005). *E. coli* transformation was performed using a XL1-Blue Electroporation Competent Cell (Agilent Technologies). DNA sequencing was performed using an ABI 3730xl Analyzer.

2.2.5 Fluorescence imaging

GFP fluorescence images of yeast culture plates were obtained using a LAS4000 lumino-image analyzer (Fujifilm) and were processed using Photoshop CS2 software (Adobe).

2.2.6 Preparation of DNA fragments for gap-repair cloning

About 10 μg of pDblet DNA prepared from *E. coli* was digested with appropriate restriction enzymes in a 100 μl solution. A total of 2 μl (- 0.2 μg) digested plasmid solution was used directly for yeast transformation. DNA fragments were amplified using KOD polymerase (Toyobo) according to the manufacturer's protocol in 50 μl solution using the primers listed in the Tables 2.4-1 and 2.4-3 along with the template DNA described. A total of 45 μl of the amplified DNA solution (containing about 10 μg DNA) was used directly for yeast transformation. The molar ratio of the digested vector and PCR products was about 1:200-300.

2.3 Results and Discussion

2.3.1 Cloning the *LEU2* marker gene

I first evaluated if efficient GRC events could be observed in *Sc. pombe*, and then constructed plasmids in it using GRC. I used the plasmid pDblet as a cloning vector because it is stable as a monomer and transforms *Sc. pombe* with high efficiency. It also shows high mitotic stability (Brun *et al.*, 1995). These features are advantageous when the constructed plasmid is recovered from the *Sc. pombe* cells to verify its structure. DNA fragments containing *Sa. cerevisiae LEU2* were used for inserted DNA. This gene can complement *Sc. pombe leu1* so that transformants harboring the plasmids (i.e., pDblet with the *LEU2* gene) could be easily distinguished by replica plating. I also tested the effect of (1) the length of the homologous region (-25 bp or -40 bp) and (2) the distance of the homologous region from the fragment end (Figure 2.5-2A).

Strain Sp286h+ was transformed with a circular vector, linearized (*Kpn*I-*Hin*dIII digested) vector, and three combinations of linearized plasmids with inserts as shown in Figure 2.5-2A. Transformants were first selected by the auxotrophic pDblet marker (uracil) in order to estimate transformation efficiency. As shown in Figure 2.5-2B, the linearized plasmids resulted in a lower number of transformants than the circular or the linearized plasmid with inserts. I then tested whether these transformants were leucine prototrophs by replica-plating the transformants onto –leucine plates as this would provide an indirect evidence of successful GRC. Almost all of the transformants from the three groups, where the linearized plasmids with inserts were combined, showed leucine synthesizing ability (Figure 2.5-2C).

These results suggest that GRC can be successfully performed in *Sc. pombe.* Because the GRC efficiencies were indistinguishable between the three groups where the linearized plasmids with inserts were combined, it is clear that a 25-bp homologous region suffices for GRC and that the recombination site does not have to be at the end of the fragment. I also constructed linearized vectors by digestion with *Xho*I to check the effect of the restriction sites used. In this case,

the number of uracil- and leucine-prototroph transformants observed was similar to that observed with the *Hin*dIII-*Kpn*I double-digested vector (data not shown), suggesting that no preferences in restriction site (for single or double restriction enzyme digestions) were observed for GRC in *Sc. pombe*.

I next examined the structure of the plasmids within transformants grown on –leucine plates by randomly recovering plasmids and digesting them with restriction enzymes and found that 70 % of plasmids recovered had a desired structure (Table 2.4-3). Plasmids without the desired structure appeared to have the *LEU2* gene in the pDblet cloning site but had some mutations in the regions (data not shown). These results indicate that GRC is a useful cloning method in *Sc. pombe*.

2.3.2 Construction of plasmids containing *nmt1* promoter + *EGFP*

I then investigated whether GRC seen in *Sc. pombe* could be applied in more advanced plasmid constructions. The blueprint of the plasmid construction is shown in Figure 2.5-3A. In this process, three DNA fragments containing the *nmt1* promoter, *EGFP* gene, and linearized pDblet should be connected. The *nmt1* promoter is the most frequently used one in *Sc. pombe*. *nmt1* has conveniently been used for constructing expression vectors that regulate gene expression in a thiamine-repressible manner (Maundrell, 1990). *EGFP* is expressed under the control of the *nmt1* promoter when the plasmid is constructed correctly. As shown in Figure 2.5-3B, most of the transformants with the linearized plasmids with inserts showed GFP fluorescence: seven out of 10 randomly selected transformants showed GFP fluorescence, while one showed weak GFP fluorescence (Figure 2.5-3C).

All plasmids recovered from the seven transformants showing GFP fluorescence were verified to have the desired structure (Table 2.4-4). I could not recover any plasmids from two of the three transformants showing no or weak fluorescence (Table 2.4-4) indicating that the DNA fragments were integrated into the genome in these transformants. The plasmid recovered from the last transformant that did not fluoresce had a truncated insert. To check if the *nmt1*

promoter and *EGFP* were joined correctly, I sequenced the connecting region: two out of seven plasmids with the desired inserts had nucleotide substitutions within the connecting region (the primer region for PCR) (Table 2.4-4). Currently I am not sure about the reason for these nucleotide substitutions.

2.3.3 Efficiency of GRC in a mutant cell without NHEJ activity

It was reported that the efficiency of homologous recombination event could be increased in a yeast strain without non-homologous end joining (NHEJ) activity (Abdel-Banat *et al.*, 2010). NHEJ is a pathway that repairs double-strand breaks (DSBs) in DNA. In the NHEJ pathway, binding of Ku heterodimer (Ku70p/Ku80p) to both ends of the DNA double-strand breaks under the participation of additional proteins, such as Lig4, promotes repair of the DSB (Kegel *et al.*, 2006). I thus tested the GRC efficiency in a *lig4Δ* mutant strain whose NHEJ is deficient (Manolis *et al.*, 2001). I performed the same experiment as described in Figure 2.5-3 (i.e. DNA fragments containing the *nmt1* promoter, *EGFP* gene, and linearized pDblet should be connected). As shown in Figure 2.5-4, 96 % (45 out of 46) transformants showed significant GFP fluorescence that was regulated by thiamine, indicating the GRC efficiency was dramatically increased in this strain. In the rest one transformant (arrowhead in Figure 2.5-4), the *EGFP* was probably integrated into genome because any plasmid could be recovered from the transformant. I recovered the plasmids from the transformants and checked the structure with restriction digestion and sequencing. All recovered plasmids had the correct structure, but three out of ten plasmids had nucleotide substitutions within the connecting region (the primer region for PCR). Currently I am not sure about the reason of these nucleotide substitutions.

These results indicate that GRC could be effectively performed in *Sc. pombe* (with 70 % efficiency in wild type, and with 95 % in the NHEJ mutant) with three DNA fragments without selection for recombination, although constructed plasmids sometimes had nucleotide substitutions within the connecting regions. I thus concluded that GRC is suitable for use as a cloning method in *Sc. pombe* and used GRC in establishment of *Sc. pombe* gTOW

(Chapter 3).

2.4 Tables

Table 2.4-1. Oligo DNA primers for construction of pDblet + *LEU2*

Primer Name	Sequence*	Description
OHM001	agctatgaccatgattacgccaagcTTCCTCAACA TAACGAG	up primer to amplify *LEU2* with 25 bp homologous sequence
OHM002	atttcacacaggaaacagctatgaccatgattacgccaagc TTCCTCAACATAACGAG	up primer to amplify *LEU2* with 41bp homologous sequence
OHM003	gactcactatagggcgaattgggtaCCAATATATA AATTAGG	down primer to amplify *LEU2* with 27 bp homologous sequence
OHM004	gcgcgcgtaatacgactcactatagggcgaattgggtaC CAATATATAAATTAGG	down primer to amplify *LEU2* with 40 pb homologous sequence
OHM005	tagtggatcccccgggctgcaggaattcgatatcaagctt CCTCAACATAACGAG	up primer to amplify *LEU2* with 40 bp homologus sequence adjucent to vector's *Hin*dIII site

* Vector and insert sequences are shown in lower and upper cases.

Table 2.4-2. Oligo DNA primers for construction of pDblet + P*nmt1-EGFP*

Oligo	Sequence*	Description
OHM014	ttaaaccagcaccgtcacccATGATTTAACAA AGCGACTA	down primer for P*nmt-EGFP* fusion
OHM015	TAGTCGCTTTGTTAAATCATgggtgacg gtgctggtttaa	up primer for *EGFP*-P*nmt1* fusion
OHM016	ctcactatagggcgaattgggtaccTGCCGGTAG AGGTGTGGTCA	down primer to amplify *EGFP*
OSBI867	TTGTGTGGAATTGTGAGCGG	up primer to amplify *Pnmt1*
OHM025	TGGGGAGAGAAAACAGGGCA	primer to sequence the junction region between P*nmt1* and *EGFP*

* *EGFP* sequence is shown in upper case and P*nmt1* sequence is shown in upper case in OHM014 and OHM015. Vector sequence is shown in lower case and insert sequence is shown in upper case in OHM016.

Table 2.4-3. Structural verification of plasmids pDblet + Leu

Insert	No. of positive clones*/tested	Positive clone (%)
Set 1	8/11	73
Set 2	9/11	82
Set 3	8/11	73

* The inserts were detected by restriction enzymes.

Table 2.4-4. Analysis of independent transformants obtained in pDblet + P*nmt1-EGFP* construction

Clone No.*1	Fluorescence on plate	Plasmid Recovery*2	Presence of desired insert*3	Presence of mutation*4
1	strong	+	+	−
2	weak	−	NA	NA
3	strong	+	+	−
4	strong	+	+	+
5	strong	+	+	+
6	no	+	−*5	NA
7	strong	+	+	−
8	no	−	NA	NA
9	strong	+	+	−
10	strong	+	+	−

*1. The number corresponds to the number of isolates cloned in Figure 2.5-3C.
*2. +: Plasmid is recovered from *Sc. pombe* in *E. coli*; − : Plasmid could not be recovered from *Sc. pombe* in *E. coli*.
*3. Presence of desired insert is checked by restriction digestion. NA: Not applicable.
*4. The region between P*nmt1* and *EGFP* is sequenced using primer OHM025.
*5. The insert is truncated.

2.5 Figures

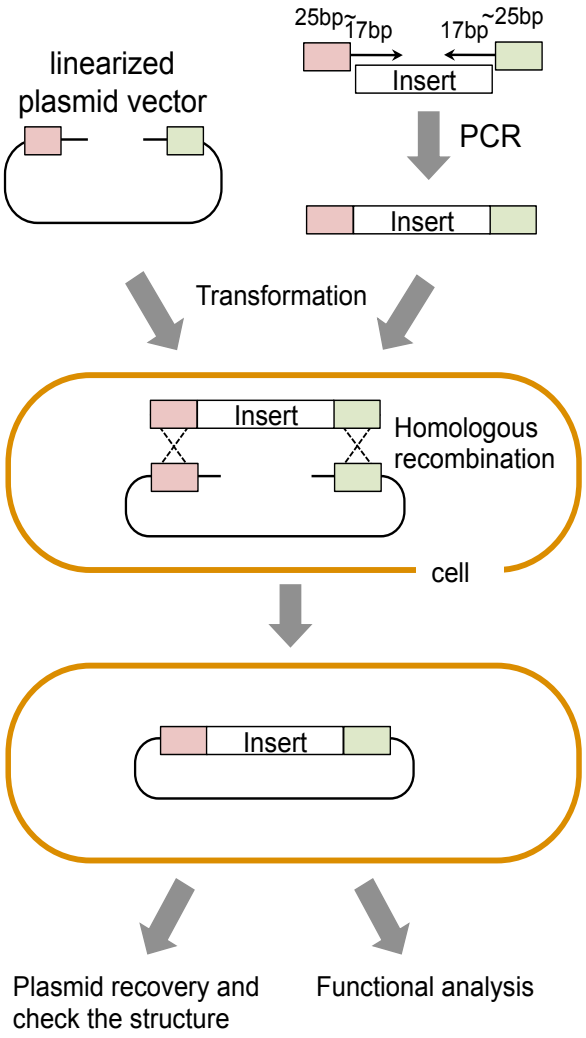

Figure 2.5-1. Basic gap-repair cloning procedure

DNA fragment(s) from a linearized plasmid vector are prepared by restriction enzyme digestion or by PCR. DNA fragment(s) from the insert are amplified by PCR, ensuring that the sequence at the end of the fragment is homologous with that of the plasmid. Both DNA fragments are then simultaneously introduced into the cell. Transformants are selected by identifying the plasmid vector marker. The fragments are connected by the homologous recombination activity that occurs within the cell. The constructed plasmid is recovered from the transformed cell into *E. coli* to amplify and check the structure of the plasmid with restriction enzyme digestion and DNA sequencing. Cells with plasmids that have the desired structure are used for functional analysis.

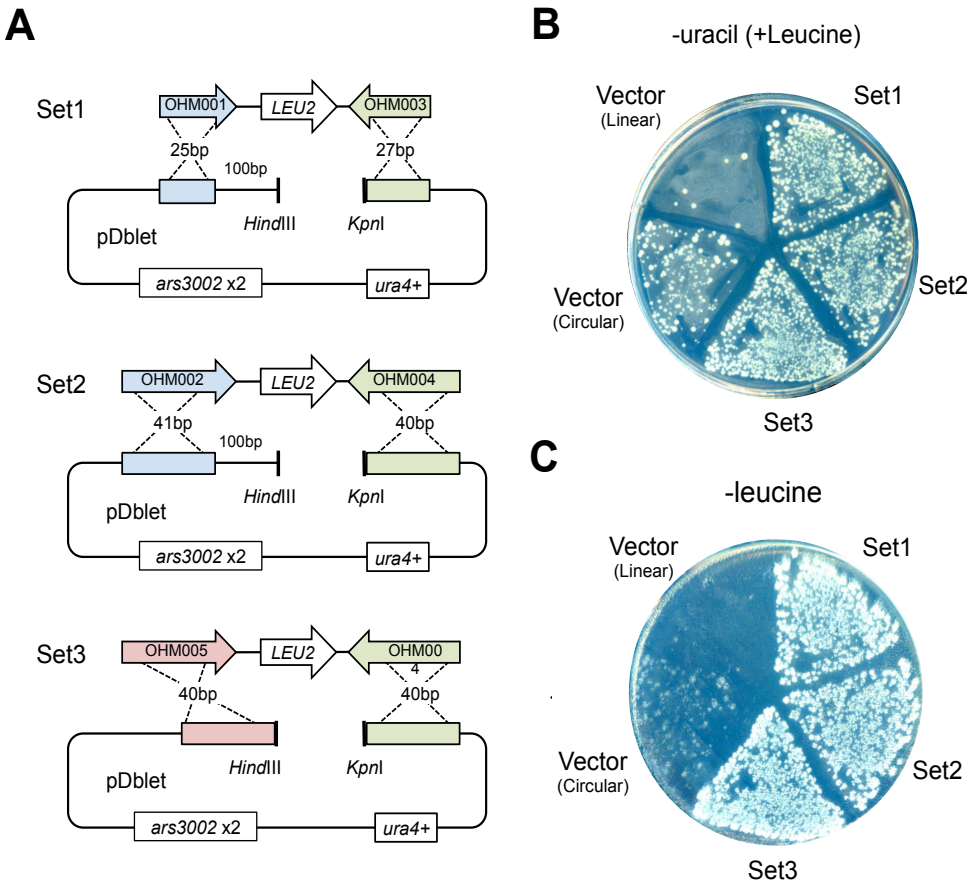

Figure 2.5-2. Cloning the *LEU2* marker gene using GRC in *Sc. pombe*

(A) Blueprint of the plasmid construction. DNA fragments containing *LEU2* genes were amplified by PCR using the indicated primer sets with pRS315 as a template. Homologous regions between the vector plasmid (pDblet) and the insert fragments are shown in the same colors.

(B) Result of transformation with the linearized (*Hin*dIII-*Kpn*I digested) vector, circular vector, and linearized vector with inserts as shown in A. Transformants of Sp286h+ were selected on –uracil plates (EMM with leucine and adenine).

(C) A replica of the transformants on the plate in B on a –leucine plate (EMM with adenine).

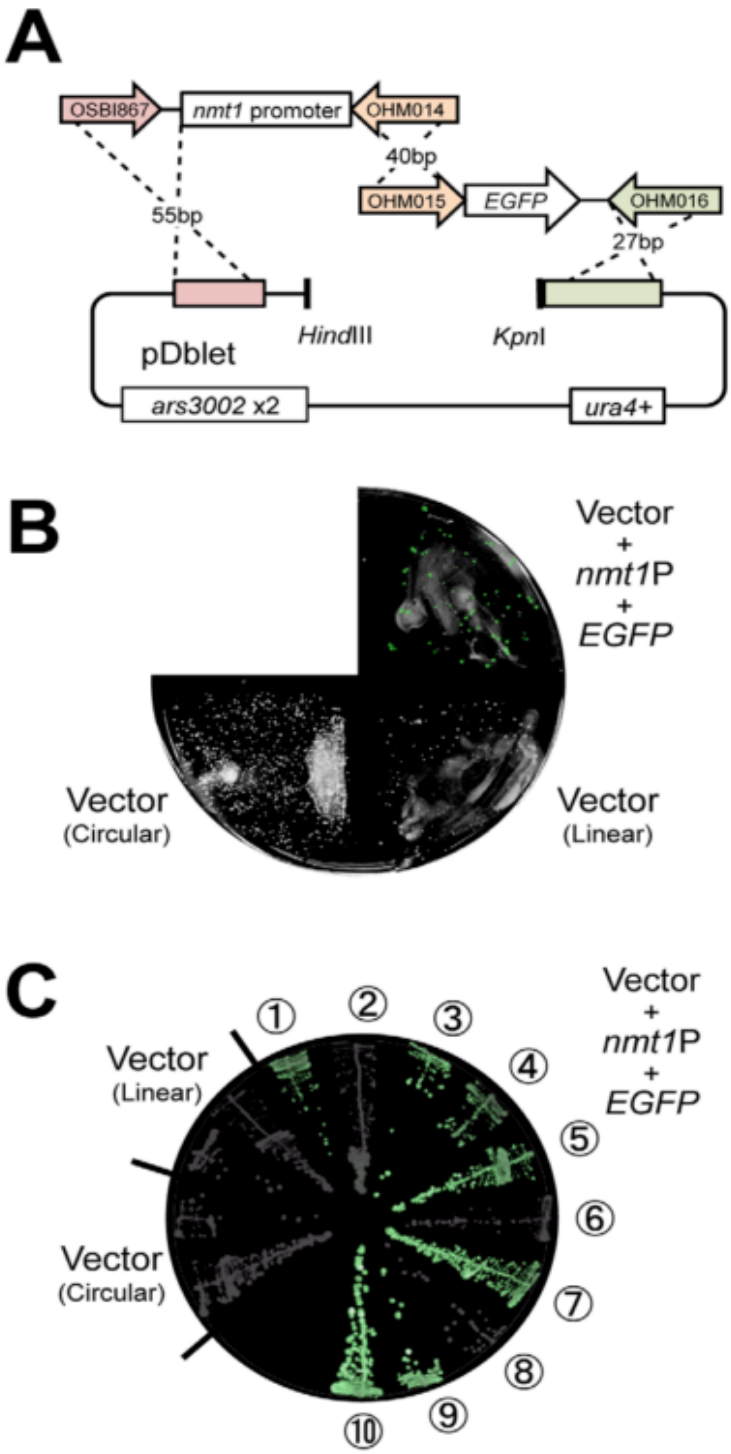

Figure 2.5-3. Construction of a plasmid containing *nmt1* promoter + *EGFP*

(A) Blueprint of the plasmid construction. DNA fragments containing *nmt*1 promoter and *EGFP* were amplified by PCR using the indicated primer sets with pHM004_nmt1-1 and pKT128 as templates, respectively. Homologous regions between the vector plasmid (pDblet) and the insert fragments are shown in the same colors.

(B) Result of transformation. Transformants of Sp286h+ were selected on –uracil plates (EMM with leucine and adenine). The fluorescent GFP image was superimposed on a bright-field image.

(C) Independent colonies from plate B were streaked on –uracil plates.

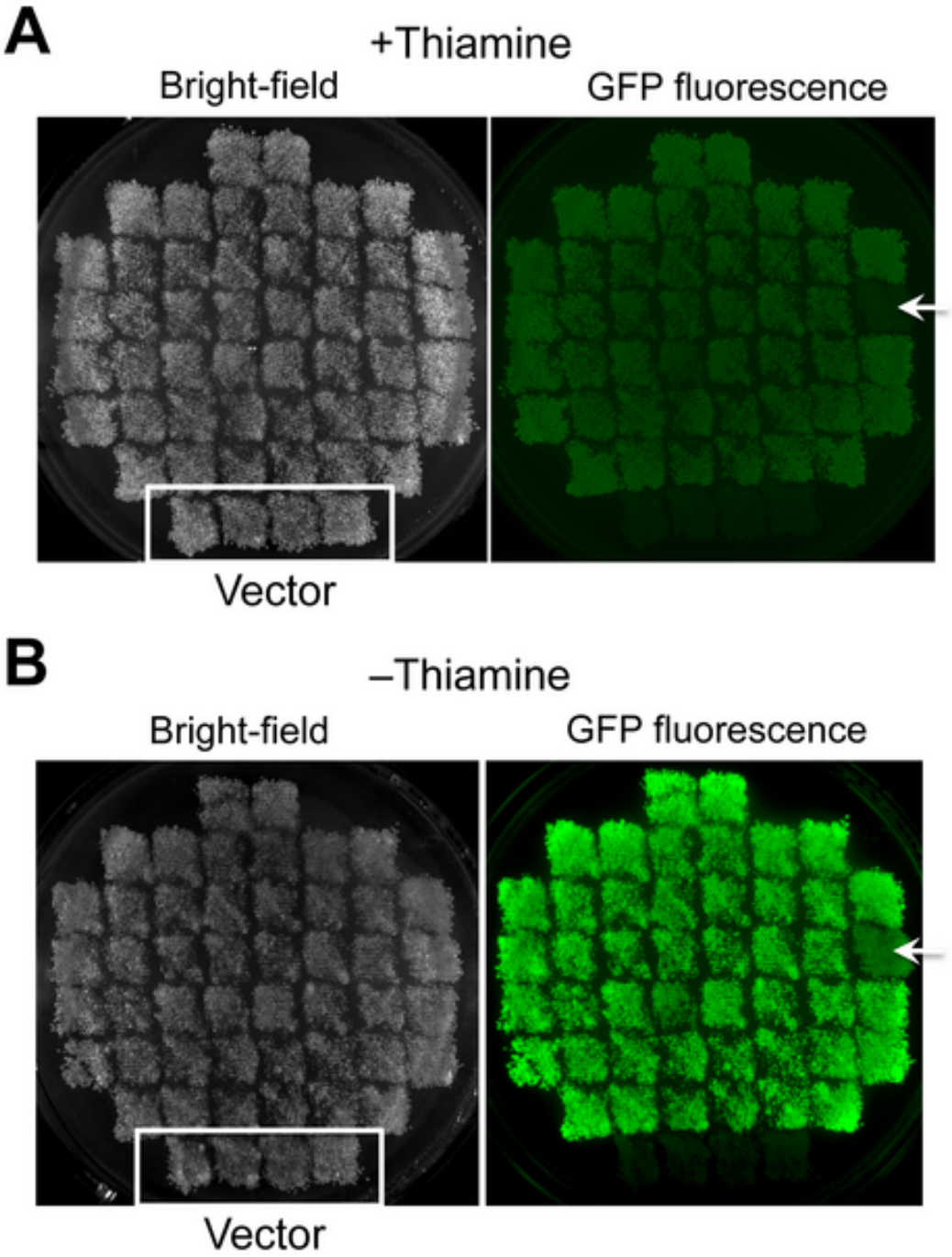

Figure 2.5-4. Construction of a plasmid containing *nmt1* promoter + *EGFP* in the *Sc. pombe lig4Δ* mutant

GRC was performed as in Figure 2.5-3 except FY4102 was used as a host strain. Transformants were randomly selected and streaked on –uracil +thiamine plate, then the transformants were replica-plated on +thiamine (A) and –thiamine (B) plates. Negative controls (transformants with the vector) were also streaked. Arrowheads indicate transformant with weak GFP fluorescence, in which GFP was integrated into genome.

Chapter 3

Development of gTOW in *Sc. pombe* and its application for robustness analysis of the cell cycle

3.1 Background

Intracellular parameters such as gene expression and enzyme activities require optimization, such that cellular functions may be performed effectively (Alon *et al.*, 1999; Zaslaver *et al.*, 2004; Dekel and Alon, 2005; Wagner, 2005). Fluctuations in these parameters lead to various cellular defects. On the other hand, in order to maintain cellular functions despite environmental change, mutation, and noise in intracellular biochemical reactions, these parameters may have certain permissible ranges, a characteristic termed robustness, which is commonly observed in various cellular systems (Barkai and Leibler, 1997; von Dassow *et al.*, 2000).

Moriya *et al.* (2006) previously reported a method designated genetic 'tug-of-war (gTOW),' by which they measured the limit of gene overexpression in the budding yeast *Saccharomyces cerevisiae*. In gTOW, a target gene with its native regulatory regions is cloned into a particular plasmid, and the copy number of the plasmid is increased by genetic selection. Next, the copy number is measured just before the cellular system halts (i.e., the cell dies), such that the overexpression limit of the target gene is evaluated as the gene copy number limit. As the gene copy number increases, relative overexpression of the gene is expected. If we can measure the copy number limit of gene overexpression, we can evaluate the degree to which the cellular system resists overexpression of the target gene (namely, robustness against gene overexpression).

Using gTOW, Moriya *et al.* (2006) previously measured the copy number limits of 30 cell-cycle regulators in budding yeast. The data were used to show the robustness profile of the cell-cycle regulatory system and to evaluate and refine the integrative mathematical model of the budding yeast cell cycle (Moriya *et al.*, 2006; Kaizu *et al.*, 2010). The fission yeast *Schizosaccharomyces pombe* is

distantly related to *Sa. cerevisiae* (Sipiczki, 2000) and, like *Sa. cerevisiae,* is an established model eukaryote for the study of the molecular biology of the cell cycle (Egel, 2004). In this chapter, I developed a gTOW method in *Sc. pombe* and determined the copy number limits of 31 cell-cycle regulator genes. The data obtained were used to compare the robustness profiles between budding and fission yeasts in order to reveal the conserved/non-conserved properties of the eukaryotic cell cycle and to evaluate and refine an integrative mathematical model to discover unknown regulations conferring robustness of the fission yeast cell cycle.

3.2 Materials and Methods

3.2.1 Strains

Sc. pombe strain FY7652 (*h- leu1-32 ura4-D18*) obtained from NBRP yeast was used for the constructions of plasmids and gTOW. In 2Dop-gTOW of *Sc. pombe*, Sp286h+ (*h+ ade6 ura4-D18 leu1-32*), a haploid progeny of Sp286 (BG_0000, Bioneer) was used. For *clp1Δ*, *cig1Δ*, *puc1Δ*, and *srw1Δ* strains, haploid progenies of BG_0465, BG_4780, BG_4172, and BG_0289 (Bioneer) were used, respectively. *Escherichia coli* strain XL1-blue (Stratagene) was used for plasmid amplification.

3.2.2 Plasmids

Plasmid vectors used in this study are listed in Table 3.5-1. Construction details of the plasmids are described below.

For construction of plasmids, DNA fragments amplified from genome or plasmid were joined using GRC described in Chapter 2 of this thesis. The plasmids constructed were recovered into *E. coli* (XL1-blue, Agilent Technologies), and the structures were checked with restriction enzyme digestion and partial nucleotide sequencing. All DNA fragments were amplified with polymerase chain reaction (PCR) using the high fidelity DNA polymerase KODplus (Toyobo) according to the manufacture protocol. Oligo DNA primers used for construction of plasmid vectors are shown in .5-2.

Construction of pTOWsp series vectors

Construction procedure of pTOWsp series vectors and their structures are shown in Figure 3.6-1. I have measured the copy number of the pHM004-835 to pHM004-840 in –leucine condition (Table 3.5-4). And select three plasmids for further use. I thus changed the names of the vectors as follows.

- pHM004 (*LEU2* promoter length is 29 bp) : pTOWsp-H
- pHM004-835 (*LEU2* promoter length is 59 bp) : pTOWsp-M
- pHM004-836 (*LEU2* promoter length is 89 bp) : pTOWsp-L

Construction of pA6R

The construction procedure of pA6R vector and its structure are shown in Figure 3.6-2.

Construction of plasmids with *Sc. pombe* cell-cycle regulator genes

Each target gene studied in this work was cloned from just after its upstream ORFs to just before its downstream ORFs, so that it contains all of its regulatory elements (i.e, its native promoter and terminator). Figure 3.6-3 is the case of *cdc2*, as an example. According to the genome annotations and nucleotide sequences obtained from *Schizosaccharomyces pombe* GeneDB, I used 23-bp in the end of neighboring ORFs for the priming sites to amplify each target gene with PCR (Figure 3.6-3 as an example). Each primer contains homologous sequence with vectors at its 5' for the gap-repair cloning. Upstream (Up) and downstream (Down) primers contain *Hin*dIII site (aagctt) and *Kpn*I site (ggtacc), respectively, for the verification of construction. Oligo DNA primers to amplify and clone the target genes are listed in Table 3.5-3.

Each target gene was amplified with the primer set from FY7652 genome with high fidelity PCR. The amplified DNA fragment was joined with the vectors digested with *Hin*dIII and *Xho*I in advance using gap-repair method. At least two independent plasmids for each construction were recovered from yeast into *E. coli* and purified for structural verifications with restriction enzyme digestion and sequencing. *cut1* was amplified as two fragments and joined into vectors with gap-repair method, because it was too large to amplify by single PCR (eF and eR primers were used for this purpose).

For construction of frameshift mutant of each gene, two DNA fragments were amplified with the primers with cgca insertion just after start codon and joined into the vectors with gap-repair method. Each frameshift mutant gene thus contains *Fsp*I site (tgcgca) in the beginning of ORF. Figure 3.6-4 is the case of *cdc2*, as an example.

3.2.3 Media and growth conditions

LB broth was used for cultivation of *E. coli*. *Sc. pombe* cells were cultured in a manner similar to that described by Moreno *et al*. (1991). EMM medium and plates were prepared using EMM broth powder (MP Biomedicals). *Sc. pombe* transformation was performed using the LiOAc method (Amberg *et al.*, 2005). *Sc. pombe* and *E. coli* were cultivated at 30 and 37˚C, respectively.

3.2.4 Measurement of plasmid copy number

Sc. pombe cells with pTOWsp containing target genes were grown in EMM without uracil, transferred into EMM without leucine and uracil, and then cultivated for 48 h (for cells with pTOWsp-L- and -M-based plasmids) or 72 h (for cells with pTOWsp-H-based plasmids). In 2Dop-gTOW, pTOW and pA6R derivatives were introduced into Sp286h+ cells, and the cells were grown in EMM without uracil and adenine; they were then transferred into EMM without leucine, uracil, and adenine and cultivated for 48h. The plasmid dosage in a yeast cell was determined using real-time PCR as described previously (Moriya *et al.*, 2006), except that the *pombe-1* primer set (5′-CCCTCAGTTGCTTCTCCTAA-3′ and 5′-GTGACTTCGTGA ATCAAGTG-3′), the *ura4-3* primer set (5′-TCTTTGGCTACTGGTTCCTA-3′ and 5′-TATGTAGTCGCTTTGAAGGT-3′), and the *ade6-1* primer set (5′-GCCCATCGCTTAAACATCA-3′ and 5′-TGCATCGGGGTCAGTAAAT-3′) were used for quantification of genomic DNA, pTOW plasmids, and pA6R plasmids, respectively. Data are averages of at least two independent experiments. The copy number determined by PCR using the *ura4-3* primer set is directly associated with the plasmid copy number in the cell because no sequence on the genomes of FY7652 or Sp286h+ is amplified by the *ura4-3* primer set. In contrast, the copy number determined by PCR using the *ade6-1* primer is one copy more than the plasmid copy number in the cell because an *ade6* sequence on the genome of Sp286h+ is amplified by the primer set. The copy number of a target gene in the wild-type cell is one copy more than the plasmid copy number as a result of one endogenous copy on the genome.

3.2.5 Flow cytometry

Cells expressing EGFP were directly analyzed by flow cytometry (FACScalibur; Becton, Dickinson and Company). EGFP fluorescence was detected as fluorescent channel 1 (FL1), and the cell size was monitored as forward-scatter channel (FSC). The data was analyzed using the FlowJo7 software.

3.2.6 Microscopic observation

Cells were fixed by 70 % ethanol for 410 min, pelleted, and resuspended in the VECTASHIELD mounting medium with DAPI (1/2 diluted with water, Vector Laboratories) and Fluorescent Brighter 28 (final concentration 10 μg/ml; Sigma). The cell suspension (2 μl) was spotted onto a glass slide and covered with an 18-mm coverslip. The coverslip was sealed with nail polish, and the slide was observed using the Leica DMI 6000B microscope (Leica Microsystems). GFP fluorescence, DAPI and Fluorescent Brighter 28 fluorescence, and RFP fluorescence were observed with GFP, A, and RFP filter cubes (Leica Microsystems), respectively.

3.3 Results

3.3.1 Development of plasmid vectors used for *Sc. pombe* genetic tug-of-war (gTOW)

The scheme of *Sc. pombe* gTOW is described in Figure 3.6-5A. The plasmid for gTOW must have the following properties: (1) the copy number in each cell is multiple; (2) the copy number is diverse in each cell; and (3) the plasmid contains a gene with a selection bias for increasing the plasmid copy number (*leu2d* in the case of *Sa. cerevisiae* gTOW). Because no *Sc. pombe* plasmid with the above properties was reported, I first constructed plasmid vectors for use in *Sc. pombe* gTOW.

Given below is a brief summary of the construction of the plasmid. I used pDblet (Brun *et al.*, 1995) for the backbone of the plasmid because it satisfies properties 1 and 2, and *Sa. cerevisiae LEU2* with promoter deletions to satisfy property 3. I first used *Sa. cerevisiae leu2d* (a *LEU2* allele used in *Sa. cerevisiae* gTOW). In *Sa. cerevisiae*, the selection bias of *leu2d* to increase the plasmid copy number can be controlled by the leucine concentration in the medium (Moriya *et al.*, 2006). However, this control proved impossible in *Sc. pombe* because the final copy numbers of the *leu2d* plasmid (pTOWsp-H) were the same even in media containing different leucine concentrations (data not shown). This is probably due to differences in the leucine-sensing mechanism between the yeasts. I thus optimized lengths of the *LEU2* promoters (Table 3.5-4) and developed three independent gTOW vectors (pTOWsp-L, pTOWsp-M, and pTOWsp-H) with different biases to increase plasmid copy numbers in *leu1Δ Sc. pombe* cells (Figure 3.6-1). Average plasmid copy numbers of the above three plasmids in the *leu1Δ* cell in the +leucine media (−uracil selection) were 8.5 ± 3.3 (all three plasmids showed no difference), and in the −leucine media were 41.3 ± 13.0, 55.4 ± 11.3, and 116.8 ± 7.0, respectively (Figure 3.6-5B; Table 3.5-4). Differences between the gTOW vectors in *Sa. cerevisiae* and *Sc. pombe* are shown in Table 3.5-5.

In each plasmid, *ura4-EGFP* was expressed, such that distribution of the

plasmid copy number within populations could be monitored. Distribution of the cells for each of the plasmids analyzed by flow cytometry is shown in Figure 3.6-5C. In the +leucine condition (orange in Figure 3.6-5C), the plasmids tended to become lost because a portion of the cells showed the same fluorescence as the negative control (gray in Figure 3.6-5C). The average of GFP fluorescence and copy number showed good correlation (Figure 3.6-5B), which indicates that GFP fluorescence is also useful in estimating the plasmid copy number within the cell.

3.3.2 Measuring plasmid copy number limits of cell-cycle regulator genes

I selected 31 cell-cycle regulator genes (except *byr4*+, Table 3.5-6) and measured their copy number limits using gTOW. These genes contain orthologs of the budding yeast cell-cycle regulator genes, which Moriya *et al.* (2006) had previously analyzed. They also contain genes implemented into an integrative mathematical model described below. In gTOW, one needs to measure how much the expression of a target gene can be increased from the native expression level; hence, whole regulatory elements on the 5′ and 3′ regions of the target ORF should be cloned into the plasmids. I thus cloned each target gene up to the neighboring ORFs (the case of *cdc2* is shown in Figure 3.6-3 as an example). In addition, I introduced frameshift mutations in five genes just after their start codons to test whether proteins expressed from these genes determine copy number limits (the structure of the frameshift mutant of *cdc2* is shown in Figure 3.6-4 as an example).

Each gene was cloned into pTOWsp-L, -M, and -H vectors, and at least two independent clones were studied for each gene. *Sc. pombe* cells with each plasmid were grown in +leucine and −leucine media. After 48 h of cultivation for pTOWsp-L and -M plasmids and 72 h for pTOWsp-H plasmids, plasmid copy numbers within the cells and GFP fluorescence of the cells were measured, and cellular morphology was observed. Cell size distribution was also monitored as forward scattering (FSC) by flow cytometry, and some examples are shown in Figure 3.6-6. Using combinations of +leucine and −leucine conditions with three

vectors, the copy number limit of each gene could be determined precisely (second and third columns in Figure 3.6-6). Using fluorescent microscopy, I could assess morphology of the cells with high target gene copy numbers (brighter GFP fluorescence, fifth and sixth columns in Figure 3.6-6). For example, in the case of *cdc25*, the copy number limit could be determined by the pTOWsp-M-based plasmids, and cells became smaller in the –leucine condition. In the case of *rum1*, both cells and nuclei enlarged, while in the case of *spg1*, cells showed multiple septation.

In addition, when I analyzed the gTOW experiments by time-lapse microscopy, I could assess morphology of the cells with high target gene copy numbers. Figure 3.6-7 shows an example of time-lapse observation of a gTOW experiment with the target gene *mik1*+, which encodes a mitotic inhibitory kinase. Daughter cells with unequally distributed plasmid copy numbers had different fates; cells with low plasmid copy numbers barely grew, and after two cellular divisions growth ceased completely (black arrowhead in Figure 3.6-7). Cells with high plasmid copy numbers grew faster because they produced leucine but were unable to divide, resulting in elongation and eventual death (white arrowhead in Figure 3.6-7). On the other hand, cells with a balanced plasmid copy number maintained normal growth and division and accumulated in the media (yellow arrowhead in Figure 3.6-7).

The copy number limits varied from 1 (one extra copy over the endogenous copy number kills the cell) to >100 (Figure 3.6-8, Table 3.5-7), indicating that the cell-cycle regulatory system has a different robustness against overexpression of each gene, as observed in *Sa. cerevisiae* cell-cycle regulation (Kaizu *et al.*, 2010). The frameshift mutants generally showed much higher copy number limits than the wild types (orange bars in Figure 3.6-8), but the frameshift mutants of *wee1* and *rum1* had lower limits than the pTOWsp-H vector alone, probably because their frameshifts do not completely shut down protein expression. Morphology of cells with high copy frameshift mutant genes was similar to that of cells with high copies of their wild types (Figure 3.6-9).

3.3.3 Comparison of robustness profiles of cell-cycle regulations between *Sa. cerevisiae* and *Sc. pombe*

I next compared the copy number limits of the cell-cycle regulator genes determined in this study with that of the *Sa. cerevisiae* homologs determined previously (Moriya *et al.*, 2006); Figure 3.6-10). *Sc. pombe* genes generally had lower copy number limits (average = 52) than those of *Sa. cerevisiae* (average = 87). Moriya *et al.* (2006) previously reported that cell-cycle regulators with lower limits constituted a fragile core that directly regulates the activity of B-type cyclin Cdk (Cyclin-dependent kinase) complexes. The orthologs that constitute the core structure of *Sc. pombe* (Cdc13, Rum1, and Wee1) also demonstrated low limits, which may indicate the presence of a conserved fragile core in eukaryotic cell-cycle regulation. In contrast, the orthologous components of the mitotic exit network (MEN) of *Sa. cerevisiae* showed very different limits from those in the septation initiation network (SIN) of *Sc. pombe,* although both networks have conserved architecture (Bardin and Amon, 2001; Krapp and Simanis, 2008). This might reflect the different physiological functions in the two yeasts (namely, budding and fission), although these components have the same origin. These results suggest that comparison of robustness profiles is a useful way to reveal the conserved/non-conserved properties of cellular systems.

3.3.4 Very low limit of *spg1* is brought about by the dosage imbalance against *byr4*

Kaizu *at al.* (2010) recently demonstrated that the M-phase phosphatase gene *CDC14* has a very low limit because of the dosage imbalance between *CDC14* and its inhibitor gene, *NET1*. Hence, I investigated whether the low limit of *spg1*, the lowest copy number gene in *Sc. pombe* cell-cycle regulators evaluated in this study, was also due to dosage imbalance. *spg1* encodes a small GTPase involved in the initiation of cellular septation; this activity is regulated by the bipartite GTPase activating protein (GAP), which is encoded by both *cdc16* and *byr4* (Furge *et al.*, 1998). The copy number limit of *cdc16* is quite high (Figure 3.6-8), and cells with high copy *cdc16* did not show any obvious phenotype (data

not shown). In contrast, the limit of *byr4* was very low (1.8 ± 0.2, measured by pTOWsp-L in the +leucine condition). And cellular lethality due to overexpression of *spg1* is nullified by the simultaneous overexpression of *byr4* (Furge *et al.*, 1998). I thus assume that activity of Spg1 is regulated by the delicate balance between Spg1 and Byr4, and hence, the limits of both *spg1* and *byr4* are quite low. To investigate whether *spg1* and *byr4* were in dosage balance, I performed two-dimensional overproduction (2Dop) gTOW (Kaizu *et al.*, 2010). As shown in .6-11B, *byr4* limits increased only when multicopy *spg1* was supplied by another plasmid. Moreover, their copy numbers were balanced (Figure 3.6-11B, dotted line). Microscopic observation also confirmed our assumption that cells can divide normally only when *spg1* and *byr4* copy numbers are balanced (Figure 3.6-11C). These results strongly support the theory that *spg1* has a very low limit because of the sensitive balance required for GTPase activity.

3.4 Discussion

3.4.1 gTOW in *Sc. pombe*

In this study, I developed a gTOW method in the fission yeast *Sc. pombe*. *Sc. pombe* gTOW vectors have different biases for increasing the plasmid copy number. These vectors also have the *EGFP* gene, such that distribution of the plasmid copy numbers can be monitored by flow cytometry, or the plasmid copy number in a single cell can be estimated under fluorescent microscopy. In *Sc. pombe,* the *nmt*1 promoter has been often used to overexpress genes, but the upper limit is difficult to determine by this method. Thus, gTOW provides another means for overexpression of genes and for obtaining unique data to investigate the robustness of cellular systems in *Sc. pombe*.

3.4.2 Robustness and fragility in cell-cycle regulation in *Sc. pombe* and *Sa. cerevisiae*

Sa. cerevisiae and *Sc. pomb*e appear to have conserved fragility in the subsystem that directly regulates B-type cyclin Cdk1 activity (Figure 3.6-10). Because these species are distantly related, with an evolutional distance of several hundred million years (Sipiczki, 2000), fragility in B-type Cdk regulation would be conserved among eukaryotes. In contrast, networks regulating cytokinesis (MEN in *Sa. cerevisiae* and SIN in *Sc. pombe*) showed different robustness profiles (Figure 3.6-10), which might reflect their different systems of cellular division (budding and fission). Hence, comparison of robustness profiles would be useful to reveal the conserved properties of cellular systems.

In the cell-cycle regulation of *Sa. cerevisiae*, the Cdk1-counteracting phosphatase gene *CDC14* had the lowest copy number limit, the reason being dosage imbalance against the inhibitor gene *NET1* (Kaizu *et al.*, 2010). The relatively high copy number limit of *clp1,* the *Sc. pombe* ortholog of *CDC14*, may be explained by the fact that Clp1 does not have a stoichiometric inhibitor (it seems that there is an ortholog of *Net1* but acts differently (Jin *et al.*, 2007). In this study, I showed that the small GTPase gene *spg1*, the gene with the lowest

copy number limit among the *Sc. pombe* cell-cycle regulators, was also in dosage balance with the GAP gene *byr4* (Figure 3.6-11). I therefore believe that dosage imbalance is a general mechanism for inducing cellular fragility in case of gene overexpression.

3.4.3 Integrative mathematical model of cell-cycle regulation in *Sc. pombe*

Robustness can be a measure of plausibility in mathematical models of biological networks (Morohashi *et al.*, 2002). Moriya *et al.* (2006) previously used copy number limits obtained from *Sa. cerevisiae* gTOW to evaluate and refine an integrative mathematical model of the *Sa. cerevisiae* cell cycle. I thus evaluated and refined the integrative mathematical model, such that the model reproduces robustness (copy number limits of genes) of the *Sc. pombe* cell cycle obtained from this study. Novak group previously published a mathematical model for *Sc. pombe* cell-cycle regulation (Novak and Tyson, 1997; Sveiczer *et al.*, 2000). Using the gTOW data obtained in this study, Novak group has modified the model, such that the model reproduce more published experimental results. They designated the model 'basic model,' the whole structure of which is shown in Figure 3.6-12A (green components; the simplified structure is shown in Figure 3.6-13). They first investigated to what degree the core model reproduced the copy number limits obtained in this study. Although they did not use the gTOW data for development of the model, the model predicted the experimental data well (Figure 3.6-12B, green circles) and appeared to capture the robustness of fission yeast cell-cycle regulation. To describe the gTOW data more extensively, they modified the basic model by adding some important regulators (M-phase phosphatase Clp1, cyclins Cig1 and Puc1) and regulations, and the parameters were optimized by-hand parameter adjustments (they designated the model 'gTOW model,' shown in red in Figure 3.6-12A; see also Figure 3.6-13). The model successfully reproduced the copy number limits obtained in this study (Figure 3.6-12B, orange squares). In addition, the model could also reproduce 42 already published mutant behaviors (Table 3.5-11). The result of time-course

simulation of the model is shown in Figure 3.6-12C. As a result, we can claim that the presented 'gTOW model' is the most detailed model of fission yeast cell-cycle regulation so far. The model provided us with the predictions that should be evaluated by further research.

One of the practical values of the existence of the integrative mathematical model, just as we have developed in this study, is that we can define the limit of our understanding and find novel biological knowledge using the model predictions as references of experimental results. I thus measured the copy number limits of the cell-cycle regulators in the deletion strains and compared the data with the model prediction in Table 3.5-12. This '2Ddelta-gTOW experiment' was performed with the deletion strain of each of four genes (*cig1*, *clp1*, *puc1*, and *srw1*). I chose these genes because the deletion of them does not give so much impact for the upper limits of the other cell-cycle regulators in the model (Figure 3.6-14A; Table 3.5-12). I thus expected uncovered regulations.

In fact, we found some discrepancies between the gTOW experimental data and the gTOW model predictions (Figure 3.6-14A). The *rum1* limit in *cig1Δ*, the *slp1* limit in *clp1Δ*, and *cdc25* limit in *srw1Δ* were much lower than the model prediction. The *pyp3* limit in s*rw1Δ* was much higher than the model prediction. These results suggested additional regulations and wrong assumptions within the current gTOW model (summarized in Figure 3.6-14B). We thus showed that the prediction of the model was quite useful reference to indicate the existence of additional (unknown) regulations conferring the robustness of the cell cycle. I propose that the following potential regulatory mechanisms provide an explanation for the 2Ddelta-gTOW data in Figure 3.6-14

(1) Low *rum1* limit in *cig1Δ:* Cig1 might be more important for Rum1 degradation than it is assumed in the model.

(2) Low *slp1* limit in *clp1Δ*: Clp1 might negatively regulate Slp1 activity or the level that is absent in *clp1Δ* background.

(3) Low *cdc25* limit in *srw1Δ*: Srw1 might be important for degradation of Cdc25.

(4) Low *pyp3* limit in *srw1Δ* in the model but not in the experiment: Pyp3

might be less important as a Cdc25 backup phosphatase than it is assumed in the model.

At this point, we did not modify the gTOW model with these suggested regulatory interactions because they are still hypothetical. These hypothetical regulations should be tested with additional experiments and the model will be refined with the regulations, just as Kaizu *et al*. (2010) did in the budding yeast case.

3.4.4 Evaluation and refinement of integrative mathematical model using robustness information

A considerable body of knowledge has been accumulated for the fission yeast *Sc. pombe* and for the molecular details of the regulation of its cell cycle (Nurse, 2002), and this knowledge has been integrated into mathematical models before (Novak and Tyson, 1997; Sveiczer *et al.*, 2000), and further developed in this study. These integrative mathematical models are expected to have very important roles in future life sciences because they can be used to predict behaviors of complicated biological systems that are difficult to handle intuitively.

These models are generally constructed according to the accumulated knowledge on the interactions between relevant molecules, but information on biochemical parameters needed to describe the strength and speed of interactions is usually lacking. Although these parameters are important to guarantee the plausibility of these models, it is sometimes technically difficult to obtain these biochemical parameters experimentally.

On the other hand, it is considered that these parameters should have some permissible ranges because biological systems have robustness (Barkai and Leibler, 1997; von Dassow *et al.*, 2000). Because the permissible ranges have emerged from interactions of components within the system, they are useful indicators for evaluation of the network structures of biological models (Morohashi *et al.*, 2002; Moriya *et al.*, 2006; Kaizu *et al.*, 2010).

In this study, we performed experiments to measure the permissible range of gene overexpression and used the data obtained to evaluate and modify the mathematical model. I believe this is a useful scheme for development of

integrative mathematical models in which direct experimental measurement of biochemical parameters is difficult.

3.5 Tables

Table 3.5-1. Plasmid

Plasmid name	Original name	Relevant feature	Source
pRS315		*LEU2*	Sikorski *et al*, 1989
pDBlet		*ars3002x2*, *ura4+*	Brun *et al*, 1995
pKT128		*EGFP*, *his5MX*	Sheff and Thorn, 2004
mRFP in pRSET-B		*mRFP*	Campbell *et al*, 2002
pHM001		pDBlet with *LEU2*	This study
pHM002		pDBlet with *leu2d*	This study
pTOWsp-H	pHM004	pHM002 with *ura4-EGFP*, *his5MX*	This study
pTOWsp-M	pHM004-835	pHM004 with longer *LEU2* promoter	This study
pTOWsp-L	pHM004-836	pHM004 with longer *LEU2* promoter	This study
pHM004-837		pHM004 with longer *LEU2* promoter	This study
pHM004-838		pHM004 with longer *LEU2* promoter	This study
pHM004-839		pHM004 with longer *LEU2* promoter	This study
pHM004-840		pHM004 with longer *LEU2* promoter	This study
pA6R		pDblet with *ade6-mRFP* instead of *ura4+*	This study

Table 3.5-2. Oligo DNA primers used for construction of plasmid vectors	
Oligo	**Sequence (5' to 3')**
OSBI0009	GGAAACAGCTATGACCATG
OSBI0582	gcatctgtgcggtatttcacaccgCATATGaatggtcaggtcattgagtg
OSBI0583	agattgtactgagagtgcac
OSBI0584	GGGATTTGTAGCTAAGCTCCATATGcctcaacataacgagaacacacagg
OSBI0585	cctgtgtgttctcgttatgttgaggCATATGGAGCTTAGCTACAAATCCC
OSBI0606	GGGATTTGTAGCTAAGCTCCATATGtatatatatttcaaggatataccat
OSBI0607	atggtatatccttgaaatatatataCATATGGAGCTTAGCTACAAATCCC
OSBI0640	gcgcgtttcggtgatgacgg
OSBI0719	tgttaattaaaccagcaccgtcaccATGCTGAGAAAGTCTTTGCTGATATG
OSBI0720	CATATCAGCAAAGACTTTCTCAGCATggtgacggtgctggtttaattaaca
OSBI0721	CTTAACTATGCGGCATCAGAGCAGATTGTACTGAGAGTGCACtcgatg aattcgagctcg
OSBI0835	TACATATAGCCAGTGGGATTTGTAGCTAAGCTCCATATGttcttacctttac atttca
OSBI0836	TACATATAGCCAGTGGGATTTGTAGCTAAGCTCCATATGgtggttagcaat cgtcttac
OSBI0837	TACATATAGCCAGTGGGATTTGTAGCTAAGCTCCATATGtatttaaggacct attgttt
OSBI0838	TACATATAGCCAGTGGGATTTGTAGCTAAGCTCCATATGttgcatcacaat acttgaag
OSBI0839	TACATATAGCCAGTGGGATTTGTAGCTAAGCTCCATATGtagaatagaga agcgttcat
OSBI0840	TACATATAGCCAGTGGGATTTGTAGCTAAGCTCCATATGaggtgagagcg ccggaaccg
OSBI0850	TTACCAATGCTTAATCAGTG
OSBI0851	ATGAGTATTCAACATTTCCG
OSBI0880	attaccctgttatccctagcggatccaaatcaactacatcttttaataat
OSBI0881	attattaaaagatgtagttgatttggatccgctagggataacagggtaat
OSBI0882	ccatgtttcaatgtgcgtatcactacaatgacctgaccattCATATGcgg
OSBI0883	ccgCATATGaatggtcaggtcattgtagtgatacgcacattgaaacatgg
OSBI0884	aaaagcaagcaaaatcatttaacagTTAGGCGCCGGTGGAGTGGCGGCCC
OSBI0885	GGGCCGCCACTCCACCGGCGCCTAActgttaaatgattttgcttgctttt
OSBI0886	TGATGACGTCCTCGGAGGAGGCCATTGCAGAATAATTTTTCCAACC AAC
OSBI0887	GTTGGTTGGAAAAATTATTCTGCAATGGCCTCCTCCGAGGACGTCA TCA

Table 3.5-3. Oligo DNA primers to amplify and clone cell-cycle regulators

No.	Gene	Up primer	Sequence (5' to 3')	Down primer	Sequence (5' to 3')
1	*ark1+*	OSBI0667	agctatgaccatgattacgccaagcttGGGGTTCGATTCCCCCTGACGGA	OSBI0668	gactcactatagggcgaattgggtaccTCATTCTTTCGTCTAGTCTATTG
2	*cdc2+*	OSBI0608	agctatgaccatgattacgccaagcttGACTTTGGCAATGATTTCTTTTA	OSBI0609	gactcactatagggcgaattgggtaccCCCGAGGAGGAAGAAATTATTTA
3	*cdc7+*	OSBI0669	agctatgaccatgattacgccaagcttCATAACCATCAGACACTTGTTTA	OSBI0670	gactcactatagggcgaattgggtaccTATATTCCTTTTTACTTCTGACA
4	*cdc10+*	OSBI0671	agctatgaccatgattacgccaagcttAGTGGAAAACGTTCTGTTAAGTA	OSBI0672	gactcactatagggcgaattgggtaccGAAAATTTAACTAATTTCCAATA
5	*cdc13+*	OSBI0610	agctatgaccatgattacgccaagcttAGCGCGTTTGCTCCTTCCCTATGA	OSBI0611	gactcactatagggcgaattgggtaccGTAAATCGATCTACTATTGATTA
6	*cdc16+*	OSBI0673	agctatgaccatgattacgccaagcttAGGCGTCGAATTGGGAGTCGACA	OSBI0674	gactcactatagggcgaattgggtaccTCCTTTGCTATGCATACGACCCA
7	*cdc18+*	OSBI0675	agctatgaccatgattacgccaagcttAAAGATGTAGAAAAAGAAGAATA	OSBI0676	gactcactatagggcgaattgggtaccCGTGTTGTTTTGTGGACTCTTTA
8	*cdc25+*	OSBI0612	agctatgaccatgattacgccaagcttCTTGCCGAGCATCTTAAGAATT	OSBI0613	gactcactatagggcgaattgggtaccCTTGGAAGCATGGTCGTTATTCA
9	*chk1+*	OSBI0677	agctatgaccatgattacgccaagcttCTGGTTTTGCATATCAGAATCCA	OSBI0678	gactcactatagggcgaattgggtaccATATTGGGTACAATGATGTATTA
10	*cig1+*	OSBI0679	agctatgaccatgattacgccaagcttATCTGATTCAAATTCGAATCTCA	OSBI0680	gactcactatagggcgaattgggtaccAATTCCCTCGATATTAATCAACA
11	*cig2+*	OSBI0681	agctatgaccatgattacgccaagcttAGCGCTATTGCTGAATACTGTTT	OSBI0682	gactcactatagggcgaattgggtaccAAAAAAGCTCAAATGTTCATTA
12	*clp1+*	OSBI0683	agctatgaccatgattacgccaagcttCTGCTCTTGAAGTTTAATTGTTC	OSBI0684	gactcactatagggcgaattgggtaccAAACTGACCCAAAGGTGAAAACA
13	*csk1+*	OSBI0685	agctatgaccatgattacgccaagcttCAGCTTTAAAAATTTAACTCGCA	OSBI0686	gactcactatagggcgaattgggtaccAAACTCCACGACTTCCAAATCCA
14	*cut1+*	OSBI0687	agctatgaccatgattacgccaagcttTTGCGGCCCATTAGTGGCAGACA	OSBI0742	gctaatttcgcattattgttggaattatgctctaggagattttggtcacc
15	*cut2+*	OSBI0689	agctatgaccatgattacgccaagcttACATGCGACGTTTGTTGTGCCCC	OSBI0690	gactcactatagggcgaattgggtaccTACATCAAGGCTGCTAAGTTTTA
16	*dfp1+*	OSBI0691	agctatgaccatgattacgccaagcttATGACACGAAAAAGGAGAATATA	OSBI0692	gactcactatagggcgaattgggtaccTTTCTGAAAATCATATGAGTCCA
17	*fkh2+*	OSBI0693	agctatgaccatgattacgccaagcttACGAGATACATCGCCGGAAGACA	OSBI0694	gactcactatagggcgaattgggtaccGGAGATCGTGAATGCAGCAGACA
18	*hsk1+*	OSBI0695	agctatgaccatgattacgccaagcttTCTAGAAAGAAGATCCAACGACA	OSBI0696	gactcactatagggcgaattgggtaccGGTGTCGTTGAGCTCATTGCCTA
19	*mik1+*	OSBI0697	agctatgaccatgattacgccaagcttTGTTTGCAAATTCTTTTTTTTT	OSBI0698	gactcactatagggcgaattgggtaccTCGTGAATTATTTAAAATAAGAT
20	*plo1+*	OSBI0699	agctatgaccatgattacgccaagcttATTAATGCACTATTTATCCCATA	OSBI0700	gactcactatagggcgaattgggtaccGATATGCGTTCTTGGATACTTCA
21	*puc1+*	OSBI0701	agctatgaccatgattacgccaagcttTATGAGCACAAATTTGGCTCGTA	OSBI0702	gactcactatagggcgaattgggtaccAGAAAATTAAAAAAAACTCACTA
22	*ras1+*	OSBI0703	agctatgaccatgattacgccaagcttAATCTTGAGAAACTACATCCTTA	OSBI0704	gactcactatagggcgaattgggtaccAAAGCGCTTTTAGGGATAGATTG

23	*res1+*	OSBI0705	agctatgaccatgattacgccaagcttAGACAGCAGTACCAAGCCAAATG	OSBI0706	gactcactatagggcgaattgggtaccGCAGGAATTGACGTCGAATTGTA
24	*res2+*	OSBI0707	agctatgaccatgattacgccaagcttACGTTACTTGGAAAATGCTCATA	OSBI0708	gactcactatagggcgaattgggtaccTGTCAAAAGTTTCAACGCATCCA
25	*rum1+*	OSBI0614	agctatgaccatgattacgccaagcttTTCTTGTTGCAATTCAGATGTCA	OSBI0615	gactcactatagggcgaattgggtaccTTTCGTTGGGATTGTTTCGATCA
26	*sid2+*	OSBI0709	agctatgaccatgattacgccaagcttAAAAATGGCAAGTTAATAAGCTG	OSBI0710	gactcactatagggcgaattgggtaccTTAACAGATTAATTTACGAGTGA
27	*slp1+*	OSBI0711	agctatgaccatgattacgccaagcttAAAAGAACGTAAATAGGAACTCA	OSBI0712	gactcactatagggcgaattgggtaccACTACCCGTTCTATTCCGTTTCA
28	*spg1+*	OSBI0713	agctatgaccatgattacgccaagcttATCAAAACTACAATTAAAACTTG	OSBI0714	gactcactatagggcgaattgggtaccACAGTTGAACGTTTAGAAATATA
29	*srw1+*	OSBI0715	agctatgaccatgattacgccaagcttTACGCGAACATTAGCTGTAGACA	OSBI0716	gactcactatagggcgaattgggtaccACAAATGCAAAGCCTCTCAATTA
30	*wee1+*	OSBI0616	agctatgaccatgattacgccaagcttGACAAGAACCAGTTTTTGGCTCA	OSBI0617	gactcactatagggcgaattgggtaccAGAAAATATTCGTCTCCCAAGCA
31	*pyp3+*	OSBI0717	agctatgaccatgattacgccaagcttGTAAAAGGGTGGATGGATATATA	OSBI0718	gactcactatagggcgaattgggtaccATGTAAATAGGATGGGAGCATCA
32	*byr4+*	OSBI	agctatgaccatgattacgccaagcttGGCTCAACGGTAATGTCAGACAT	OSBI	gactcactatagggcgaattgggtaccAACCTCCTTGGCAACCCCAATAA
		F_fs primer		**R_fs primer**	
2_fs	*cdc2-fs*	OSBI0725	tcttttagtggtttgcaATGcgcaGAGAATTATCAAAAAGTCGA	OSBI0726	TCGACTTTTTGATAATTCTCtgcgCATtgcaaaccactaaaaga
5_fs	*cdc13-fs*	OSBI0727	cgtttcttcttttcctcATGcgcaACTACCCGTCGTTTAACTCG	OSBI0728	CGAGTTAAACGACGGGTAGTtgcgCATgaggaaaagaagaaacg
8_fs	*cdc25-fs*	OSBI0729	gttaaacctcaactaaaATGcgcaGATTCTCCGCTTTCTTCACT	OSBI0730	AGTGAAGAAAGCGGAGAATCtgcgCATtttagttgaggtttaac
25_fs	*rum1-fs*	OSBI0731	tggattgtcagttcgctATGcgcaGAACCTTCAACACCACCTAT	OSBI0732	ATAGGTGGTGTTGAAGGTTCtgcgCATagcgaactgacaatcca
30_fs	*wee1-fs*	OSBI0733	acattttccatacagaaaacATGcgcaAGCTCTTCTTCTAATAC	OSBI0734	GTATTAGAAGAAGAGCTtgcgCATgttttctgtatggaaaatgt
		eF primer		**eR primer**	
14	*cut1+*	OSBI0768	ggtgaccaaaatctcctagagcataattccaacaataatgcgaaattagc	OSBI0769	gctaatttcgcattattgttggaattatgctctaggagattttggtcacc

Table 3.5-4. Copy numbers of *Sc. pombe* gTOW vectors

Plasmid name	*LEU2* promoter[*1]		Copy number ± SD[*2]	
pHM001	-341	(*LEU2*)	5.9	± 2.1
pHM004-840	-209		63.1	± 1.2
pHM004-839	-179		80.9	± 15.6
pHM004-838	-149		89.2	± 9.2
pHM004-837	-119		78.8	± 8.1
pTOWsp-L	-89		41.3	± 13.0
pTOWsp-M	-59		55.4	± 11.3
pTOWsp-H	-29	(*leu2d*)	116.8	± 7.0

*1 Length from ATG is shown with negative number.

*2 Copy number −leucine condition.

Table 3.5-5. Comparison of the vectors

Species	Vector Name	Plasmid Origin	1st selection	2nd selection	Others
Sa. cerevisiae	pTOW (pSBI40)	2μ DNA	*URA3*	*leu2d*	
Sc. pombe	pTOWsp-H, -M, -L	*ars3002* x2	*ura4+*	*LEU2* derivative	*EGFP-sphis5MX*

Table 3.5-6. *Schizosaccharomyces pombe* genes is analyzed in this study

No.	Gene	Description
1	*ark1+*	Aurora kinase
2	*cdc2+*	Cyclin dependent kinase
3	*cdc7+*	Septation kinase
4	*cdc10+*	G1 phase transcription factor
5	*cdc13+*	B type cyclin, M phase
6	*cdc16+*	With Byr4, a two-component GEF for the GTPase Spg1
7	*cdc18+*	S phase initiator / MCM loader
8	*cdc25+*	CDK tyrosine phosphatase
9	*chk1+*	Checkpoint kinase, damage response
10	*cig1+*	B-type cyclin, function not clear
11	*cig2+*	B-type cyclin in S phase
12	*clp1+*	Phosphatase, involved in septation
13	*csk1+*	CDK-activating kinase
14	*cut1+*	Promotes anaphase, Separase
15	*cut2+*	APC substrate, blocks Cut1, Securin
16	*dfp1+*	regulatory subunit of CDC7-type kinase
17	*fkh2+*	Fork head transcription factor
18	*hsk1+*	DBF4-Dependent Kinase
19	*mik1+*	CDK tyrosine kinase, overlaps with *wee1+*
20	*plo1+*	Polo-like kinase
21	*puc1+*	Cyclin, acts in G1 at cell-cycle entry/exit
22	*pyp3+*	CDK tyrosine phosphatase
23	*ras1+*	Ras homolog
24	*res1+*	Partner to Cdc10 transcription factor
25	*res2+*	Partner to Cdc10 transcription factor
26	*rum1+*	CDK inhibitor, functionally similar to Sic1
27	*sid2+*	Ser/Thr kinase, functions as part of a network in mitosis
28	*slp1+*	APC activator
29	*spg1+*	GTPase, involved in septation and mitotic exit
30	*srw1+*	APC activator, WD protein
31	*wee1+*	CDK tyrosine kinase
32	*byr4+*	With Cdc16p, a two-component GEF for the GTPase Spg1

Table 3.5-7. Plasmid copy number is determined by gTOW experiment

No.	Gene Name	Plasmid copy number (±SD)*1			
		+leucine	L (-leucine)	M (-leucine)	H (-leucine)
	vector	8.5 ± 3.3	41.3 ± 13.0	55.4 ± 11.3	116.8 ± 7.0
1	*ark1+*	7.2 ± 4.5	36.1 ± 7.2	63.0 ± 11.4	**149.0 ± 18.2**
2	*cdc2+*	2.4 ± 1.1	26.2 ± 4.4	52.1 ± 8.8	**97.0 ± 12.1**
3	*cdc7+*	2.0 ± 0.8	8.7 ± 0.7	**10.5 ± 1.9**	2.5 ± 1.0
4	*cdc10+*	8.2 ± 1.2	27.7 ± 5.1	66.1 ± 7.9	**69.5 ± 10.6**
5	*cdc13+*	1.4 ± 0.7	**4.5 ± 1.9**	2.3 ± 0.9	1.5 ± 0.7
6	*cdc16+*	5.7 ± 2.6	31.2 ± 3.0	48.2 ± 3.5	**106.0 ± 12.2**
7	*cdc18+*	6.0 ± 3.6	28.7 ± 6.6	39.0 ± 4.8	**44.2 ± 7.8**
8	*cdc25+*	3.8 ± 2.0	22.6 ± 3.4	**38.7 ± 15.1**	29.4 ± 13.7
9	*chk1+*	5.4 ± 1.3	35.2 ± 9.3	55.9 ± 4.6	**112.7 ± 18.0**
10	*cig1+*	3.7 ± 1.6	17.5 ± 4.9	**42.8 ± 20.1**	1.9 ± 0.6
11	*cig2+*	1.6 ± 0.7	**15.9 ± 6.8**	14.9 ± 4.7	1.4 ± 0.7
12	*clp1+*	1.6 ± 1.0	**6.9 ± 3.2**	5.0 ± 0.3	2.3 ± 2.6
13	*csk1+*	9.5 ± 3.2	52.9 ± 19.9	77.7 ± 9.6	**218.0 ± 7.4**
14	*cut1+*	2.9 ± 0.7	43.5 ± 8.1	**56.6 ± 21.3**	3.0 ± 0.7
15	*cut2+*	5.8 ± 2.2	26.0 ± 3.8	**32.2 ± 4.6**	10.3 ± 13.5
16	*dfp1+*	5.2 ± 2.4	26.8 ± 4.5	41.3 ± 4.0	**70.3 ± 5.4**
17	*fkh2+*	5.6 ± 1.2	17.6 ± 2.0	**24.5 ± 2.2**	4.9 ± 1.0
18	*hsk1+*	8.8 ± 4.7	43.5 ± 8.7	77.7 ± 13.2	**200.2 ± 12.4**
19	*mik1+*	5.3 ± 3.7	39.5 ± 8.2	65.9 ± 6.6	**102.8 ± 7.5**
20	*plo1+*	6.3 ± 2.1	**34.7 ± 7.7**	31.9 ± 3.6	3.8 ± 2.2
21	*puc1+*	5.2 ± 2.0	30.3 ± 3.6	72.9 ± 8.6	**154.9 ± 30.5**
22	*ras1+*	8.8 ± 1.5	38.4 ± 2.6	77.8 ± 8.5	**105.1 ± 29.1**
23	*res1+*	3.8 ± 1.9	24.6 ± 1.1	**28.3 ± 7.4**	17.1 ± 9.2
24	*res2+*	4.2 ± 1.7	31.6 ± 2.4	75.9 ± 9.2	**161.6 ± 35.2**
25	*rum1+*	2.4 ± 0.4	12.9 ± 2.2	**13.8 ± 2.3**	3.8 ± 1.7
26	*sid2+*	6.8 ± 4.0	31.6 ± 3.8	62.5 ± 8.2	**143.0 ± 11.5**
27	*slp1+*	4.0 ± 1.5	**27.7 ± 1.6**	26.2 ± 10.3	2.8 ± 2.4
28	*spg1+*	0.6 ± 0.5	**0.9 ± 0.5**	0.9 ± 0.3	1.0 ± 0.3
29	*srw1+*	5.4 ± 2.1	32.5 ± 7.7	57.5 ± 9.1	**114.7 ± 19.1**
30	*wee1+*	0.9 ± 0.4	**2.4 ± 0.8**	2.0 ± 1.0	2.3 ± 1.3
31	*pyp3+*	11.1 ± 3.1	39.9 ± 8.7	60.5 ± 7.2	**187.0 ± 24.5**
2_fs	*cdc2-fs*	13.1 ± 1.5			**181.4 ± 4.7**
5_fs	*cdc13-fs*	11.0 ± 0.4			**173.3 ± 30.6**
8_fs	*cdc25-fs*	10.4 ± 2.6			**231.1 ± 42.9**
25_fs	*rum1-fs*	2.1 ± 0.2			**89.8 ± 11.5**
30_fs	*wee1-fs*	6.2 ± 1.0			**58.8 ± 24.3**

Table 3.5-8. Mean GFP fluorescence in gTOW experiment

No.	Gene Name	Mean GFP fluorescence (±SD)*1							
		+leucine		L (-leucine)		M (-leucine)		H (-leucine)	
	vector	52.5	± 8.4	239.9	± 73.5	334.6	± 113.4	851.5	± 94.9
1	*ark1+*	48.1	± 9.2	202.6	± 58.8	349.2	± 131.6	**709.5**	**± 84.4**
2	*cdc2+*	25.6	± 3.7	175.0	± 29.3	305.0	± 33.3	**520.3**	**± 63.5**
3	*cdc7+*	30.3	± 13.6	72.9	± 44.1	**81.7**	**± 66.1**	13.6	± 3.4
4	*cdc10+*	42.6	± 10.9	172.8	± 35.4	319.3	± 36.1	**379.8**	**± 62.7**
5	*cdc13+*	17.4	± 1.6	**33.0**	**± 5.0**	27.4	± 5.9	10.8	± 2.4
6	*cdc16+*	38.5	± 7.2	129.5	± 26.1	207.5	± 80.5	**443.8**	**± 69.8**
7	*cdc18+*	44.1	± 8.9	163.0	± 24.2	221.2	± 33.4	**179.0**	**± 8.3**
8	*cdc25+*	22.7	± 2.0	185.0	± 16.1	**317.8**	**± 58.5**	85.0	± 41.0
9	*chk1+*	44.9	± 7.8	189.4	± 46.5	338.0	± 53.3	**543.0**	**± 60.0**
10	*cig1+*	24.3	± 5.0	132.8	± 23.1	**331.0**	**± 142.7**	18.6	± 5.4
11	*cig2+*	16.2	± 1.2	**75.2**	**± 8.6**	96.2	± 9.5	13.9	± 6.5
12	*clp1+*	21.0	± 3.3	**47.4**	**± 13.2**	47.2	± 6.3	12.8	± 7.9
13	*csk1+*	51.5	± 7.7	215.6	± 91.0	416.5	± 155.0	**956.0**	**± 59.4**
14	*cut1+*	32.7	± 15.2	204.8	± 87.2	**433.2**	**± 61.0**	23.1	± 5.3
15	*cut2+*	32.5	± 4.8	110.3	± 17.0	**176.8**	**± 15.6**	58.6	± 24.9
16	*dfp1+*	39.7	± 8.2	135.4	± 27.3	226.8	± 23.6	**310.0**	**± 32.1**
17	*fkh2+*	29.3	± 5.9	141.6	± 19.4	**165.0**	**± 9.5**	24.1	± 5.8
18	*hsk1+*	45.0	± 8.5	161.8	± 74.2	361.8	± 87.8	**791.0**	**± 79.0**
19	*mik1+*	43.2	± 8.9	186.6	± 57.4	320.0	± 82.2	**430.3**	**± 33.1**
20	*plo1+*	39.5	± 8.2	**151.0**	**± 74.2**	146.8	± 63.4	30.0	± 16.0
21	*puc1+*	37.4	± 10.0	141.7	± 8.4	486.0	± 170.4	**765.5**	**± 17.7**
22	*ras1+*	34.9	± 5.1	185.3	± 69.2	490.6	± 58.9	**472.5**	**± 115.5**
23	*res1+*	34.6	± 1.8	164.3	± 15.5	**259.8**	**± 58.0**	133.5	± 34.0
24	*res2+*	37.9	± 8.6	189.0	± 61.5	393.2	± 98.4	**897.0**	**± 110.2**
25	*rum1+*	24.1	± 2.7	84.4	± 8.4	**94.2**	**± 4.3**	20.5	± 2.9
26	*sid2+*	42.0	± 7.4	160.0	± 58.3	255.4	± 68.3	**694.3**	**± 91.4**
27	*slp1+*	28.8	± 3.3	**175.4**	**± 11.4**	193.0	± 17.2	22.9	± 3.6
28	*spg1+*	10.1	± 2.4	**14.2**	**± 1.5**	8.8	± 2.0	4.7	± 0.5
29	*srw1+*	41.7	± 6.1	236.3	± 91.5	366.0	± 65.1	**780.8**	**± 85.8**
30	*wee1+*	16.0	± 3.5	**21.9**	**± 0.5**	13.7	± 11.9	7.1	± 2.4
31	*pyp3+*	41.7	± 9.1	224.9	± 156.5	247.0	± 16.7	**722.8**	**± 116.6**
2_fs	*cdc2-fs*	44.8	± 11.4					**827.0**	**± 72.8**
5_fs	*cdc13-fs*	40.0	± 6.7					**724.5**	**± 61.1**
8_fs	*cdc25-fs*	37.0	± 5.8					**731.3**	**± 118.8**
25_fs	*rum1-fs*	38.8	± 3.9					**433.0**	**± 63.2**
30_fs	*wee1-fs*	39.8	± 4.4					**273.5**	**± 78.7**

*1 L, M, and H stand the experiments done with pTOWsp-L, pTOWsp-M, and pTOWsp-H, respectively. Numbers in bold letters were used as upper limits.

Table 3.5-9. Comparison of the copy number limits of orthologs in *Sc. pombe* and *Sa. cerevisiae*

Functional Category	*Sc. pombe*		*Sa. cerevisiae**	
	Gene	Copy #	Copy #	Gene
CDK	*cdc2+*	97.0	83.7	*CDC28*
G1 cyclin	*puc1+*	154.9	55.7	*CLN1*
			115.9	*CLN2*
			181.2	*CLN3*
B-type cyclin	*cdc13+*	4.5	71.1	*CLB1*
			30.3	*CLB2*
	cig1+	42.8	17.9	*CLB3*
			104.8	*CLB4*
	cig2+	15.9	12.8	*CLB5*
			141.2	*CLB6*
G1 transcription factor	*cdc10+*	69.5	154.3	*SWI6*
	res1+	28.3	56.9	*SWI4*
	res2+	161.6	94.6	*MBP1*
MCM loader	*cdc18+*	44.2	78.1	*CDC6*
CDK inhibitor	*rum1+*	13.8	30.9	*SIC1*
CDK-tyrosine kinase	*wee1+*	2.4	22.8	*SWE1*
	mik1+	102.8		
CDK-tyrosine phosphatase	*cdc25+*	38.7	197.0	*MIH1*
	pyp3+	187.0		
SIN / MEN components	*cdc16+*	106.0	127.9	*BUB2*
	cdc7+	10.5	166.6	*CDC15*
	clp1+	6.9	0.8	*CDC14*
	spg1+	0.9	86.7	*TEM1*
Separase	*cut1+*	56.6	163.7	*ESP1*
Securin	*cut2+*	32.2	55.8	*PDS1*
APC activator	*srw1+*	114.7	62.1	*CDH1*
	slp1+	27.7	69.6	*CDC20*

Table 3.5-10. Copy number limits of cell-cycle regulators in the wild type (WT) and cell cycle mutant strains

Strain*1	Target Gene	Copy Number (± SD)*2	%/WT	P-value *3
WT	*cdc10+*	20.9 ± 6.2		
WT	*cdc13+*	1.6 ± 0.6		
WT	*cdc18+*	26.2 ± 4.3		
WT	*cdc25+*	23.0 ± 5.8		
WT	*cig1+*	18.2 ± 7.7		
WT	*cig2+*	16.8 ± 11.1		
WT	*clp1+*	3.1 ± 1.4		
WT	*mik1+*	49.4 ± 20.3		
WT	*puc1+*	33.7 ± 9.6		
WT	*rum1+*	10.8 ± 10.3		
WT	*slp1+*	17.2 ± 3.7		
WT	*srw1+*	24.4 ± 5.5		
WT	*wee1+*	1.7 ± 1.3		
WT	*pyp3+*	41.4 ± 15.4		
WT	vecter	32.0 ± 11.6		
cig1Δ	*cdc10+*	31.7 ± 7.0	151	5.2E-02
cig1Δ	*cdc13+*	2.1 ± 0.4	130	2.7E-01
cig1Δ	*cdc18+*	36.1 ± 7.2	138	3.2E-02
cig1Δ	*cdc25+*	34.2 ± 8.1	149	4.6E-02
cig1Δ	*cig1+*	19.1 ± 18.3	105	9.2E-01
cig1Δ	*cig2+*	19.3 ± 8.3	115	6.8E-01
cig1Δ	*clp1+*	1.9 ± 0.1	61	8.5E-02
cig1Δ	*mik1+*	48.4 ± 11.6	98	9.3E-01
cig1Δ	*puc1+*	22.8 ± 11.8	67	1.8E-01
cig1Δ	*rum1+*	2.4 ± 0.9	22	1.4E-02
cig1Δ	*slp1+*	14.3 ± 11.3	83	5.7E-01
cig1Δ	*srw1+*	54.7 ± 23.1	224	1.1E-02
cig1Δ	*wee1+*	1.1 ± 0.2	62	4.3E-01
cig1Δ	*pyp3+*	51.8 ± 9.9	125	2.3E-01
cig1Δ	vecter	51.1 ± 5.3	160	1.2E-01
clp1Δ	*cdc10+*	15.5 ± 0.3	74	1.9E-01
clp1Δ	*cdc13+*	2.5 ± 0.4	155	7.0E-02
clp1Δ	*cdc18+*	29.0 ± 7.3	111	2.1E-01
clp1Δ	*cdc25+*	20.5 ± 2.5	89	5.2E-01
clp1Δ	*cig1+*	8.6 ± 5.7	47	1.0E-02
clp1Δ	*cig2+*	11.0 ± 4.0	65	4.2E-01
clp1Δ	*clp1+*	2.5 ± 0.5	81	5.1E-01
clp1Δ	*mik1+*	24.3 ± 3.6	49	8.5E-02
clp1Δ	*puc1+*	25.7 ± 13.5	76	2.6E-01
clp1Δ	*rum1+*	6.8 ± 1.2	63	5.3E-01
clp1Δ	*slp1+*	3.0 ± 2.1	18	9.0E-06
clp1Δ	*srw1+*	17.0 ± 13.5	70	2.4E-01
clp1Δ	*wee1+*	1.2 ± 0.7	72	5.8E-01
clp1Δ	*pyp3+*	26.8 ± 4.1	65	1.6E-01
clp1Δ	vecter	19.6 ± 4.9	61	1.3E-01
puc1Δ	*cdc10+*	20.3 ± 23.0	97	9.5E-01
puc1Δ	*cdc13+*	20.3 ± 23.0	121	4.3E-01
puc1Δ	*cdc18+*	37.0 ± 6.7	141	1.2E-02
puc1Δ	*cdc25+*	48.8 ± 18.4	212	8.4E-03
puc1Δ	*cig1+*	21.7 ± 17.4	119	6.7E-01
puc1Δ	*cig2+*	14.9 ± 9.9	89	7.8E-01

puc1Δ	*clp1+*	2.8 ± 0.5	93	7.0E-01
puc1Δ	*mik1+*	51.7 ± 11.9	105	8.3E-01
puc1Δ	*puc1+*	30.7 ± 7.1	91	6.4E-01
puc1Δ	*rum1+*	7.0 ± 1.0	64	5.5E-01
puc1Δ	*slp1+*	13.9 ± 7.2	81	3.8E-01
puc1Δ	*srw1+*	65.5 ± 23.1	268	2.1E-03
puc1Δ	*wee1+*	1.5 ± 0.3	87	7.9E-01
puc1Δ	*pyp3+*	56.3 ± 21.3	136	2.6E-01
puc1Δ	vecter	53.5 ± 20.4	167	7.7E-02
srw1Δ	*cdc10+*	20.4 ± 4.7	97	8.9E-01
srw1Δ	*cdc13+*	0.7 ± 0.1	44	5.2E-02
srw1Δ	*cdc18+*	23.1 ± 3.0	88	8.2E-01
srw1Δ	*cdc25+*	0.3 ± 0.1	1	2.5E-06
srw1Δ	*cig1+*	20.6 ± 12.8	113	7.2E-01
srw1Δ	*cig2+*	16.3 ± 12.0	97	9.5E-01
srw1Δ	*clp1+*	1.4 ± 1.1	45	1.1E-01
srw1Δ	*mik1+*	27.3 ± 4.4	55	1.2E-01
srw1Δ	*puc1+*	35.1 ± 17.8	104	8.8E-01
srw1Δ	*rum1+*	4.6 ± 2.9	43	3.5E-01
srw1Δ	*slp1+*	12.5 ± 3.2	73	1.1E-01
srw1Δ	*srw1+*	24.0 ± 3.0	98	9.1E-01
srw1Δ	*wee1+*	1.0 ± 0.4	56	3.7E-01
srw1Δ	*pyp3+*	20.7 ± 1.6	50	6.0E-02
srw1Δ	vecter	12.7 ± 2.9	40	2.9E-02

*1 For WT, *clp1*Δ, *cig1*Δ, *puc1*Δ , and *srw1*Δ strains, haploid progenies of BG_0000, BG_0465, BG_4780, BG_4172, and BG_0289 (Bioneer) were used, respectively.
*2 Copy numbers were determined using pTOWsp-M vector.
*3 P-value of the two-tailed student t-test against wild type.

Table 3.5-11. Investigated mutant phenotypes

Mutants	Parameter changes	Phenotype	References	Cdc13max at periodic cycles	Re-license	Comment
wild type (WT)	-	WT	-	1.15	yes	OK
wee1ts	T9=0.15	semi-WT	(Nurse and Thuriaux, 1980)	0.57	yes	OK
wee1Δ	T9=0	semi-WT	(Nurse and Thuriaux, 1980)	0.63	yes	OK
mik1Δ	T12=0	nearly WT	(Lundgren *et al.*, 1991)	1.15	yes	OK
mik1Δ wee1ts	T12=0, T9=0.15	cut	(Lundgren *et al.*, 1991)	0.58	no	OK
mik1Δ wee1ts cig2Δ	T12=0, T9=0.15, T4=0	semi-WT	(Bueno and Russell, 1993)	0.58	yes	OK
pyp3Δ	T0=0	nearly WT	(Millar *et al.*, 1992)	1.34	yes	OK
cdc25ts	T7=0.1	G2 block	(Russell and Nurse, 1986)	-	no	OK
cdc25Δ	T7=0	G2 block	(Russell and Nurse, 1986)	-	no	OK
wee1ts cdc25Δ	T9=0.15, T7=0	quantized cycles	(Sveiczer *et al.*, 1996)	0.70	no	low amplitude oscillator
wee1ts cdc25ts	T9=0.15, T7=0.1	semi-wee1	(Grallert *et al.*, 1998)	0.63	yes	OK
wee1Δ cdc25Δ	T9=0, T7=0	semi-wee1	(Sveiczer *et al.*, 2000)	0.57	yes	OK
wee1ts cdc25Δ mik1Δ	T9=0.15, T7=0, T12=0	quantized cycles	(Lundgren *et al.*, 1991)	0.70	no	low amplitude oscillator
cig1Δ	T6=0	nearly WT	(Bueno and Russell, 1993)	1.15	yes	OK
cig2Δ	T4=0	nearly WT	(Bueno and Russell, 1993)	1.33	yes	OK
cig1Δ cig2Δ	T4=0, T6=0	nearly WT	(Martin-Castellanos *et al.*, 1996)	1.33	yes	OK
puc1Δ	Puc1=0	nearly WT	(Forsburg and Nurse, 1994)	1.14	yes	OK
cig1Δ wee1ts	T6=0, T9=0.15	semi-WT	(Bueno and Russell, 1993)	0.56	yes	OK
cig2Δ wee1ts	T4=0, T9=0.15	semi-WT	(Bueno and Russell, 1993)	0.56	yes	OK
cig1Δ cig2Δ wee1ts	T4=0, T6=0, T9=0.15	semi-WT	(Martin-Castellanos *et al.*, 2000)	0.56	yes	OK
puc1Δ wee1ts	T0=0, T9=0.15	semi-WT	(Martin-Castellanos *et al.*, 2000)	0.58	yes	OK
rum1Δ	ksrum=0	nearly WT	(Moreno and Nurse, 1994)	1.10	yes	OK
rum1Δ cig2Δ	ksrum=0, T4=0	nearly WT	(Martin-Castellanos *et al.*, 1996)	1.29	yes	OK
rum1Δ wee1ts	ksrum=0, T9=0.15	too small	(Moreno and Nurse, 1994)	0.58	no	OK
srw1Δ	T5=0	nearly WT	(Kitamura *et al.*, 1998)	1.17	yes	OK
srw1Δ cig2Δ	T5=0, T4=0	nearly WT	(Kitamura *et al.*, 1998)	1.38	yes	OK
srw1Δ wee1ts	T5=0, T9=0.15	too small	(Kitamura *et al.*, 1998)	0.59	no	OK

srw1Δ rum1d	T5=0, ksrum=0	nearly WT	(Yamaguchi *et al.*, 2000)	1.11	yes	OK
srw1Δ rum1Δ wee1ts	T5=0, ksrum=0, T9=0.15	too small	(Sveiczer *et al.*, 2000)	0.56	no	OK
srw1Δ mik1Δ	T5=0, T12=0	nearly WT	(Kitamura *et al.*, 1998)	1.18	yes	OK
slp1ts	T3=0.01	M block	(Kim *et al.*, 1998)	-	no	OK
clp1Δ	T2=0	smaller than WT	(Trautmann *et al.*, 2001)	1.10	yes	OK
clp1Δ wee1ts	T2=0, T9=0.15	semi-WT	(Trautmann *et al.*, 2001)	0.58	yes	OK
cdc13Δ	ksc13=0	endoreplication	(Hayles *et al.*, 1994)	-	yes	OK
cdc13Δ cig1Δ	ksc13=0, T6=0	endoreplication	(Mondesert *et al.*, 1996)	-	yes	OK
cdc13Δ cig2Δ	ksc13=0, T4=0	G1 block	(Mondesert *et al.*, 1996)	-	no	OK
HU	krepl=0	S block	(Enoch *et al.*, 1992)	-	no	OK
cdc13Δ HU	ksc13=0, krepl=0	S block	(Zarzov *et al.*, 2002)	-	no	OK
cdc18Δ	ksc1810=0, ksc18=0	cut	(Kelly *et al.*, 1993)	1.15	no	OK
cdc18Δ HU	ksc1810=0, ksc18=0, krepl=0	cut	(Hermand and Nurse, 2007)	1.15	no	OK
rad3Δ	Rad3=0	nearly WT	(Martinho *et al.*, 1998)	1.15	yes	OK
rad3Δ HU	Rad3=0 krepl=0	cut	prediction	1.15	no	OK
cdc18TA	kdc1813=0, kdc18c2=0, kdc18c2'=0	G2 block	(Hermand and Nurse, 2007)	-	no	OK
cdc18TA rad3D	kdc1813=0, kdc18c2=0, kdc18c2'=0, Rad3=0	nearly WT	(Hermand and Nurse, 2007)	1.15	yes	OK

Table 3.5-12. Testing gTOW in single deletion mutants *in silico*

	WT	*Cdc10Δ*	*Cdc13Δ*	*Cdc18Δ*	*Cdc25Δ*	*Cig1Δ*	*Cig2Δ*	*Clp1Δ*	*Mik1Δ*	*Puc1Δ*	*Pyp3Δ*	*Rum1Δ*	*Slp1Δ*	*Srw1Δ*	*Wee1Δ*
		G1 block	endorepl.	cut	G2 block	~WT	~WT	~WT	~WT	~WT	~WT	~WT	M block	~WT	~0.5*WT
cdc10+	61.0		1.0				1.0		22.0	53.0	2.0			65.0	256.0
cdc13+	6.7				2.3-6.7				6.0			2.3		3.7	5.7
cdc18+	62.0		1.0				1.0		86.0	50.0	2.0	64.0		70.0	256.0
cdc25+	21.0		38.0				256.0	15.0	14.0	256.0	41.0	8.0		12.0	10.0
cig1+	40.0		20.0				26.6	46.7			30.0				4.0
cig2+	23.0		1.0					22.0	15.0	24.0	28.0	7.0		17.0	1.0
clp1+	6.0		256.0				2.0		7.0	5.0	3.0	7.0		8.0	256.0
mik1+	22.0		1.0				10.0	27.0		12.0	6.0	24.0		35.0	124.0
puc1+	256.0		9.0						140.0						1.0
pyp3+	240.0		1.0				256.0	198.0	235.0	220.0		8.0		21.0	2.0
rum1+	7.0		3.0		9.0-33.0		2.0			5.0	6.0		12.0-35.0	8.0	1.0
slp1+	31.0		256.0				7.0	39.0	32.0	27.0	11.0	39.0		37.0	3.0
srw1+	92.0		256.0			93.0	21.0	115.0	95.0	81.0	31.0	117.0			15.0
wee1+	1.3		256.0				1.0	1.4	1.4	1.2	1.1	1.4		1.4	

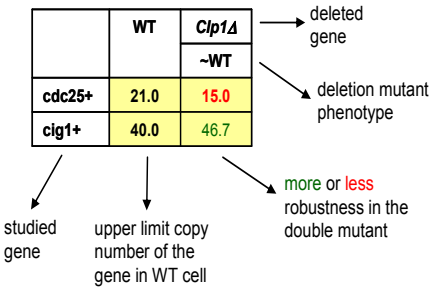

wild type behaviour
endoreplication cycles
not viable
small cells

red letter : upper limit is lower in the mutant than in WT

green letter : upper limit is higher in the mutant than in WT

bold coloured letter : difference between WT and the mutant upper limits is larger than 25%

3.6 Figures

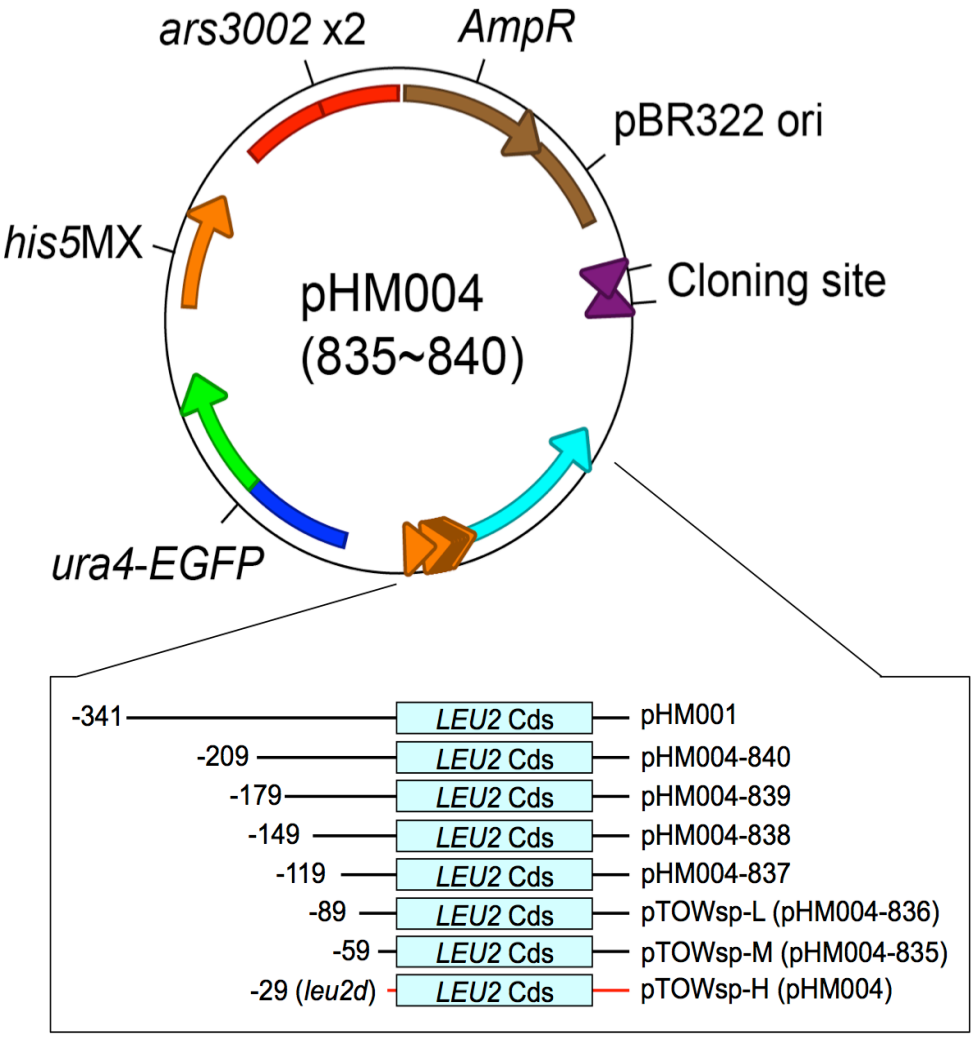

Figure 3.6-1. Structure of the pTOWsp vectors

Step1: Construction of pHM001

1. Amplify budding yeast *LEU2* gene using pRS315 as a template with primers OSBI0582 - OSBI0584.
2. Amplify fission yeast *ura4+* gene using pDBlet as a template with primers OSBI0583 - OSBI0585.
3. Cut pDBlet with a restriction enzyme *Nde*I.
4. Join the three DNA fragments above with gap-repair method.

Step2: Construction of pHM002

1. Amplify budding yeast *leu2d* gene using pRS315 as a template with primers OSBI0582 - OSBI0606.
2. Amplify fission yeast *ura4+* gene using pDBlet as a template with primers OSBI0583 - OSBI0607.
3. Cut pDBlet with a restriction enzyme *Nde*I.
4. Join the three DNA fragments above with gap-repair method.

Step3: Construction of pHM004

1. Amplify a DNA fragment containing *leu2d* and *ura4+* genes using pHM002 as a template with primers OSBI009 - OSBI0719.
2. Amplify *EGFP-sphis5MX* cassette using pKT128 as a template with primers OSBI0720 - OSBI0721.
3. Cut pDBlet with a restriction enzyme *Nde*I.
4. Join the three DNA fragments above with gap-repair method.

Step4: Construction of pHM004-835 to 840

1. Amplify DNA fragments containing *LEU2* genes with deletions of the promoter using pHM001 as a template with primers OSBI009 - OSBI 0835 to 0840.
2. Amplify *ura4-EGFP-sphis5MX* gene cassette using pHM004 as a template with primers OSBI0585 - OSBI0640.
3. Cut pDBlet with a restriction enzyme *Nde*I.
4. Join the three DNA fragments above with gap-repair method.

Step5: Changing vector's names

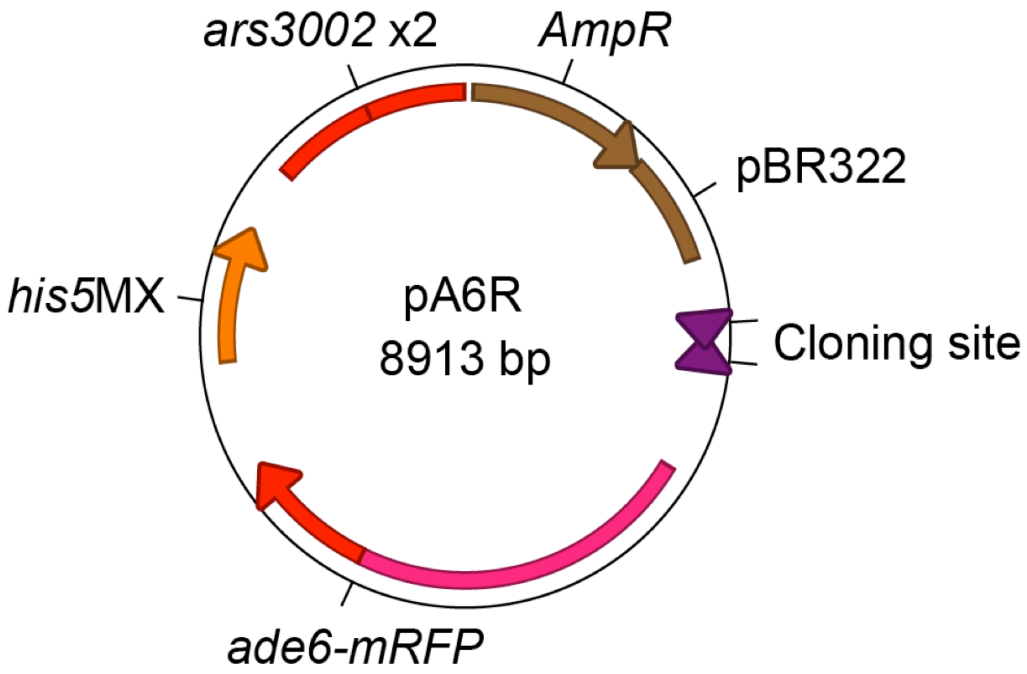

Figure 3.6-2. Structure of the pA6R

1. Amplify two DNA fragments containing the plasmid backbone using pHM004 as a template with primers OSBI0881 - OSBI0850 and OSBI0851- OSBI0882.
2. Amplify two DNA fragments containing *ade6* (promoter and ORF) and *ade6* terminator using *Sc. pombe* genome as a template with primers OSBI0883 - OSBI0886 and OSBI0880 - OSBI0885, respectively.
3. Amplify a DNA fragment containing *mRFP* using pRSET-B as a template with primers OSBI0884- OSBI0887.
4. Join the five DNA fragments above with the gap-repair method.

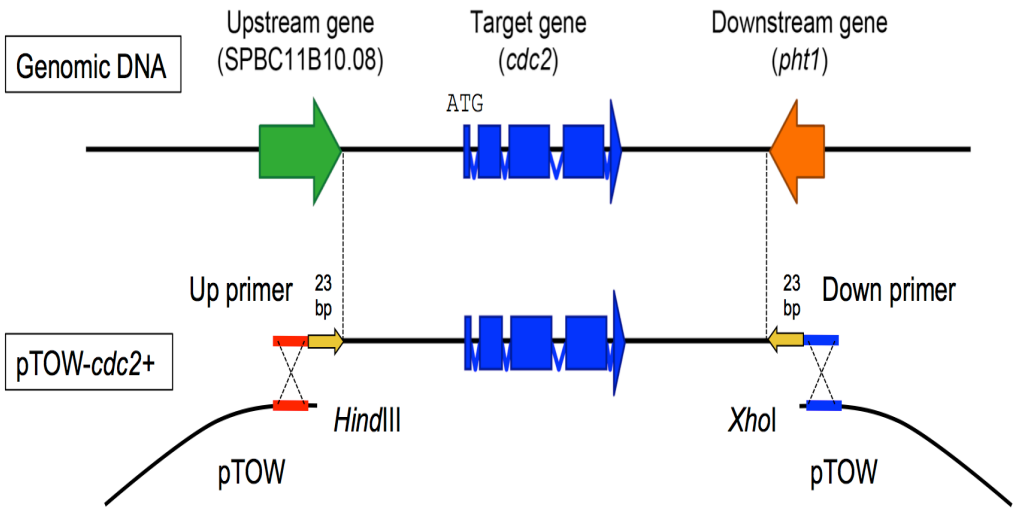

Figure 3.6-3. Design of primers to amplify and clone the target genes

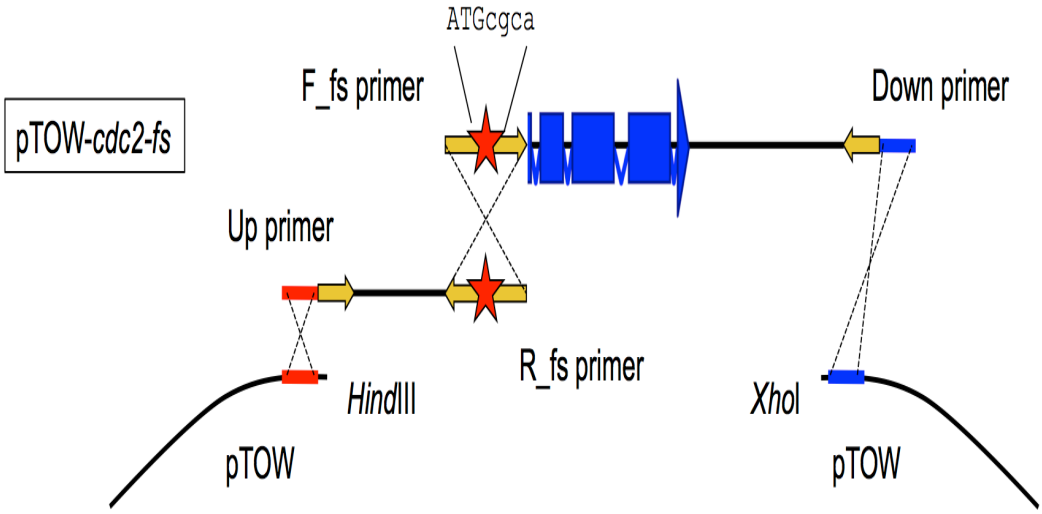

Figure 3.6-4. Design of primers to construct frame-shift mutant genes

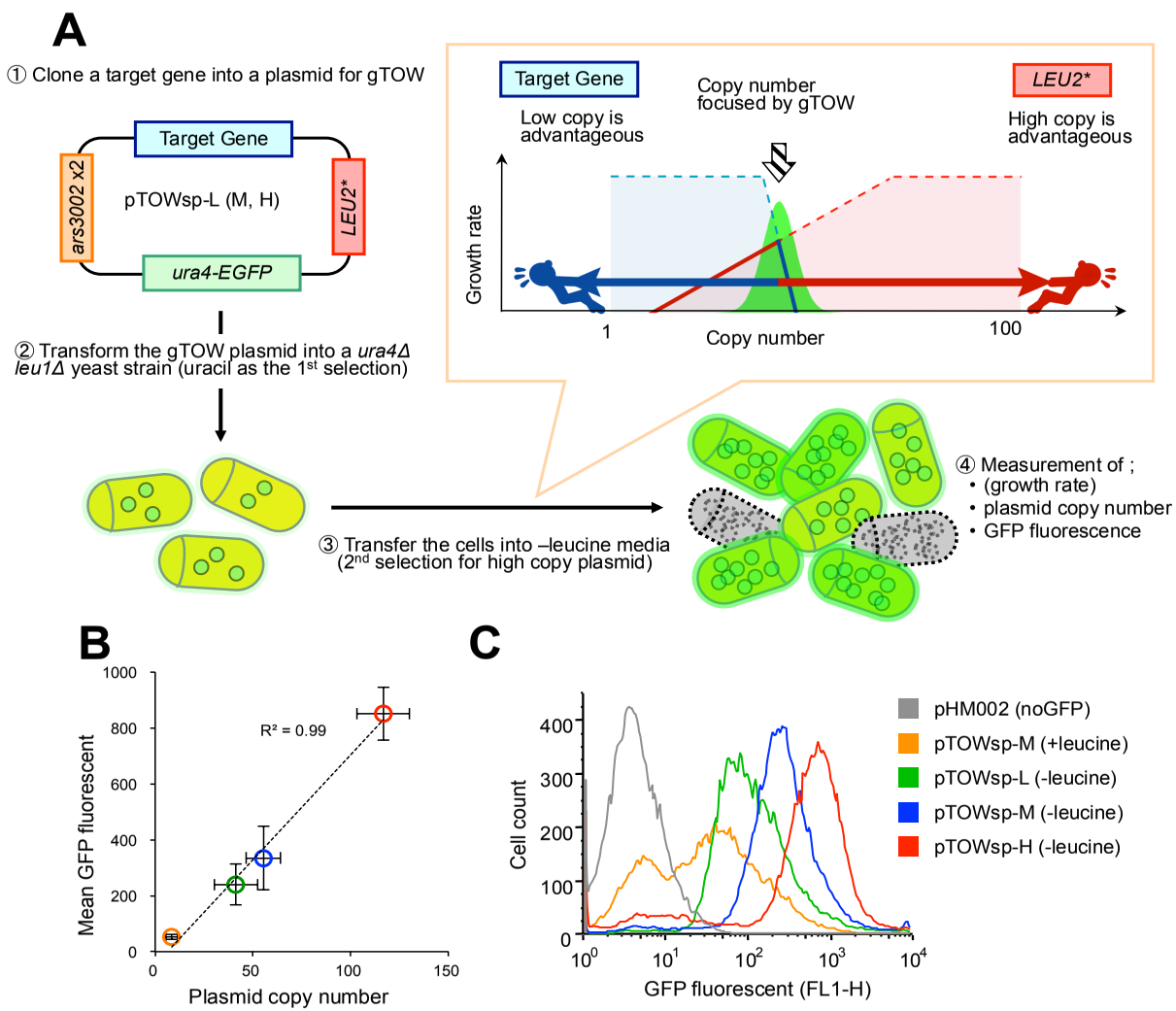

Figure 3.6-5. gTOW in *Sc. pombe*

(A) The four steps in the gTOW experiment. (1) Each target gene is cloned into a plasmid for gTOW. (2) The plasmid is introduced into the *leu1Δ ura4Δ* cell (first selection is uracil). The plasmid copy number becomes 10 per cell due to *ars3002X2* ORI. If the copy number limit of the target gene < 10 per cell, then the plasmid copy number is determined according to the limit. (3) The cells are transferred into –leucine media. In this condition, cells with a high plasmid copy number are selected according to the strength of expression of the leucine synthesizing enzyme gene *LEU2*. On the other hand, if the increase in the target gene (i.e., overexpression) is toxic to the cell, then the plasmid copy number must be less than the toxicity limit. The resulting tug-of-war of both selection biases determines the plasmid copy number within the cell, the number being close to the copy number limit of overexpression of the target gene. (4) To estimate the copy number limit of the target gene, the growth rate, GFP fluorescence of the cell, and the plasmid copy number within the cell are measured. In gTOW, the growth rate of the cell with the plasmid and the plasmid copy number within the cell should be mutually related (Moriya *et al.*, 2006). I observed this trend in *Sc. pombe*, but measuring growth rate with a microplate reader, as described previously (Moriya *et al.*, 2006), was unstable in this species. I thus cannot show the growth rate of the cell.
(B) Comparison of the plasmid copy number determined by real-time PCR with mean GFP fluorescence of the cell determined by flow cytometry. A linear correlation between the plasmid copy number and the GFP fluorescence is observed.
(C) Flow cytometric analysis of cellular distribution for each pTOW plasmid. pHM002 represents the control without GFP. In the +leucine condition, no difference is observed among pTOWsp-L, -M, and -H.

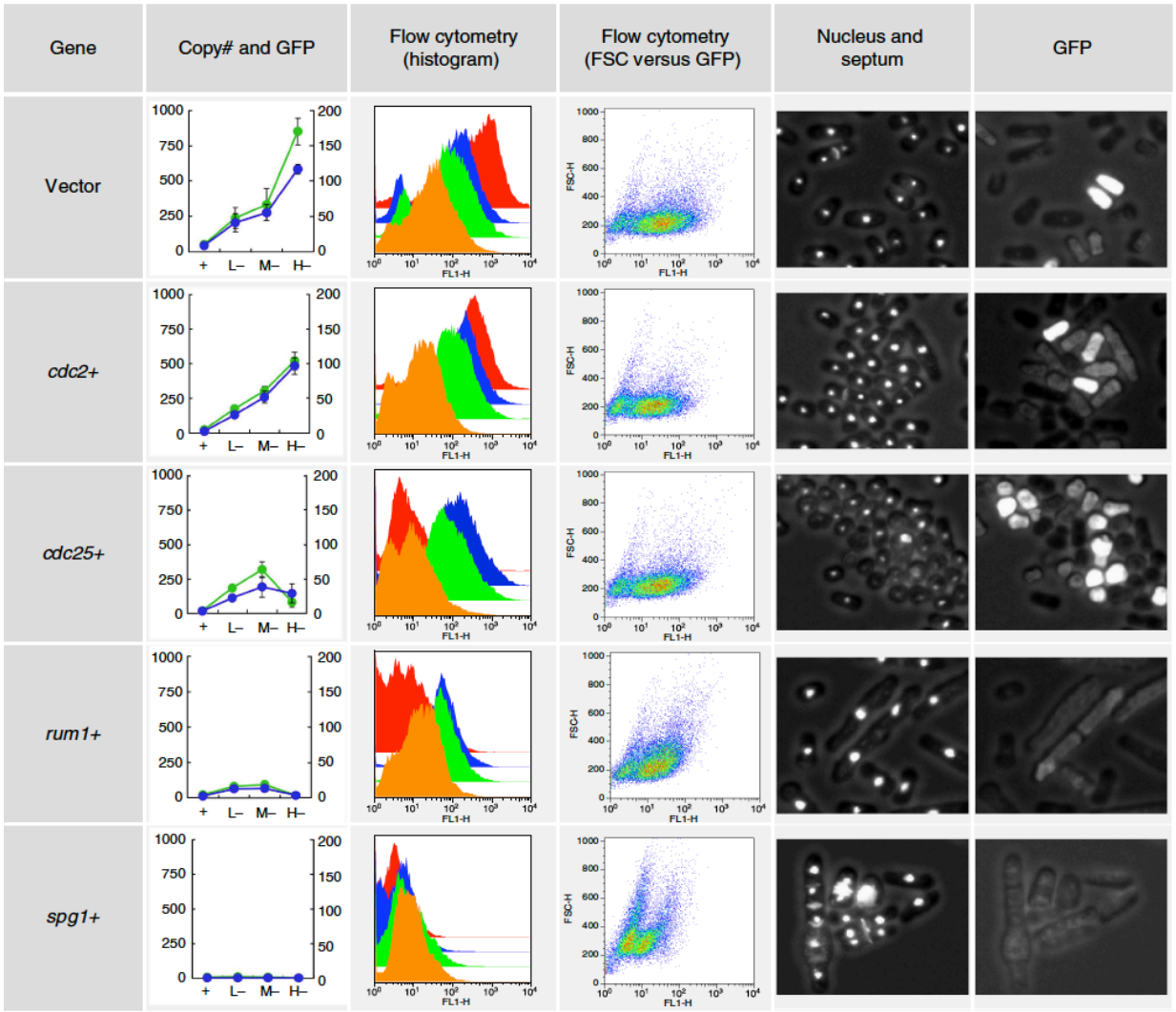

Figure 3.6-6. Examples of gTOW experiments with cell-cycle regulators in *Sc. pombe*

The experimental results obtained by gTOW with empty vector, *cdc2+*, *cdc25+*, *rum1+*, and *spg1+* are shown.

First column: The plasmid copy number (blue graph, right vertical axis) and the mean GFP fluorescence (green graph, left vertical axis) in gTOW in +leucine (indicated as '+') and −leucine with each vector (pTOWsp-L, -M, and -H) are shown (indicated as 'L−,' 'M−,' and 'H−,' respectively). The original data are shown in Tables 3-7 and 3-8.

Second column: Cell distribution with GFP fluorescence in gTOW experiments in +leucine (orange graph) and −leucine conditions with −L vector (green graph), −M vector (blue graph), and −H vector (red graph) are shown. Some experiments showed bimodality distributions. This is probably due to the plasmid loss, which is a property of the ars-based plasmid.

Third column: Scatter plot between GFP fluorescence (FL-1) and cell size (FSC). Cells were cultured in the +leucine condition.

Fourth column: Fluorescent microscopic image of the cells cultured in the +leucine condition. Nucleus and septum are stained.

Fifth column: GFP fluorescence of the cells in the fourth column. The brightness reflects the plasmid copy number within the cell. The whole data set of above analysis for the genes analyzed in this study is provided upon request.

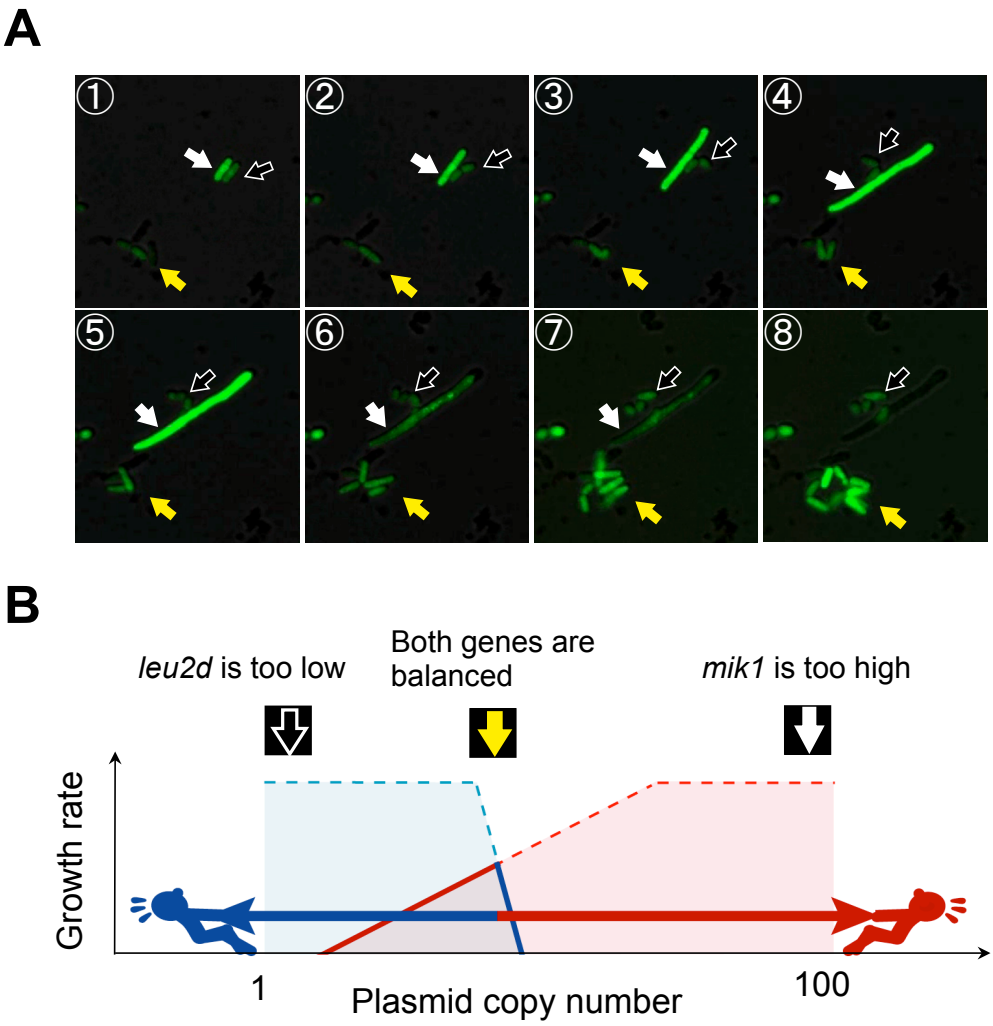

Figure 3.6-7. Time-laps observation of gTOW experiments with the target gene *mik1+*

(A) FY7052 cells harboring the pTOWsp-H plasmid with the mitotic CDK inhibitor *mik1+* were cultivated in EMM without leucine and were observed under fluorescent microscopy. The plasmid copy number in each cell was estimated from the intensity of GFP fluorescence. The black arrowhead with a white frame indicates a cell with very low plasmid copy number to synthesize a sufficient amount of leucine to support growth. The cell stops proliferating after the second cell division (frame 6). The white arrowhead indicates a cell with a sufficiently high plasmid copy number to synthesize enough leucine to support rapid cellular growth, but this number is beyond the copy number limit of *mik1+*. The cell thus cannot divide, becomes elongated (frames 3–5), and eventually dies (frame 6). The yellow arrowhead indicates cells with balanced plasmid copy number; the cells can grow and divide because they synthesize sufficient leucine. Cells with a plasmid copy number close to the limit of *mik1+* thus become concentrated during cultivation.
(B) Assumed cellular situations in gTOW experiment are shown (A).

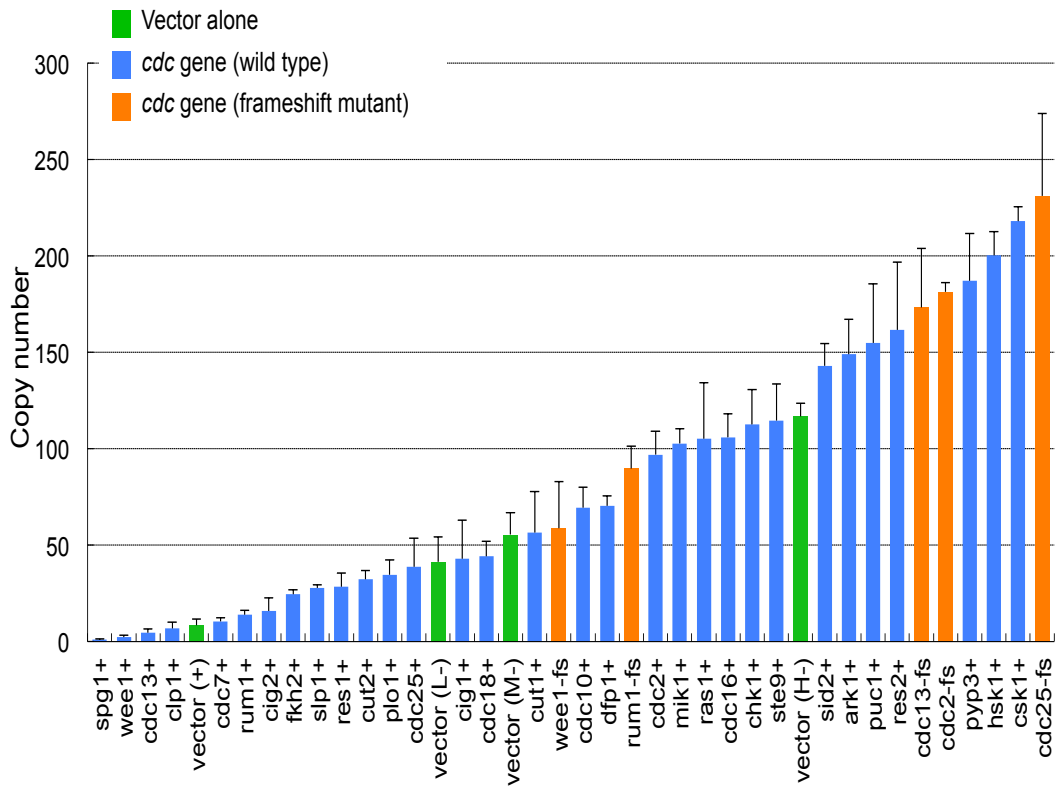

Figure 3.6-8. Copy number limits of 30 cell-cycle regulators in *Sc. pombe*

The green bar indicates the plasmid copy number obtained in the gTOW experiment with each vector. The blue bar indicates the maximum plasmid copy number for each target gene obtained in the gTOW experiment with three different vectors. The orange bar indicates the maximum plasmid copy number for each target gene with frameshift mutation. The original data are shown in Table 3.5-7. Because the cell has an endogenous copy of the target gene, the copy number limit for the target gene is the plasmid copy number plus 1.

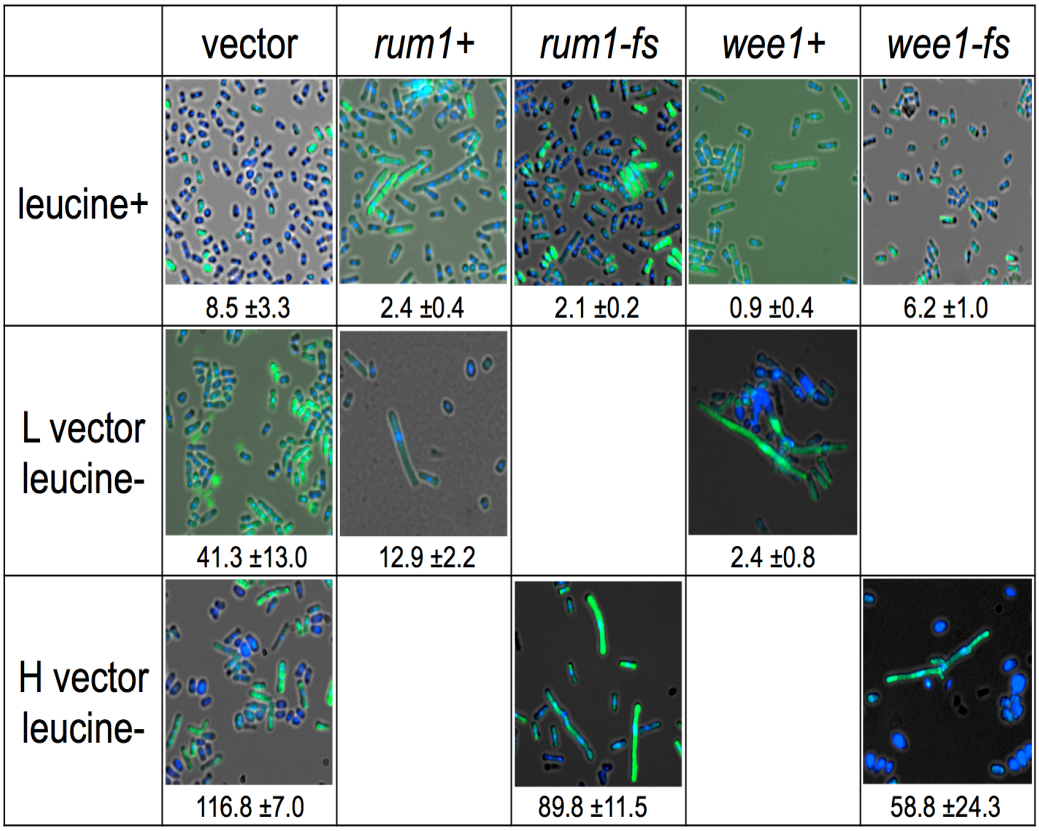

Figure 3.6-9. Frameshift mutants of *rum1* and *wee1* are leaky

Cells harboring pTOW plasmid with the indicated gene were cultured in –leucine condition. GFP fluorescence, nucleus, and septum were observed as shown in Figure 3.6-6.

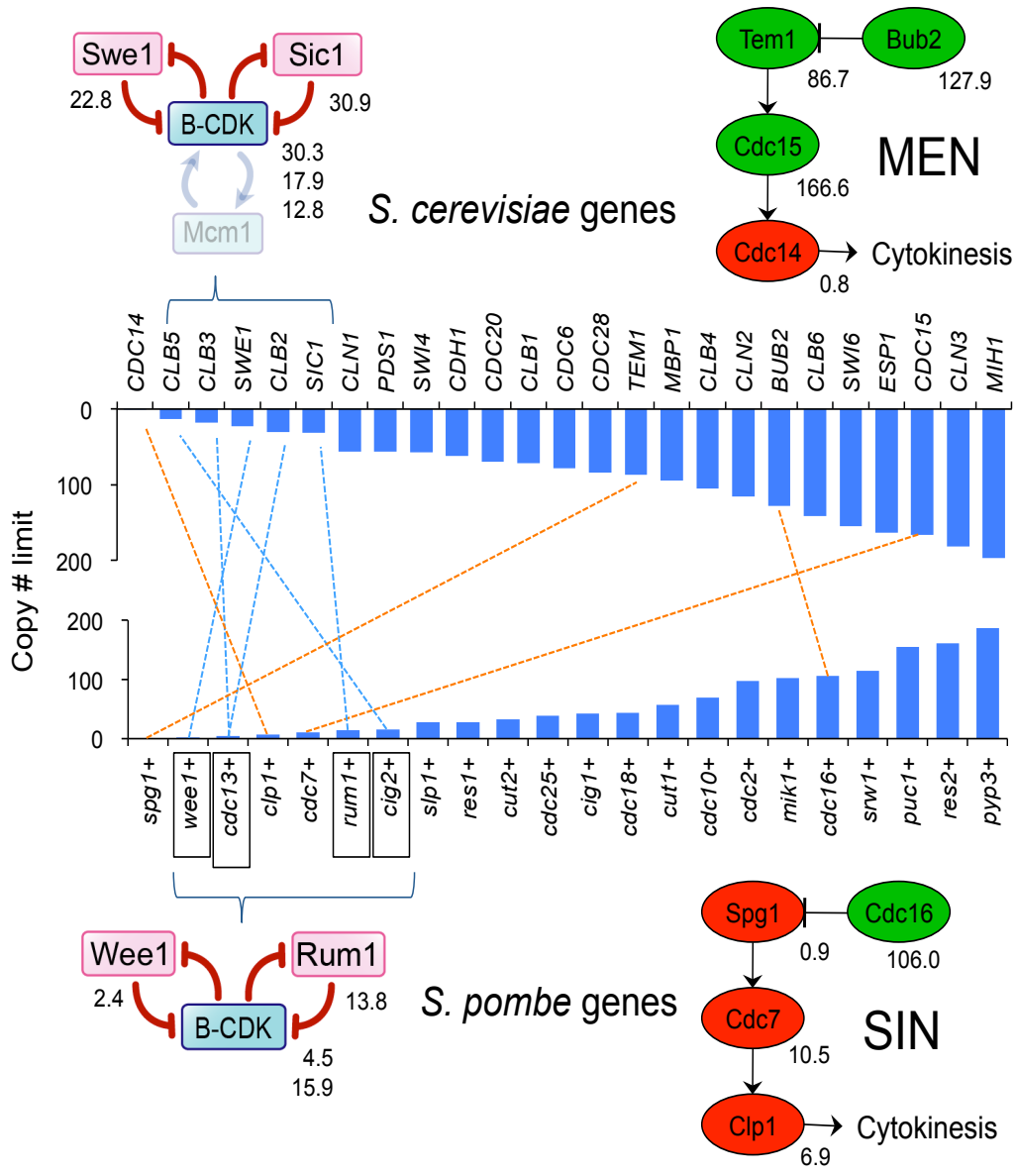

Figure 3.6-10. Comparison of robustness profiles of cell-cycle regulation between *Sa. cerevisiae* and *Sc. pombe*

The dotted blue line connects the functional orthologs within the "fragile core" conserved in both yeasts (left). The dotted orange line connects the functional orthologs involved in the cytokinesis regulatory pathway of both yeasts (MEN and SIN). Some components involved in both MEN and SIN are omitted from the diagrams because their copy number limits were not measured. Data for *Sa. cerevisiae* are obtained from a previous study (Moriya *et al.*, 2006). The original data are shown in Table 3.5-9.

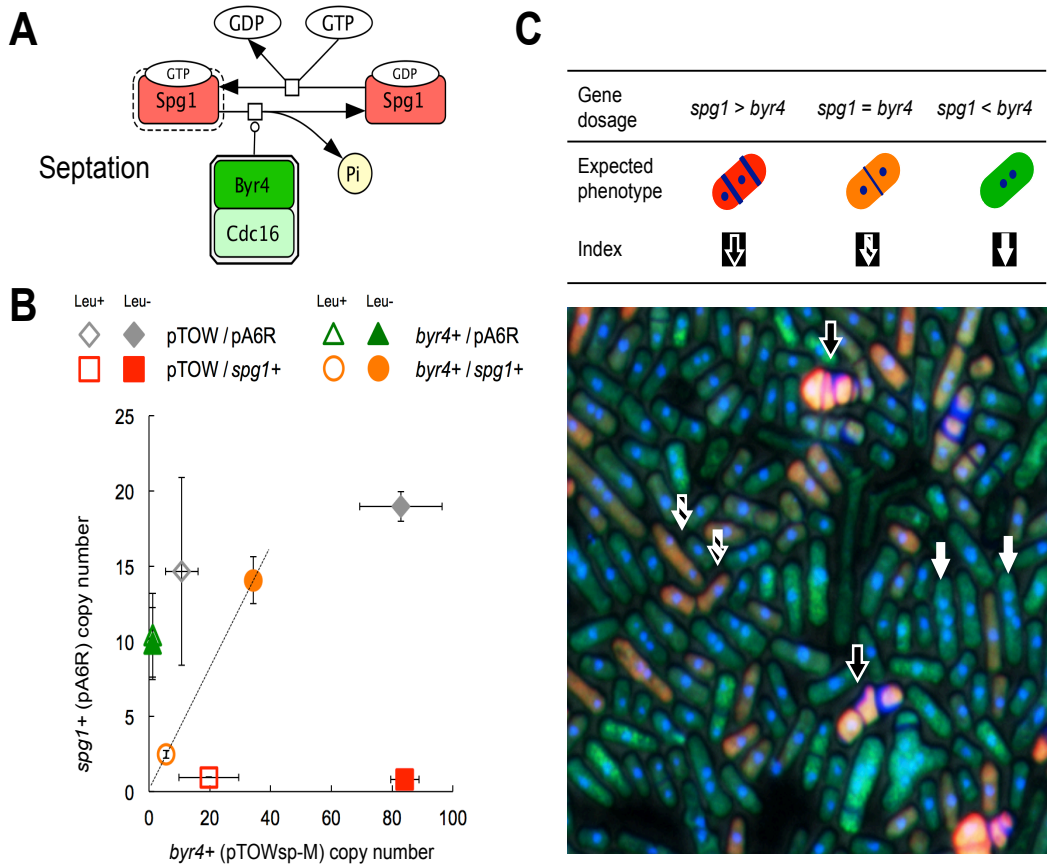

Figure 3.6-11. Very low limit of *spg1* is brought about by the dosage imbalance against *byr4*

(A) To trigger cellular septation, GTPase Spg1 and its GAP Byr4 function in an antagonistic fashion. The molecular interactions are given with Systems Biology Graphical Notation (SBGN) using CellDesigner 4.1 (www.celldesigner.org).

(B) Two-dimensional overproduction (2Dop) gTOW experiment between *spg1* and *byr4*. The copy numbers of *spg1* and *byr4* can be increased only when both gene copy numbers are balanced (dotted line). Extra copies of *spg1*+ are supplied by the pA6R plasmid, and extra copies of *byr4*+ are supplied by the pTOWsp-M plasmid.

(C) Microscopic image of cells by 2Dop gTOW experiment involving *spg1* and *byr4*. Sp286h+ cells with pTOWsp-M with *byr4* and pA6R with *spg1* were cultivated in EMM with leucine. GFP (reflecting the *byr4* copy number), RFP (reflecting the *spg1* copy number), the nucleus, and the septum were observed. Expected phenotypes of the cells within the dosage balance between *spg1* and *byr4*, and the indices within the image are shown.

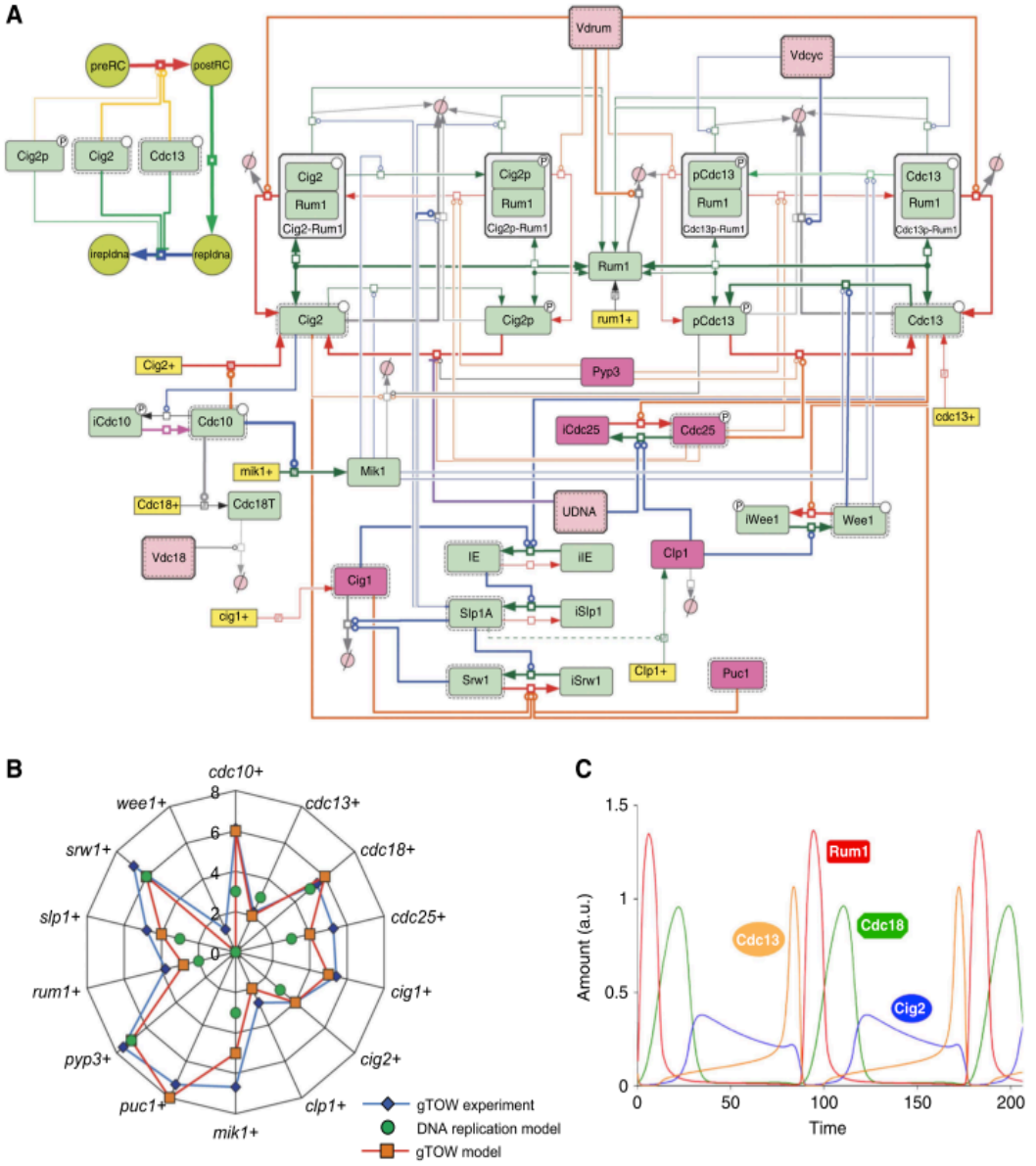

Figure 3.6-12. Mathematical model reproducing gTOW data

(A) Whole structure of the mathematical model of the fission yeast cell cycle developed in this study (gTOW model) given with Systems Biology Graphical Notation (SBGN) using CellDesigner 4.1. Pink colored components are the ones added to the 'basic model' to make the 'gTOW model'.
(B) Comparison of the copy number limits of cell-cycle regulators between the data obtained by gTOW and prediction of the mathematical model. Scale of the axis = log2.
(C) Time-course simulation result of the gTOW model.

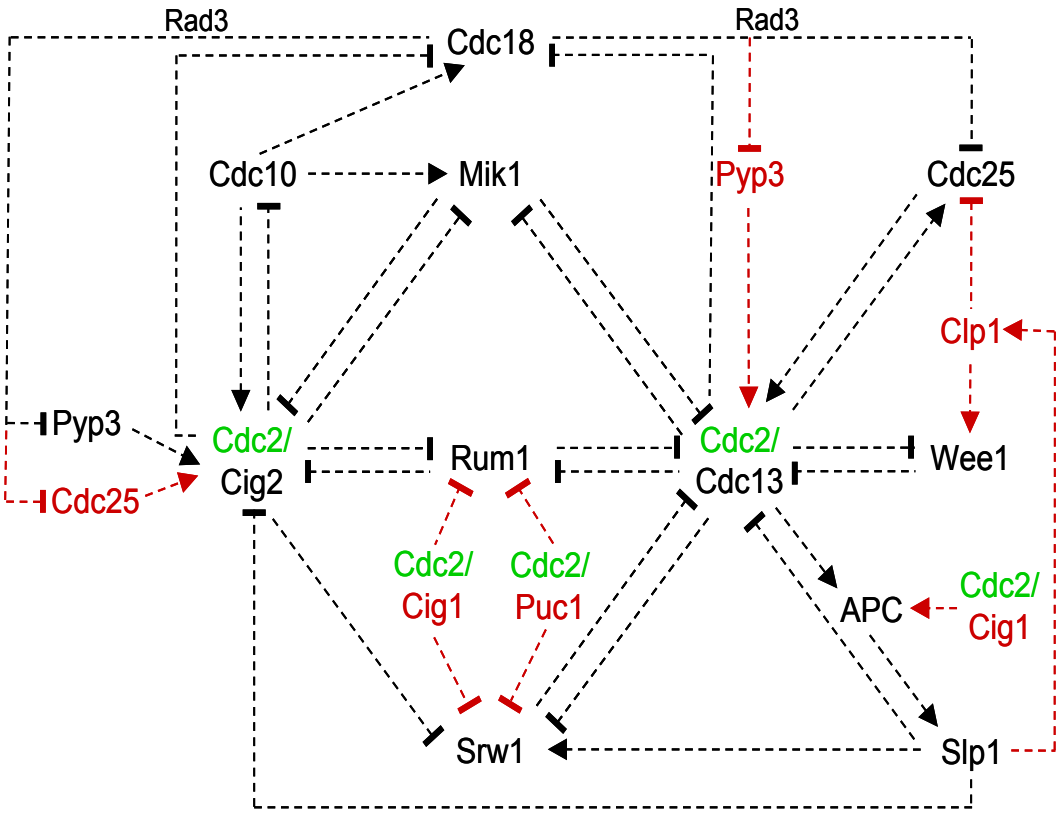

Figure 3.6-13. Regulatory interactions among cell cycle regulators in the fission yeast cell cycle control network

Arrows and blocked end lines represent stimulation of synthesis (or activation) and repression of synthesis (or inhibition). Black letters and arrows represent components and interaction in the original "basic model". Red colors show the additions to the "gTOW model", while the green Cdc2 signs show that Cdc2 explicitly appears only in the extended "Cdc2-level model".

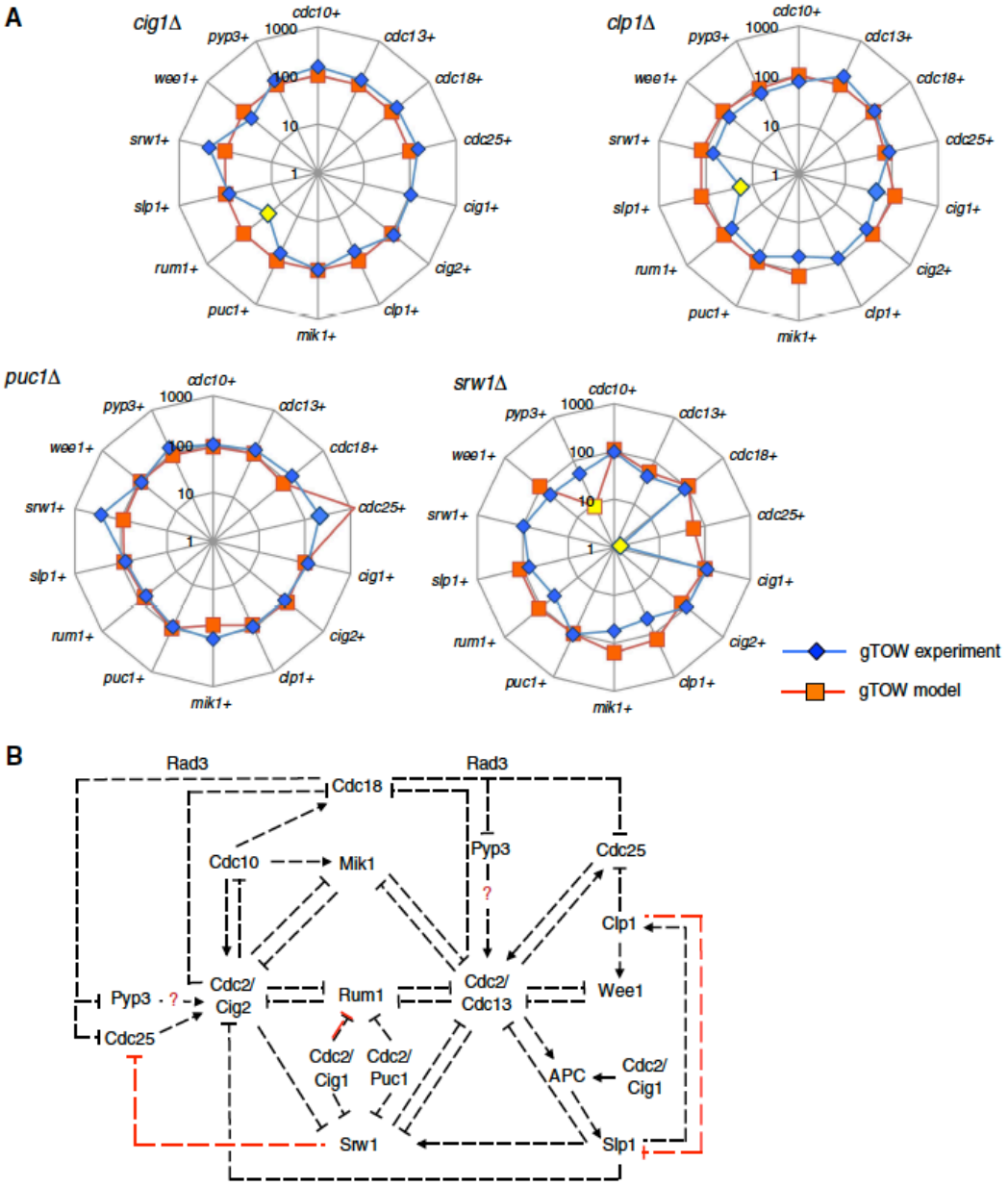

Figure 3.6-14. Testing the gTOW model with 2Ddelta-gTOW

(A) Comparison of upper limits of cell-cycle regulators in *clp1Δ*, *cig1Δ*, *puc1Δ*, and *srw1Δ* strains between the model prediction (orange) and experimental data (blue). The percentage of mutant/wild type is shown. Yellow marker indicates that the upper limit in the mutant strain is significantly less than the wild type (copy number < 30% and P-value < 0.05). The large discrepancy between the model and experiment in the upper limit of *pyp3+* in the *srw1Δ* is also shown in yellow marker. The complete experimental data set is shown in Table 3.5-10.

(B) Regulatory interactions among cell-cycle regulators in the fission yeast cell-cycle control network mathematically reconstituted in the gTOW model. Arrows and blocked end lines represent the simulation of synthesis (or activation) and repression of synthesis (or inhibition). Red lines indicate the potential novel regulations proposed by comparison of the gTOW model and 2Ddelta-gTOW data shown in (A). Red question marks refer the regulations with uncertain strengths in the model. Possible mechanisms for these regulations are described in Discussion.

Chapter 4

Correlation between protein levels and gene copy numbers of the cell-cycle regulators in *Sc. pombe*

4.1 Background

The cell cycle is a series of events that lead to cellular duplication. The engine of the eukaryotic cell cycle is the regulation of the activity of cyclin-dependent protein kinase (CDK). In the cell cycle, there are multiple feedback loops that precisely govern each event, including cell growth, DNA replication, and chromosome separation (Sveiczer *et al.*, 2000; Ayte *et al.*, 2001; Moriya *et al.*, 2006; Aligianni *et al.*, 2009; Kaizu *et al.*, 2010; Lu *et al.*, 2012).
Using gTOW, I measured the copy number limits of 31 cell-cycle regulator genes in the fission yeast (Chapter 3). The limits ranged from <2 copies to >100 copies.

A major drawback of gTOW is that the amount of protein expressed from the target gene may not be linearly correlated with the copy number. On the other hand, if there is inconsistency between the copy number and protein amount, regulation within the gene expression system is suggested. If there is a strong negative feedback regulation within the gene expression system, the protein amount will not increase with the increase in copy number, whereas if there is a positive feedback regulation, the protein amount will dramatically increase with the increase in copy number.

In this study, I attempted to measure protein amounts with the increase in copy number in gTOW and to uncover possible feedback in fission yeast cell cycle regulation.

4.2 Materials and Method

4.2.1 Strains and plasmids used in this study

The plasmids and yeast strains used in this study are listed in Table 4.5-1 and Table 4.5-2, respectively. TAP plasmids and TAP strains were constructed as shown in Figure 4.6-1. All primers used to construct plasmids and strains are listed in Tables 4-3 through 4-6. For each construct, two DNA fragments were amplified by polymerase chain reaction (PCR) with primers OHM844 and Up-tag and OHM845 and Down-tag using corresponding pTOWsp-M-target plasmid (Chapter 3) as a template. A TAPtag-*KanMX* cassette, which was constructed from pKT232 (Sheff and Thorn, 2004) and pTOWug2-ESP1-TAP (Moriya *et al.*, 2006; Kaizu *et al.*, 2010), was amplified by PCR with primers OHM179 and OHM182. All three DNA fragments were combined by GRC in *Sc. pombe* as described in Chapter 2. This procedure also removes the unnecessary *his5MX* gene from the vector, leading to a vector backbone identical to pTOWspd5-M. Each constructed plasmid was recovered from the *Sc. pombe* cells and the structure was checked by restriction enzyme digestion and partial sequencing. To construct TAP strains, the TAP-*KanMX* cassette containing parts of the coding region of the target gene and the 3′ region for homologous recombination was amplified by PCR with primers Up-int and OSBI870 using corresponding TAP plasmid as a template and introduced into *Sc. pombe* cells to integrate the cassette into the genomic region of the target gene. G418 (final conc. 150 mg/mL) was used for the selection of *KanMX*. The genomic integration of TAP-*KanMX* was checked by PCR.

4.2.2 Growth media, culture conditions, and DNA methods

Cultivation of *Sc. pombe* cells, transformation of yeast, yeast DNA isolations (yeast DNA miniprep), and DNA miniprep from *E. coli* were performed as described in Chapter 2 and 3.

4.2.3 Measurement of plasmid copy number and TAP-tagged protein level

The sample preparation scheme to measure plasmid copy numbers and protein amounts is shown in Figure 4.6-2. Each TAP strain with the empty vector or corresponding TAP plasmid was cultured in 6 mL Edinburgh minimal medium (EMM) with leucine (for 24 h) or without leucine (for 48 h). Each sample (200 μL) was used to measure the plasmid copy number using real-time PCR as described in Chapter 3. An aliquot of 2.5 mL (+leucine) or 5.0 mL (−leucine) of the preculture was transferred into 10 mL of the fresh EMM medium, so that the optical density at 600 nm (OD_{600}) became approximately 0.5. After 6 h cultivation, cells of 4 OD_{600} (i.e., if the OD600 was 1.0, cells were collected from 4 mL culture) were collected. The proteins in the cells were extracted by treating the cell with 0.3 N NaOH for 10 min and separated by SDS polyacrylamide gel electrophoresis (NuPage 4-12% Bis-Tris Gel, Invitrogen). We performed two electrophoresis for each sample. One gel was stained with Coomassie® G-250 (SimplyBlue™ SafeStain, Invtrogen), and the other gel was subjected to Western blotting using peroxidase-antiperoxidase (P19011; Sigma-Aldrich) as described previously (Moriya *et al*, 2006; Kaizu *et al*, 2010). The density of a 50 kDa band (corresponding to the size of tubulin) of each sample was measured from the scanned Coomassie-stained gel using the gel analysis option of ImageJ 1.44o software to estimate the total protein amount for normalization. The intensity of the corresponding protein band in each Western blot was measured using an LAS-4000 image analyzer (Fujifilm/GE Healthcare), and data within the linear detection range among the serial dilutions of the samples were used. The fold increase in protein level upon the increase of the copy number was then calculated as; *Dilution* × (*TAPint_TAPplasmid* / *TAPint_vector*) / (*Coom_TAPplasmid* / *Coom_vector*). *Dilution* indicates the fold dilution of the sample. *TAPint_TAPplasmid* and *Coom_TAPplasmid* indicate the intensity of detected TAP-tagged protein and that of the Coomassie-stained 50 kDa protein of the sample with the TAP plasmid. *TAPint_vector* and *Coom_vector* indicate the intensities in the sample with the empty vector.

4.3 Results

4.3.1 Construction of plasmids and yeast strains used to measure protein amounts

As the targets of this study, I chose 31 cell-cycle regulators that I had analyzed by gTOW in Chapter 3 (listed in Table 4.5-7). Because specific antibodies against most of the cell-cycle regulators were not available, I used tandem affinity purification (TAP) to detect the target proteins (Rigaut *et al.*, 1999). I constructed C-terminally TAP-tagged cell-cycle regulator genes on the gTOW plasmid, pTOWspd5-M (the plasmid construction procedure is shown in Figure 4.6-1). We have gTOW vectors with three different maximum plasmid copy numbers, but here I chose the "middle" vector because it covers the widest range of limit copy numbers (see Chapter 3). Figure 4.6-3A shows the general structure of the plasmid used in this study. Each tagged-target protein is expressed from its native promoter, but its terminator is not a native one (the terminator of the *ADH1* gene from *Sa. cerevisiae*). I attempted to construct 31-tagged genes but failed to construct those of *spg1* and *wee1*, probably owing to their high toxicity in *Sc. pombe* cells (see Chapter 3). Here I designate these plasmids TAP plasmids. Because C-terminal TAP-tagging might affect the activity of the target proteins, I indirectly evaluated their activities by measuring the copy number limits of tagged genes and compared them with those of native genes. As shown in Figure 4.6-4, the tagged gene and the native gene showed similar copy number limits overall (Pearson's $r = 0.65$). However, the tagged genes of *dfp1* and *slp1* showed increased copy number limits, suggesting that their activities were reduced. In contrast, the tagged genes of *cut1*, *puc1*, *res1*, and *rum1* showed reduced copy number limits, suggesting that their activities were increased. I did not study *slp1* any further because its activity seemed to be disrupted.

I next replaced each target gene on the *Sc. pombe* chromosome with the same TAP-tagged gene in the plasmid, so that the target protein expressed from one copy of the target gene was detected (the construction procedure is shown in Figure 4.6-1). I could not obtain a *cut1-TAP* strain, possibly because C-terminal

TAP-tagging changed the activity of Cut1 as described above (Table 4.5-7). I also could not obtain *cdc13-TAP*, *res1-TAP*, or *res2-TAP* strains, for unknown reasons (Table 4.5-7). Here I designate these yeast strains TAP strains.

4.3.2 Quantification of proteins expressed from high-copy plasmids

I next measured each TAP-tagged cell-cycle regulators expressed in the TAP strains with the empty vector or the TAP plasmid cultivated in the medium with or without leucine using quantitative Western blotting. The aim of this study was not to quantify the absolute amount of the target protein, but to measure the fold increase in the protein amount expressed from the TAP plasmid over that expressed from the genomic copy (a single copy). To avoid the saturation of quantification in Western blotting, I performed a serial dilution of the protein expressed in the strain with TAP plasmid. The results of the measurements are shown in Figure 4.6-5. I could not detect TAP-tagged Cdc13, Res1, Res2, or Srw1 expressed from their TAP plasmids, although the plasmid constructions were confirmed. I also could not detect TAP-tagged Cdc2, Dfp1, Puc1, and Srw1 expressed in their TAP strains. The reason for these failures is unknown. Some of these proteins may have expression levels below the detection range of Western blotting. I succeeded in measuring the amounts of 20 cell-cycle regulator-TAP proteins as summarized in Table 4.5-7.

To assess the reproducibility of the measurement, I performed control experiments using a truncated *pyp3*-TAP construct (Pyp3*-TAP). I fused a TAP tag just after the first exon of Pyp3 to create a fusion protein containing a part of Pyp3 (96 amino acids) of a total of 303 amino acids. Because most of the protein phosphatase domain of Pyp3 was removed by this procedure, I considered that this TAP-tagged protein possessed no activity and no feedback regulation. The result of one of four repetitive experiments with Pyp3*-TAP is shown in Figure 4.6-5. I simultaneously measured the copy number (CN) of TAP plasmid in the cell of each experiment and compared it with the fold increase in the protein level (protein increase: PI) measured as described above. I then calculated the PI/CN

ratio, which corresponds to the protein amount expressed from each copy of the gene when the gene copy number increases (Table 4.5-8). Figure 4.6-6 shows the relationship between the copy numbers and the protein increases. As expected, the protein amounts increased according to the increase in copy number in four control experiments with Pyp3*-TAP. The PI/CN ratios under the +leucine and −leucine condition were 2.94 (1.11) and 1.37 (0.63), respectively. For some genes, I could not analyze the −leucine condition because their copy number limits were too low for *leu2-89* to support growth under this condition (see Chapter 3).

As shown in Figure 4.6-6, overall in 20 cell-cycle regulator-TAP proteins analyzed, there was significant correlation between copy numbers and the fold increases in protein levels (Pearson's $r = 0.67$), suggesting that there is no general compensation for gene dosage in the expression of cell-cycle regulators in *Sc. pombe*. However, I also discovered variations between abundances of protein levels and gene copy numbers in some genes. For example, *cdc10* showed a high PI/CN ratio under both +leucine and −leucine conditions (7.03 and 9.20, respectively), and *cdc16* showed a low PI/CN ratio under both conditions (0.38 and 0.28, respectively) (Figure 4.6-5 and Table 4.5-8). These results suggest the existence of feedback regulations in the expression of these genes.

4.4 Discussion

In this study, using gTOW and quantitative Western blotting with TAP-tagged protein, I measured protein amounts when the copy numbers of their genes were increased. I found several genes showing mismatches between their copy numbers and the fold increases in their proteins. These mismatches appear to reflect the operation of feedback regulation within the expression systems of these genes. The expression system of *cdc10*, whose protein was greatly increased relative to its copy number (Figure 4.6-5 and Figure 4.6-6), appears to include positive feedback regulation. *cdc10* encodes a component of a transcription factor called MBF (*Mlu*I cell cycle box binding factor) that activates transcription during the G1/S transition and is in fact known to exert positive feedback by activating its own transcription (Aligianni *et al.*, 2009). Finding of this study thus supports the existence of positive feedback and correspondingly supports the feasibility of our approach to find feedback mechanisms in gene expression systems.

The methodology used in this study, i.e., measuring a protein amount when its gene copy number is increased by gTOW, was effective for uncovering the operation of feedback regulation in the expression systems of target genes. On the other hand, protein amounts and copy numbers showed a roughly linear correlation (Figure 4.6-6). Moryia *et al*. (2006) previously obtained a similar result in budding yeast (2006). In budding yeast, a general lack of compensation for gene dosage was suggested by protein measurement in heterozygous deletion mutants (Springer *et al.*, 2010). These results together indicate that there is no buffering/compensatory mechanism responding to a change in gene copy number in yeasts.

4.5 Tables

Table 4.5-1. Plasmids

Name	Description	Source
pTOWspdh5-M	*ColE1ori*, *AmpR*, *ars3002x2*, *ura4-EGFP*, *leu2-89*	Moriya, 2012
pTOW-ark1T	pTOWspdh5-M containing *ark1-TAP-KanMX4*	This study
pTOW-cdc7T	pTOWspdh5-M containing *cdc7-TAP-KanMX4*	This study
pTOW-cdc10T	pTOWspdh5-M containing *cdc10-TAP-KanMX4*	This study
pTOW-cdc13T	pTOWspdh5-M containing *cdc13-TAP-KanMX4*	This study
pTOW-cdc16T	pTOWspdh5-M containing *cdc16-TAP-KanMX4*	This study
pTOW-cdc18T	pTOWspdh5-M containing *cdc18-TAP-KanMX4*	This study
pTOW-cdc25T	pTOWspdh5-M containing *cdc25-TAP-KanMX4*	This study
pTOW-chk1T	pTOWspdh5-M containing *chk1-TAP-KanMX4*	This study
pTOW-cig1T	pTOWspdh5-M containing *cig1-TAP-KanMX4*	This study
pTOW-cig2T	pTOWspdh5-M containing *cig2-TAP-KanMX4*	This study
pTOW-clp1T	pTOWspdh5-M containing *clp1-TAP-KanMX4*	This study
pTOW-csk1T	pTOWspdh5-M containing *csk1-TAP-KanMX4*	This study
pTOW-cug2T	pTOWspdh5-M containing *cut2-TAP-KanMX4*	This study
pTOW-fkh2T	pTOWspdh5-M containing *fkh2-TAP-KanMX4*	This study
pTOW-hsk1T	pTOWspdh5-M containing *hsk1-TAP-KanMX4*	This study
pTOW-mik1T	pTOWspdh5-M containing *mik1-TAP-KanMX4*	This study
pTOW-plo1T	pTOWspdh5-M containing *plo1-TAP-KanMX*4	This study
pTOW-ras1T	pTOWspdh5-M containing *ras1-TAP-KanMX4*	This study
pTOW-rum1T	pTOWspdh5-M containing *rum1-TAP-KanMX4*	This study
pTOW-sid2T	pTOWspdh5-M containing *sid2-TAP-KanMX4*	This study
pTOW-pyp3T	pTOWspdh5-M containing *pyp3-TAP-KanMX4*	This study
pTOW-mik1kdT	pTOWspdh5-M containing *mik1kd-TAP-KanMX4*	This study

Table 4.5-2. Strains

Name	Genotype	Source
FY7652	*h- leu1-32 ura4-D18*	NBRPyeast
AC0001	*h- leu1-32 ura4-D18 ark1::ark1-TAP-KanMX4*	This study
AC0002	*h- leu1-32 ura4-D18 cdc7::cdc7-TAP-KanMX4*	This study
AC0003	*h- leu1-32 ura4-D18 cdc10::cdc10-TAP-KanMX4*	This study
AC0004	*h- leu1-32 ura4-D18 cdc13::cdc13-TAP-KanMX4*	This study
AC0005	*h- leu1-32 ura4-D18 cdc16::cdc16-TAP-KanMX4*	This study
AC0006	*h- leu1-32 ura4-D18 cdc18::cdc18-TAP-KanMX4*	This study
AC0007	*h- leu1-32 ura4-D18 cdc25::cdc25-TAP-KanMX4*	This study
AC0008	*h- leu1-32 ura4-D18 chk1::chk1-TAP-KanMX4*	This study
AC0009	*h- leu1-32 ura4-D18 cig1::cig1-TAP-KanMX4*	This study
AC0010	*h- leu1-32 ura4-D18 cig2::cig2-TAP-KanMX4*	This study
AC0011	*h- leu1-32 ura4-D18 clp1::clp1-TAP-KanMX4*	This study
AC0012	*h- leu1-32 ura4-D18 csk1::csk1-TAP-KanMX4*	This study
AC0013	*h- leu1-32 ura4-D18 cut2::cut2-TAP-KanMX4*	This study
AC0014	*h- leu1-32 ura4-D18 fkh2::fkh2-TAP-KanMX4*	This study
AC0015	*h- leu1-32 ura4-D18 hsk1::hsk1-TAP-KanMX4*	This study
AC0016	*h- leu1-32 ura4-D18 mik1::mik1-TAP-KanMX4*	This study
AC0017	*h- leu1-32 ura4-D18 plo1::plo1-TAP-KanMX4*	This study
AC0018	*h- leu1-32 ura4-D18 ras1::ras1-TAP-KanMX4*	This study
AC0019	*h- leu1-32 ura4-D18 rum1::rum1-TAP-KanMX4*	This study
AC0020	*h- leu1-32 ura4-D18 sid2::sid2-TAP-KanMX4*	This study
AC0021	*h- leu1-32 ura4-D18 pyp3::pyp3-TAP-KanMX4*	This study
AC0022	*h- leu1-32 ura4-D18 mik1::mik1kd-TAP-KanMX4*	This study
AC0023	*h- leu1-32 ura4-D18 pyp3::pyp3*-TAP-KanMX4*	This study

Table 4.5-3. "Up-tag" primers to construct TAP plasmids

	Gene	Name	Sequence (5' to 3')
1	*ark1*	OHM27	TATCCTCCTCGCCCTTGCTCACCATATGGGAAGATTCAGAACTTTTGC
2	*cdc2*	OHM29	TATCCTCCTCGCCCTTGCTCACCATATGATGAAAATCACGAAGATAAT
3	*cdc7*	OHM31	TATCCTCCTCGCCCTTGCTCACCATATGCTGCGTTAATGGCTGCTTTG
4	*cdc10*	OHM33	TATCCTCCTCGCCCTTGCTCACCATATGTGCTTGATGTTCTTTAACAA
5	*cdc13*	OHM35	TATCCTCCTCGCCCTTGCTCACCATATGCCATTCTTCATCTTTCATGT
6	*cdc16*	OHM37	TATCCTCCTCGCCCTTGCTCACCATATGTGTTAGTCGGTCAATCAGAA
7	*cdc18*	OHM39	TATCCTCCTCGCCCTTGCTCACCATATGTCTTCTGTCAAAAAATCGTT
8	*cdc25*	OHM41	TATCCTCCTCGCCCTTGCTCACCATATGAAATCTTCTAAGTGTAGAGA
9	*chk1*	OHM43	TATCCTCCTCGCCCTTGCTCACCATATGATTTTGTGAAACATCTGTAA
10	*cig1*	OHM45	TATCCTCCTCGCCCTTGCTCACCATATGAATCACACTTAGTACCCAGT
11	*cig2*	OHM47	TATCCTCCTCGCCCTTGCTCACCATATGGTGACCATCATTTGTTAAAG
12	*clp1*	OHM49	TATCCTCCTCGCCCTTGCTCACCATATGAGAAATTAGCCGGCTTTTAG
13	*csk1*	OHM51	TATCCTCCTCGCCCTTGCTCACCATATGTGCATATTGTGAAAGCCTAG
14	*cut1*	OHM53	TATCCTCCTCGCCCTTGCTCACCATATGTGGAATAATATAAGCAGGTAT
15	*cut2*	OHM55	TATCCTCCTCGCCCTTGCTCACCATATGTAACAATCCTGTATCCAAAG
16	*dfp1*	OHM57	TATCCTCCTCGCCCTTGCTCACCATATGATCTGGCCTTAAGGGACGTT
17	*fkh2*	OHM59	TATCCTCCTCGCCCTTGCTCACCATATGAGCACTACTTTTAACATTAGA
18	*hsk1*	OHM61	TATCCTCCTCGCCCTTGCTCACCATATGAGCTCCATCCTGCAAAGCATC
19	*mik1*	OHM63	TATCCTCCTCGCCCTTGCTCACCATATGAGTTTCTAACCAACTGTTATG
20	*plo1*	OHM65	TATCCTCCTCGCCCTTGCTCACCATATGACTCACTTCCATTTTCGACG
21	*puc1*	OHM67	TATCCTCCTCGCCCTTGCTCACCATATGCAAAGTACGCTCAGTATCCT
22	*ras1*	OHM69	TATCCTCCTCGCCCTTGCTCACCATATGACATATAACACAACATTTAG
23	*res1*	OHM71	TATCCTCCTCGCCCTTGCTCACCATATGAGATCCACTTTGATCTGTAT
24	*res2*	OHM73	TATCCTCCTCGCCCTTGCTCACCATATGTTTTTCTCGGGTTAATG
25	*rum1*	OHM75	TATCCTCCTCGCCCTTGCTCACCATATGTCGTAATAAATTGTGCCTGT
26	*sid2*	OHM77	TATCCTCCTCGCCCTTGCTCACCATATGTAATAGAGTCCCGAAAGAAGGAG
27	*slp1*	OHM79	TATCCTCCTCGCCCTTGCTCACCATATGACGGATTGTTATGCTGCTGG

28	*spg1*	OHM81	TATCCTCCTCGCCCTTGCTCACCATATGGCGATCGATGTATTCCAAAAT
29	*srw1*	OHM83	TATCCTCCTCGCCCTTGCTCACCATATGCCGTATTTTCATTGTAGGGT
30	*wee1*	OHM85	TATCCTCCTCGCCCTTGCTCACCATATGAACATTCACCTGCCAATCTT
31	*pyp3*	OHM87	TATCCTCCTCGCCCTTGCTCACCATATGTAACTGAGGAAGAAGAAATTC
32	*dnt1*	OHM89	TATCCTCCTCGCCCTTGCTCACCATATGCACTAGGGCCGCCAAGCCA
33	*byr4*	OHM91	TATCCTCCTCGCCCTTGCTCACCATATGTTGTTCGGCATTAAGTATAT

Table 4.5-4. "Down-tag" primers to construct TAP plasmids

	Gene	Name	Sequence (5' to 3')
1	*ark1*	OHM28	CCGGCGGCATGGACGAGCTGTACAAGCTTTAACCGCCA TCTTGGTACTT
2	*cdc2*	OHM30	CCGGCGGCATGGACGAGCTGTACAAGCTTTAATTTTCGT CTCTTATTAT
3	*cdc7*	OHM32	CCGGCGGCATGGACGAGCTGTACAAGCTTTGAACACTA TTAAACGCATT
4	*cdc10*	OHM34	CCGGCGGCATGGACGAGCTGTACAAGCTTTAATATTGCT TTTTGTGGTT
5	*cdc13*	OHM36	CCGGCGGCATGGACGAGCTGTACAAGCTTTAATTTAGT GTATTGTGCAT
6	*cdc16*	OHM38	CCGGCGGCATGGACGAGCTGTACAAGCTTTAATACTAG GGTAGGGTTTT
7	*cdc18*	OHM40	CCGGCGGCATGGACGAGCTGTACAAGCTTTAGTACTAT CATTTCTTTCT
8	*cdc25*	OHM42	CCGGCGGCATGGACGAGCTGTACAAGCTTTAATGATTTT AGGCTGACTC
9	*chk1*	OHM44	CCGGCGGCATGGACGAGCTGTACAAGCTTTAATTGCAC ATCTTTTGAAA
10	*cig1*	OHM46	CCGGCGGCATGGACGAGCTGTACAAGCTTTGAGTTTGCT TTCAGAAGTT
11	*cig2*	OHM48	CCGGCGGCATGGACGAGCTGTACAAGCTTTAACGAACG CTCTTATAAAT
12	*clp1*	OHM50	CCGGCGGCATGGACGAGCTGTACAAGCTTTAATAAACC TGTAATTACTG
13	*csk1*	OHM52	CCGGCGGCATGGACGAGCTGTACAAGCTTTAAAATTTA CTCTCAGGATT
14	*cut1*	OHM54	CCGGCGGCATGGACGAGCTGTACAAGCTTTAAACTGTC TAAAATTCTTA
15	*cut2*	OHM56	CCGGCGGCATGGACGAGCTGTACAAGCTTTAAAAAGAT TCCGAATTTTC
16	*dfp1*	OHM58	CCGGCGGCATGGACGAGCTGTACAAGCTTTGAGAAAAT AGCCCGTGTCT
17	*fkh2*	OHM60	CCGGCGGCATGGACGAGCTGTACAAGCTTTAATGCCAA CAAATTCACCT
18	*hsk1*	OHM62	CCGGCGGCATGGACGAGCTGTACAAGCTTTGAGAAGAT TTGCTGGCAAT
19	*mik1*	OHM64	CCGGCGGCATGGACGAGCTGTACAAGCTTTGAGGGATT CTGTGTGCGAA
20	*plo1*	OHM66	CCGGCGGCATGGACGAGCTGTACAAGCTTTAATAATAC CGTTAATCTAT
21	*puc1*	OHM68	CCGGCGGCATGGACGAGCTGTACAAGCTTTAACTTTAA CATTGCTTCTT
22	*ras1*	OHM70	CCGGCGGCATGGACGAGCTGTACAAGCTTTAGCAAGTA TTATTGCAGAA
23	*res1*	OHM72	CCGGCGGCATGGACGAGCTGTACAAGCTTTAATTTTTTT GGTTTTAAAT
24	*res2*	OHM74	CCGGCGGCATGGACGAGCTGTACAAGCTTTGAATCTTG GAAACTTTCATTTA
25	*rum1*	OHM76	CCGGCGGCATGGACGAGCTGTACAAGCTTTAACTTTTTT TCGCATTTTG
26	*sid2*	OHM78	CCGGCGGCATGGACGAGCTGTACAAGCTTTAATCAAAG GGAAATTT

27	*slp1*	OHM80	CCGGCGGCATGGACGAGCTGTACAAGCTTTGAACAACA CCAGTTTCTTT
28	*spg1*	OHM82	CCGGCGGCATGGACGAGCTGTACAAGCTTTGATTTTTAA TGCTTTACCA
29	*srw1*	OHM84	CCGGCGGCATGGACGAGCTGTACAAGCTTTAATGCAAC ACATTCACTCT
30	*wee1*	OHM86	CCGGCGGCATGGACGAGCTGTACAAGCTTTAAACCTTTT AGAGACTCTT
31	*pyp3*	OHM88	CCGGCGGCATGGACGAGCTGTACAAGCTTTAGCCTTTG GTTTAGAGTTT
32	*dnt1*	OHM90	CCGGCGGCATGGACGAGCTGTACAAGCTTTAAATTTCTT GTTTTTGATTA
33	*byr4*	OHM92	CCGGCGGCATGGACGAGCTGTACAAGCTTTAAACAAGG TTTTGTCTTTA

Table 4.5-5. "Up-int" primers to construct TAP strains

	Gene	Name	Sequence (5' to 3')
1	*ark1*	OHM0183	GGTGGAGGGAAAAGAGCATA
2	*cdc2*	OHM0184	CCCGGTGACTCTGAGATCGAC
3	*cdc7*	OHM0185	AAAGAAAAGTTAACTCATAA
4	*cdc10*	OHM0186	ACTGTCAATGAAAACAACAA
5	*cdc13*	OHM0187	TACCTTGCCAGGGAAATGCT
6	*cdc16*	OHM0188	CCGAGAGCAGCTCATCGATC
7	*cdc18*	OHM0189	CTTCAACAGAAAGCCATCCT
8	*cdc25*	OHM0190	GACAGACGAATGAATAGTCA
9	*chk1*	OHM0191	GACAGTCTACGACTACTTGC
10	*cig1*	OHM0192	GCCAAATATCTTCAAGAAGT
11	*cig2*	OHM0193	GCTGCCGCAATGTATTTGAG
12	*clp1*	OHM0194	GATTCAGAAATACAAAATGA
13	*csk1*	OHM0195	GCAGGATCCGTTTACCTTAT
14	*cut1*	OHM0196	ACTACATTCAATCAACTGGA
15	*cut2*	OHM0197	ACAACACCCGCTACCTTGAA
16	*dfp1*	OHM0198	AGAGATATCGCAGAGTTGAA
17	*fkh2*	OHM0199	AAGCAAGCCAAGGAAATGGA
18	*hsk1*	OHM0200	GACTGTAACAAAAGGATTTC
19	*mik1*	OHM0201	GAAAATGGTGTTGAATGGCA
20	*plo1*	OHM0202	ACTTCCAATACCATGCTTTTCATG
21	*puc1*	OHM0203	AACATCGTAAACGAACATGT
22	*ras1*	OHM0204	CGTGTAGTTTCAAGAGCTGA
23	*res1*	OHM0205	GTAACTTACTTTTCTCAAATATGGAG
24	*res2*	OHM0206	GACGGACTTTCGTTAAATAACGA
25	*rum1*	OHM0207	AAGCCCAAACTCTTGTTTGC
26	*sid2*	OHM0208	CGTACAGCATATCGTCCTCC
27	*slp1*	OHM0209	CACTTCACTGATTTGGAGCCC
28	*spg1*	OHM0210	ATCAAGAAGAGATTACCAAACAG
29	*srw1*	OHM0211	TTGTTGTGGTCAAAGCAAAC
30	*wee1*	OHM0212	TCTTCAACAGACAACGGTTC
31	*pyp3*	OHM0213	TCATATTCTCCGGACTTTGA
32	*dnt1*	OHM0214	GAATTGTCTAAAACGTTTTCTCC
33	*byr4*	OHM0215	CGGAAGATCCCTTTAGCGGG

Table 4.5-6. Other PCR primers

Name	Sequence (5' to 3')
OHM179	ATGGTGAGCAAGGGCGAGGAGGATATGGAAAAGAGAAGATGGAAA
OHM182	CTTGTACAGCTCGTCCATGCCGCCGGTCGATGAATTCGAGCTCGT
OHM844	AAGTTCTTGAAAACAAGAATCTTTTTATTGTCAGTACTCTTTATTTGTA CAATTCATCCATACCATGGGTAATACCAGCA
OHM845	TGCTGGTATTACCCATGGTATGGATGAATTGTACAAATAAAGAGTACT GACAATAAAAAGATTCTTGTTTTCAAGAACTT
OSBI870	GGTGGAGGGAAAAGAGCATA

Table 4.5-7. Fission yeast cell cycle regulatory genes analyzed in this study

	Gene Name	Copy Number changed?[*1]	TAP plasmid Construction succeeded?[*2]	Protein detected?[*2]	TAP strain Construction succeeded?[*2]	Protein detected?[*2]
1	*ark1*					
2	*cdc2*				No?[3]	No
3	*cdc7*					
4	*cdc10*					
5	*cdc13*			No	No	n.d.
6	*cdc16*					
7	*cdc18*					
8	*cdc25*					
9	*chk1*					
10	*cig1*					
11	*cig2*					
12	*clp1*					
13	*csk1*					
14	*cut1*	Yes			No	n.d.
15	*cut2*					
16	*dfp1*	Yes			No?[3]	No
17	*fkh2*					
18	*hsk1*					
19	*mik1*					
20	*plo1*					
21	*puc1*	Yes			No?[3]	No
22	*ras1*					
23	*res1*			No	No	n.d.
24	*res2*	Yes		No	No	n.d.
25	*rum1*	Yes				
26	*sid2*					
27	*slp1*	Yes	n.d.	n.d.	n.d.	n.d.
28	*spg1*		No	n.d.	n.d.	n.d.
29	*srw1*			No		No
30	*wee1*		No	n.d.	n.d.	n.d.
31	*pyp3*					

n.d.: Construction or protein detection was not done.

*1. Blank means “No”

*2. Blank means “Yes”.

*3. The integration of TAP-*KanMX* into the corresponding genomic region of the target gene was confirmed by PCR, but the TAP-tagged protein was not detected.

Table 4.5-8. Relationship between copy number and protein increase

	+Leucine			−Leucine		
	Protein increase	Copy number*	PI/CN Ratio	Protein increase	Copy number*	PI/CN Ratio
ark1	4.0	6.2	0.64	147.9	59.5	2.49
cdc7	1.3	1.6	0.83	ND	ND	ND
cdc10	36.6	5.2	7.03	400.4	43.5	9.20
cdc16	2.2	5.7	0.38	19.6	70.6	0.28
cdc18	7.6	3.1	2.47	ND	ND	ND
cdc25	5.6	2.9	1.93	ND	ND	ND
chk1	13.2	10.1	1.31	616.7	106.4	5.80
cig1	1.5	4.7	0.31	ND	ND	ND
cig2	4.7	2.5	1.89	ND	ND	ND
clp1	1.8	2.1	0.87	ND	ND	ND
csk1	18.0	5.5	3.27	61.1	43.8	1.40
cut2	4.7	4.1	1.16	ND	ND	ND
fkh2	1.4	3.2	0.44	ND	ND	ND
hsk1	17.3	11.7	1.48	153.8	114.0	1.35
mik1	13.8	7.3	1.89	ND	46.6	ND
plo1	4.1	3.9	1.04	ND	ND	ND
ras1	18.6	12.6	1.47	72.7	83.1	0.87
rum1	3.7	1.5	2.49	ND	ND	ND
sid2	3.0	10.8	0.28	136.9	88.4	1.55
pyp3	12.7	5.8	2.20	145.1	72.0	2.02
Control 1#	15.8	6.2	2.53	99.2	115.6	0.86
Control 2#	14.8	4.3	3.45	180.2	79.8	2.26
Control 3#	8.5	3.9	1.74	113.1	89.6	1.26
Conlrol 4#	15.4	7.4	1.83	100.2	95.4	1.05

4.6 Figures

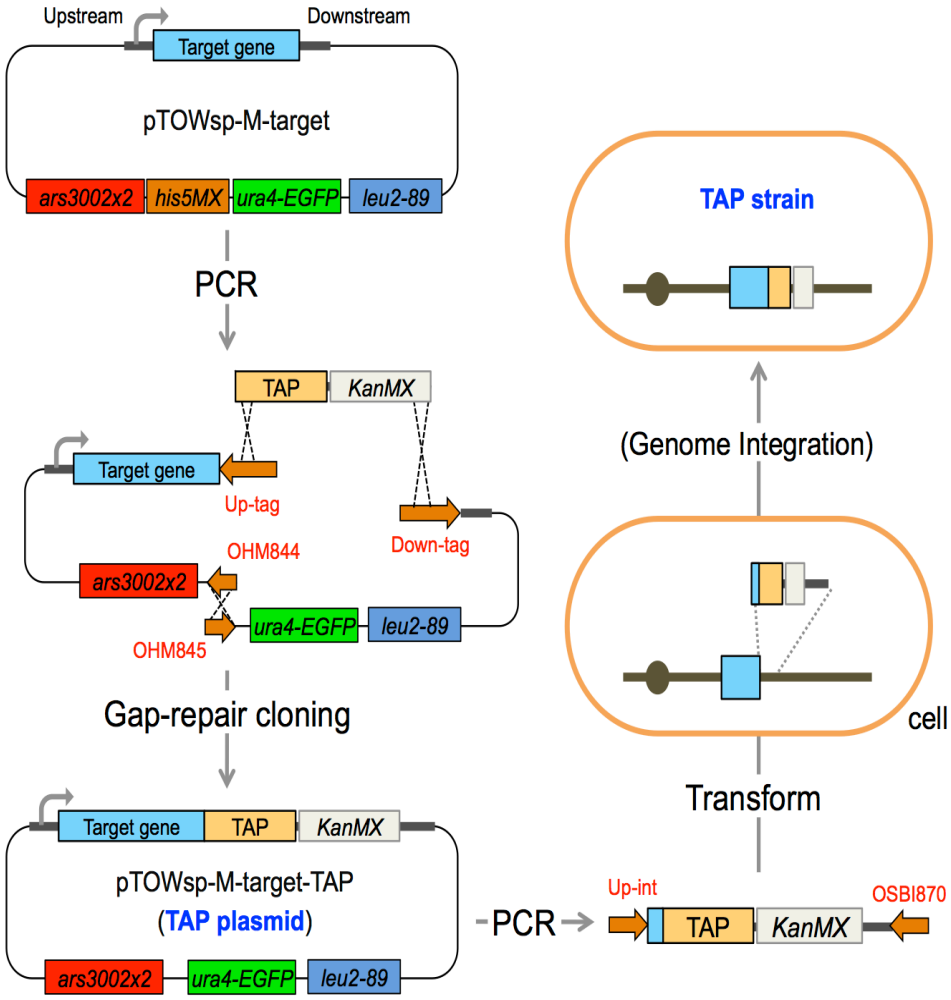

Figure 4.6-1. Construction procedure of the TAP plasmid and the TAP strain used in this study

The detail of this figure is explained in Materials and Methods of the main text. Red letters indicate PCR primers listed in Tables 4-3 to 4-6.

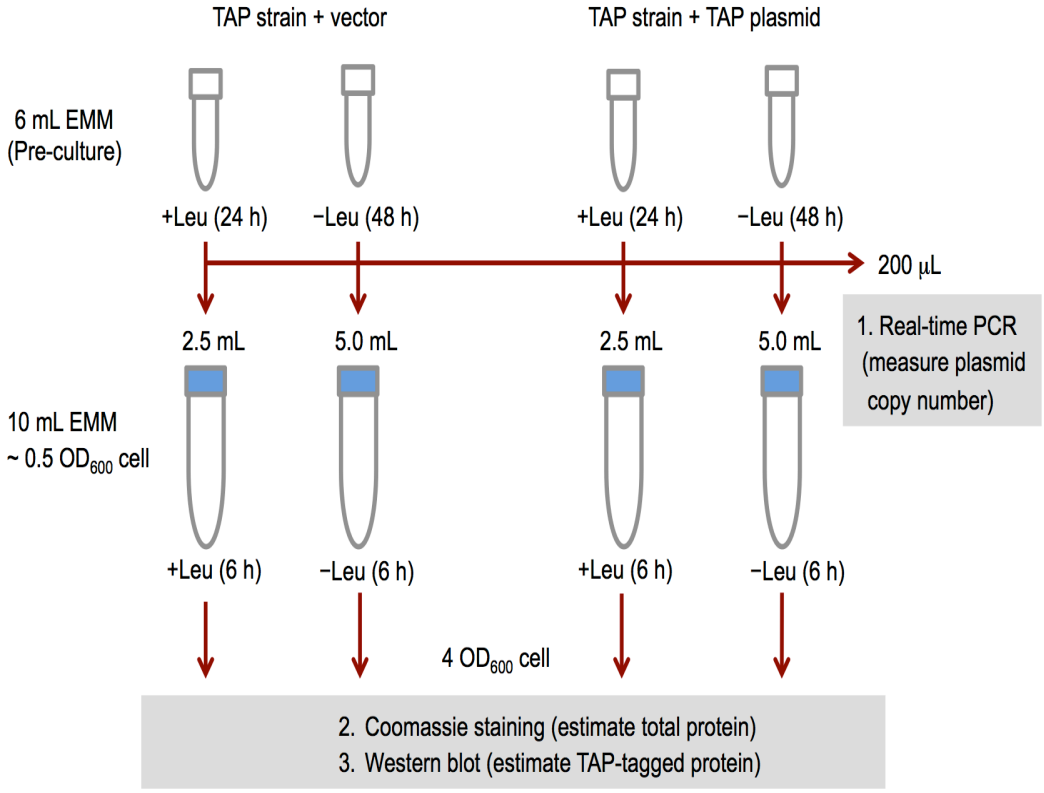

Figure 4.6-2. Sample preparation to measure the plasmid copy number and the protein amount

The detail of this figure is explained in Materials and Methods.

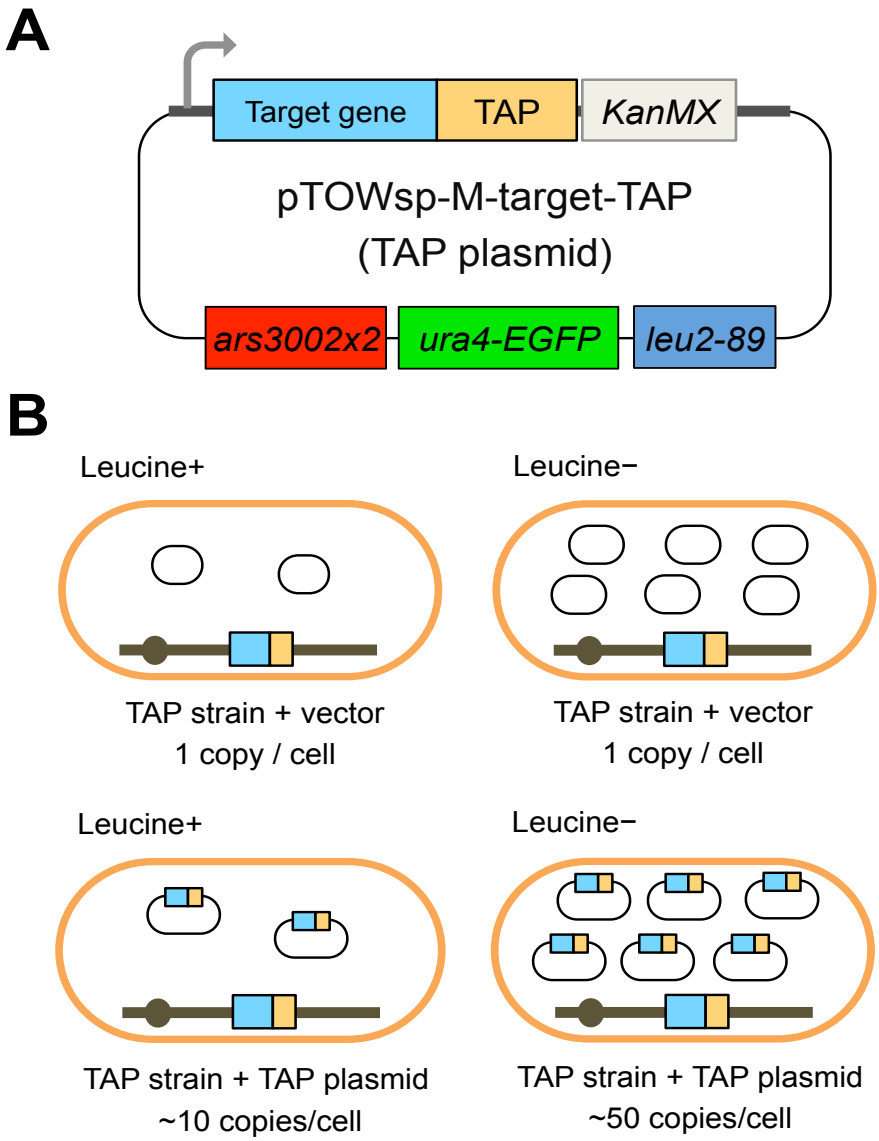

Figure 4.6-3. The plasmid and strains used in this study

A. The general construct used to detect TAP-tagged cell-cycle regulators. The target protein is expressed from its native promoter and is fused to the TAP tag on its C-terminal. The plasmid is for gTOW analysis, and the plasmid copy number within a cell increases up to several tens of copies in the medium without leucine. B. *Sc. pombe* strains for measuring the increase in protein levels with the increase in copy number. Each cell-cycle regulator genes-*TAP* strain was transformed with the empty vector or the corresponding ell-cycle regulator genes-*TAP* plasmid, cultivated in medium with or without leucine. The target ell-cycle regulator genes-*TAP* copy number is indicated in each strain under +leucine and −leucine conditions.

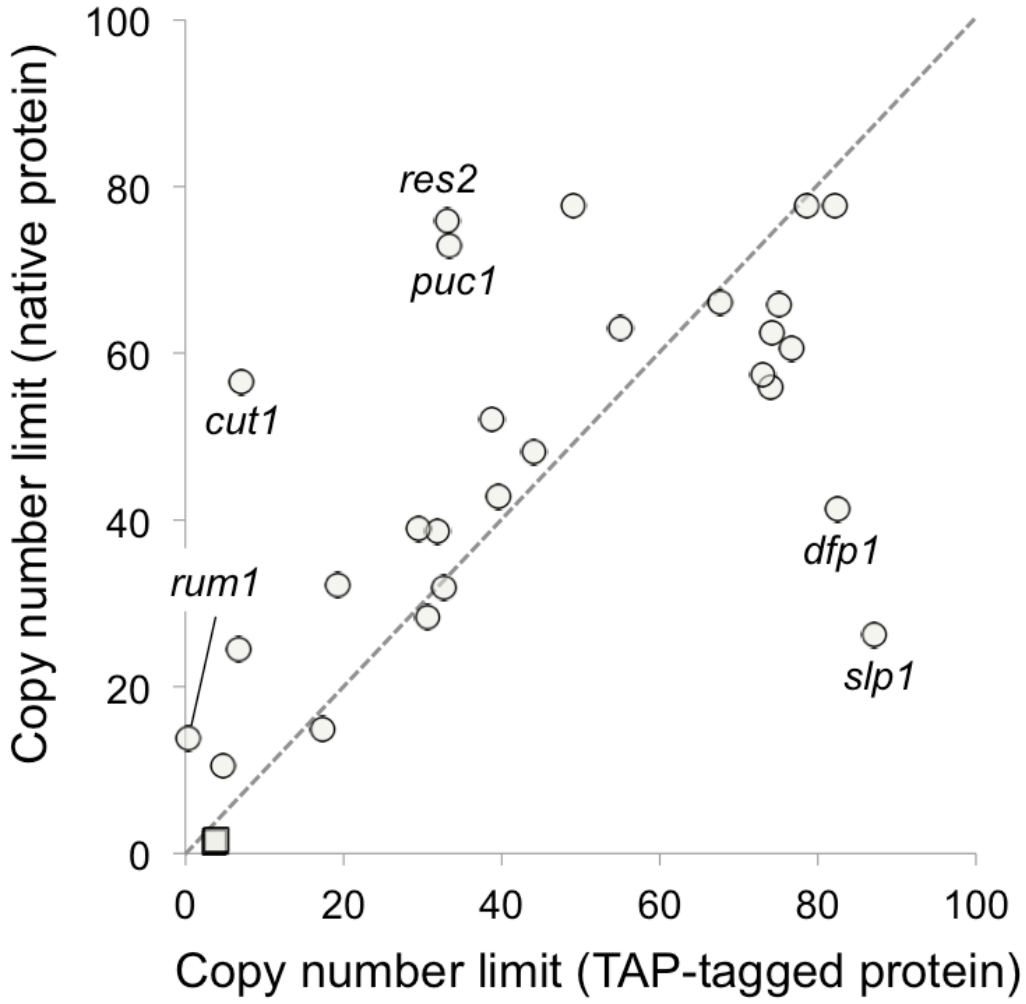

Figure 4.6-4. Relationship between the copy numbers of native and TAP-tagged genes

Names of genes whose copy numbers varied between native and TAP-tagged are shown. Circles indicate the genes whose copy numbers were measured under the −leucine condition, and squares indicate those whose copy numbers were measured under the +leucine condition. The copy numbers of native genes were obtained from the ones studied in Chapter 3. The average of more than three independent experiments was shown.

Figure 4.6-5 (1/3)

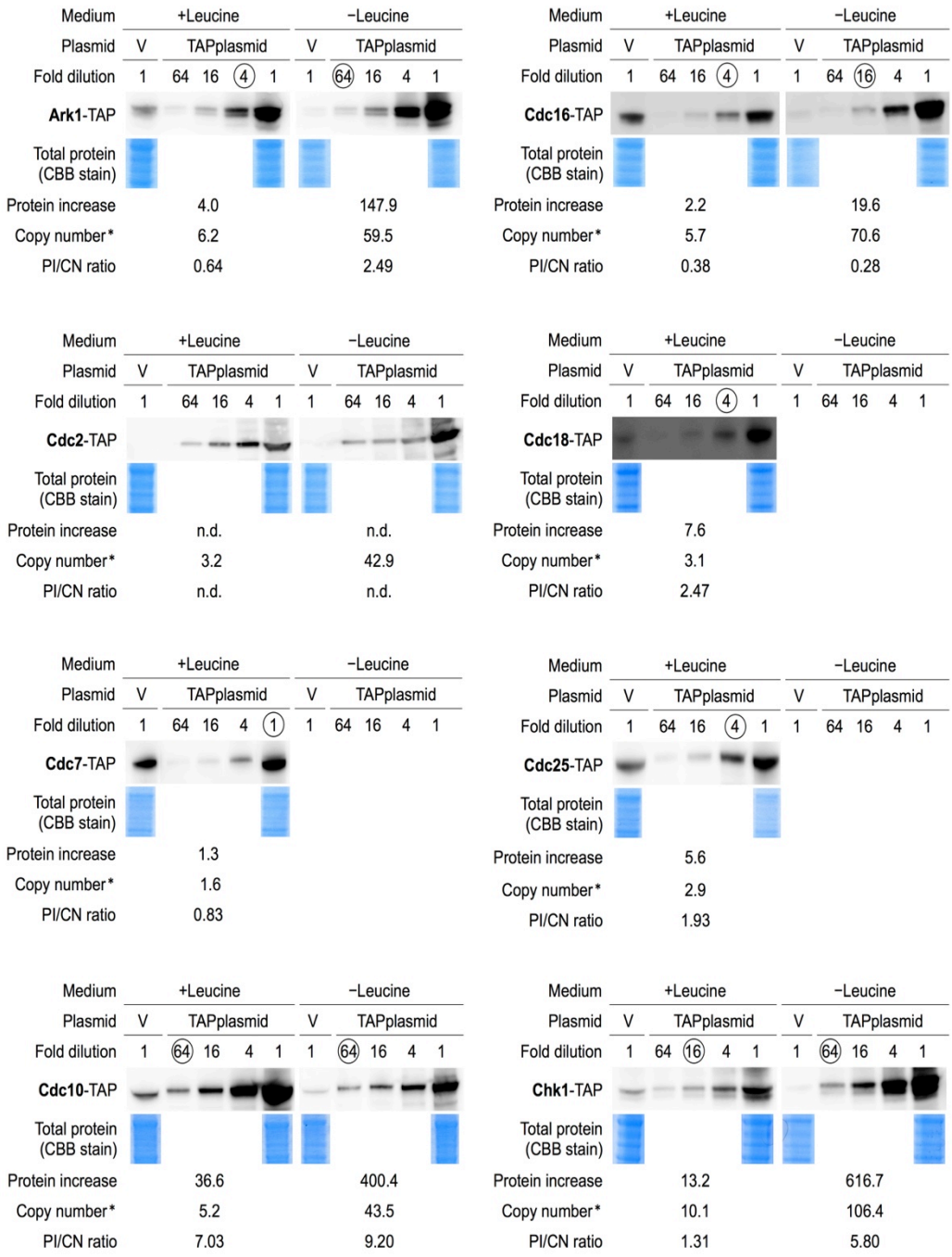

Figure 4.6-5 (2/3)

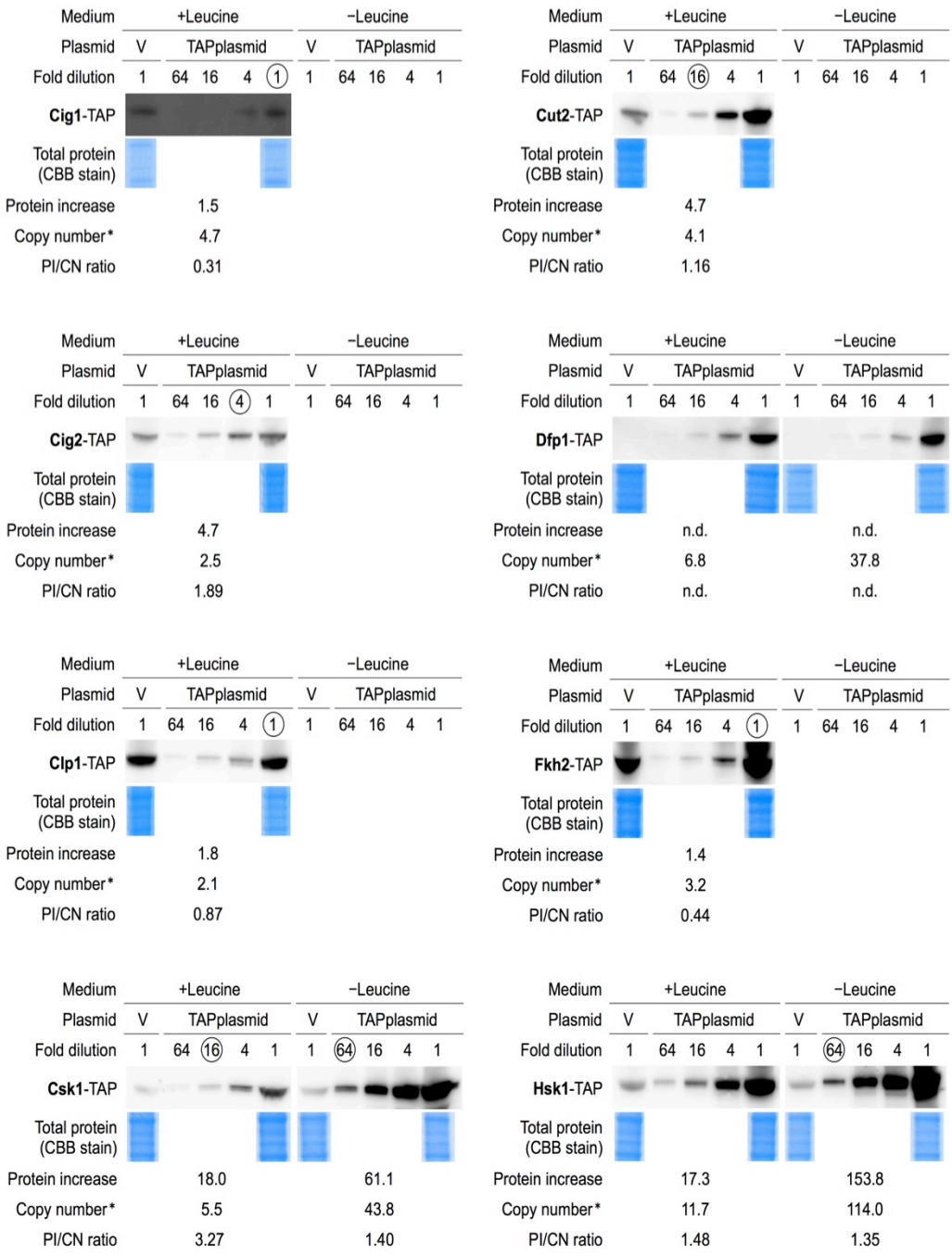

Figure 4.6-5 (3/3)

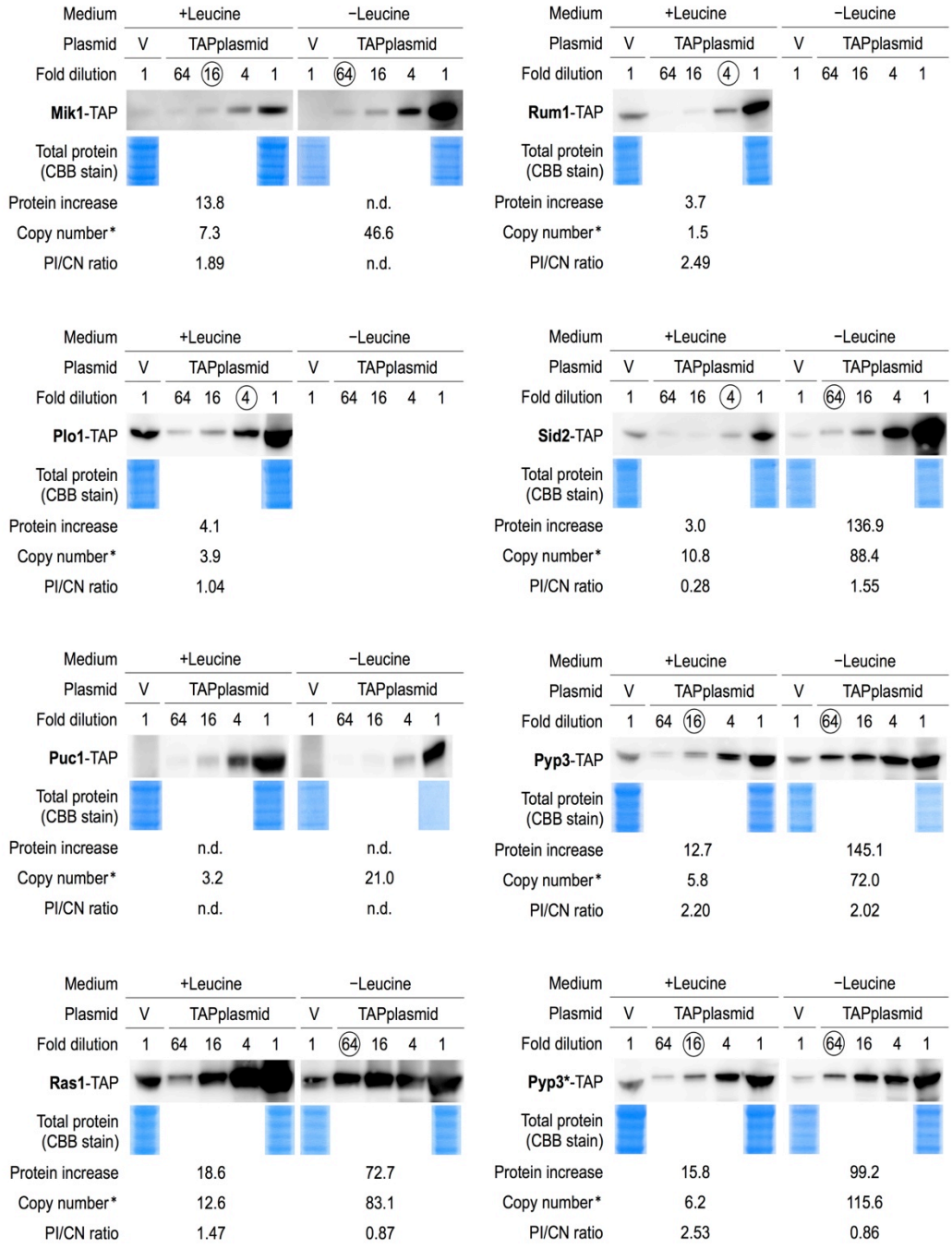

Figure 4.6-5. Results of measurements of the fold protein increases and the copy numbers of cell-cycle regulators-*TAP*

Encircled numbers indicate the fold dilutions used to measure the intensity of cell-cycle regulator -TAP proteins. Total protein was visualized with Coomassie® G-250 staining

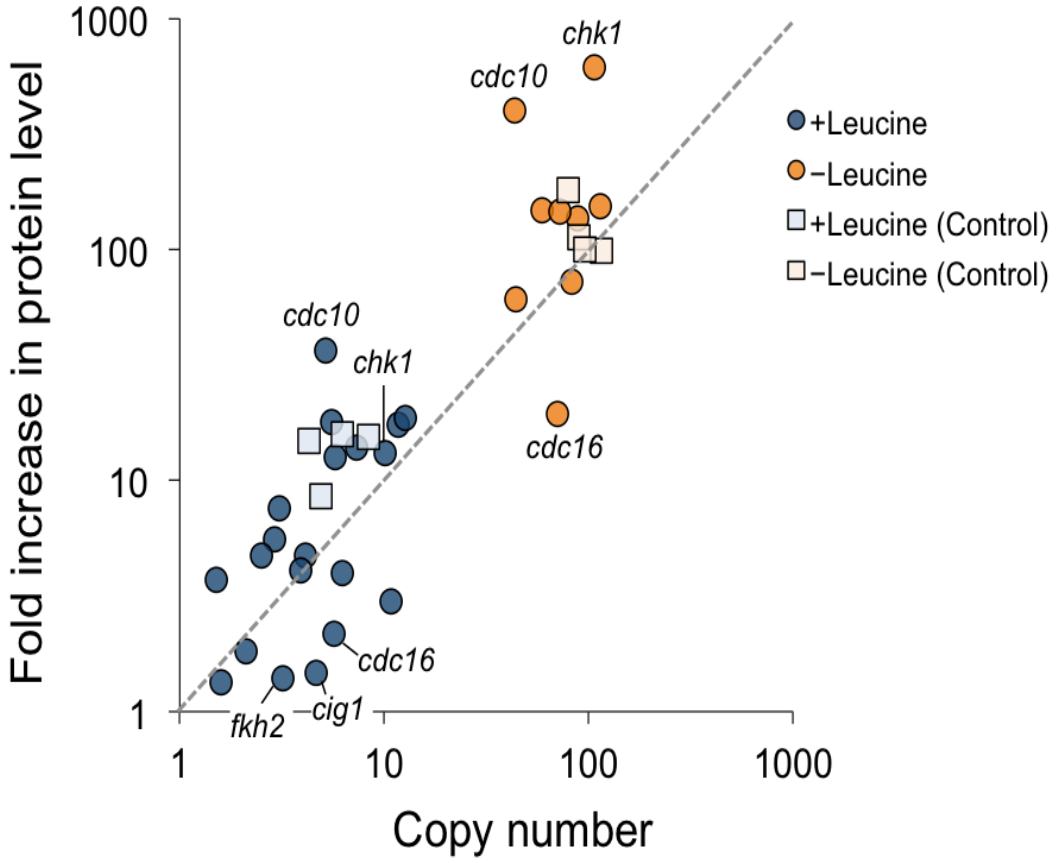

Figure 4.6-6. Relationship between folds increases in protein level and copy numbers

Squares indicate the results of control experiments using Pyp3*-TAP. The names of genes that showed high variation between protein increases and copy numbers are indicated.

Acknowledgements

I would like to express my gratitude to Prof. Kazuhiro Kutsukake for his valuable advice and helpful supports. Assosiate Prof. Hisao Moriya, as my academic supervisor, kindly gave me an opportunity and good environment to complete this thesis during the period of my doctor course. Discussion with him has been always quite interesting, exciting, and stimulating. I am very grateful to Prof. Bela Novak, Dr. Attila Csikász-Nagy, and Dr. Orsolya Kapuy for their valuable cooperation in my experiments. I would like to thank Mr. Koji Makanae, Dr. Masataka Sasabe, Ms. Ai Kinomoto, Mr. Miyaji Shoudai, Mr. Yoshihiro Mori and Ms. Reiko Kintaka for discussion and technical advice.

References

Abdel-Banat, B.M.A., Nonklang, S., Hoshida, H., and Akada, R. (2010). Random and targeted gene integrations through the control of non-homologous end joining in the yeast *Kluyveromyces marxianus*. *Yeast 27*, 29-39.

Aligianni, S., Lackner, D.H., Klier, S., Rustici, G., Wilhelm, B.T., Marguerat, S., Codlin, S., Brazma, A., de Bruin, R.A.M., and Bahler, J. (2009). The Fission Yeast Homeodomain Protein Yox1p Binds to MBF and Confines MBF-Dependent Cell-Cycle Transcription to G1-S via Negative Feedback. *PloS Genetics* 5.

Alon, U., Surette, M.G., Barkai, N., and Leibler, S. (1999). Robustness in bacterial chemotaxis. *Nature* 397, 168-171.

Amberg, D., Burke, D., and Strathern, N. (2005). Methods in Yeast Genetics: Cold Spring Harber Laboratory Press.

Ayte, J., Schweitzer, C., Zarzov, P., Nurse, P., and DeCaprio, J.A. (2001). Feedback regulation of the MBF transcription factor by cyclin Cig2. *Nature Cell Biology* 3, 1043-1050.

Bardin, A.J., and Amon, A. (2001). Men and sin: what's the difference? *Nature Reviews Mol Cell Biology* 2, 815-826.

Barkai, N., and Leibler, S. (1997). Robustness in simple biochemical networks. *Nature* 387, 913-917.

Baum, B., Wuarin, J., and Nurse, P. (1997). Control of S-phase periodic transcription in the fission yeast mitotic cycle. *EMBO Journal* 16, 4676-4688.

Brun, C., Dubey, D.D., and Huberman, J.A. (1995). pDblet, a stable autonomously replicating shuttle vector for *Schizosaccharomyces pombe*. *Gene* 164, 173-177.

Bueno, A., and Russell, P. (1993). Two fission yeast B-type cyclins, cig2 and Cdc13, have different functions in mitosis. *Molecular and Cellular Biology* 13, 2286-2297.

Csikasz-Nagy, A., Battogtokh, D., Chen, KC., Novak, B., Tyson, JJ. (2006) Analysis of a Generic Model of Eukaryotic Cell-Cycle Regulation. *Biophysical Journal* 90, 4361-4379.

Cross, F.R., Archambault, V., Miller, M., and Klovstad, M. (2002). Testing a mathematical model of the yeast cell cycle. *Molecular Biology of the Cell* 13, 52-70.

Davis, L., and Smith, G.R. (2001). Meiotic recombination and chromosome segregation in *Schizosaccharomyces pombe*. *Proceedings of the National Academy of Sciences of the United States of America* 98, 8395-8402.

Dekel, E., and Alon, U. (2005). Optimality and evolutionary tuning of the expression level of a protein. *Nature 436*, 588-592.

Egel, R. (2004). The Molecular Biology of *Schizosaccharomyces pombe*: Springer Verlag.

Enoch, T., Carr, A.M., and Nurse, P. (1992). Fission yeast genes involved in coupling mitosis to completion of DNA replication. *Genes & Development 6*, 2035-2046.

Fantes, J., and Beggs, J. (2000). The Yeast Nucleus. Oxfird Univ. Press,.

Forsburg, S.L., and Nurse, P. (1994). Analysis of the *Schizosaccharomyces pombe* cyclin puc1: evidence for a role in cell cycle exit. *Journal of Cell Science* 107, 601-613.

Furge, K.A., Wong, K., Armstrong, J., Balasubramanian, M., and Albright, C.F. (1998). Byr4 and Cdc16 form a two-component GTPase-activating protein for the Spg1 GTPase that controls septation in fission yeast. *Current Biology* 8, 947-954.

Grallert, A., Grallert, B., Ribar, B., and Sipiczki, M. (1998). Coordination of initiation of nuclear division and initiation of cell division in *Schizosaccharomyces pombe*: genetic interactions of mutations. *Journal of Bacteriology* 180, 892-900.

Hayles, J., Fisher, D., Woollard, A., and Nurse, P. (1994). Temporal order of S phase and mitosis in fission yeast is determined by the state of the $p34^{cdc2}$ -mitotic B cyclin complex. *Cell 78*, 813-822.

Hermand, D., and Nurse, P. (2007). Cdc18 enforces long-term maintenance of the S phase checkpoint by anchoring the Rad3-Rad26 complex to chromatin. *Molecular Cell*. 26, 553-563.

Ho, C.H., Magtanong, L., Barker, S.L., Gresham, D., Nishimura, S., Natarajan, P., Koh, J.L.Y., Porter, J., Gray, C.A., Andersen, R.J., Giaever, G., Nislow, C., Andrews, B., Botstein, D., Graham, T.R., Yoshida, M., and Boone, C. (2009). A molecular barcoded yeast ORF library enables mode-of-action analysis of bioactive compounds. *Nature Biotechnology* 27, 369-377.

Humphrey, T. (2000). DNA damage and cell cycle control in *Schizosaccharomyces pombe*. *Mutation Research* 451, 211-226.

Jin, Q.W., Ray, S., Choi, S.H., and McCollum, D. (2007). The nucleolar

Net1/Cfi1-related protein Dnt1 antagonizes the septation initiation network in fission yeast. *Molecular Biology of the Cell* 18, 2924-2934.

Kaizu, K., Moriya, H., and Kitano, H. (2010). Fragilities caused by dosage imbalance in regulation of the budding yeast cell cycle. *PLoS Genetics* 6, e1000919.

Kegel, A., Martinez, P., Carter, S.D., and Aström, S.U. (2006). Genome wide distribution of illegitimate recombination events in *Kluyveromyces lactis*. *Nucleic Acids Research* 34, 1633-1645.

Kelly, T.J., Martin, G.S., Forsburg, S.L., Stephen, R.J., Russo, A., and Nurse, P. (1993). The fission yeast *cdc18*+ gene product couples S phase to START and mitosis. *Cell* 74, 371-382.

Kim, S.H., Lin, D.P., Matsumoto, S., Kitazono, A., and Matsumoto, T. (1998). Fission yeast Slp1: an effector of the Mad2-dependent spindle checkpoint. *Science* 279, 1045-1047.

Kitamura, K., Maekawa, H., and Shimoda, C. (1998). Fission yeast Ste9, a homolog of Hct1/Cdh1 and Fizzy-related, is a novel negative regulator of cell cycle progression during G1-phase. *Molecular Biology of the* Cell 9, 1065-1080.

Kitano, H. (2002). Systems biology: a brief overview. *Science* 295, 1662-1664.

Kitano, H. (2004). Biological robustness. *Nature Reviews Genetics* 5, 826-837.

Krapp, A., and Simanis, V. (2008). An overview of the fission yeast septation initiation network (SIN). *Biochemical Society Transactions* 36, 411-415.

Leupold, U. (1950). Die Verebung von Homothallie und Heterothallie beo *Schizosaccharomyces pombe*. C.R. Lab. Carlsberg 24, 381-475.

Li, F., Long, T., Lu, Y., Ouyang, Q., and Tang, C. (2004). The yeast cell-cycle network is robustly designed. *Proceedings of the National Academy of Sciences of the United States of America* 101, 4781-4786.

Lu, L.X., Domingo-Sananes, M.R., Huzarska, M., Novak, B., and Gould, K.L. (2012). Multisite phosphoregulation of Cdc25 activity refines the mitotic entrance and exit switches. *Proceedings of the National Academy of Sciences of the United States of America* 109, 9899-9904.

Lundgren, K., Walworth, N., Booher, R., Dembski, M., Kirschner, M., and Beach, D. (1991). *mik1* and *wee1* cooperate in the inhibitory tyrosine phosphorylation of *cdc2*. *Cell* 64, 1111-1122.

Ma, H., Kunes, S., Schatz, P.J., and Botstein, D. (1987). Plasmid construction by homologous recombination in yeast. *Gene* 58, 201-216.

Manolis, K.G., Nimmo, E.R., Hartsuiker, E., Carr, A.M., Jeggo, P.A., and Allshire, R.C. (2001). Novel functional requirements for non-homologous DNA end joining in *Schizosaccharomyces pombe*. *EMBO Journal* 20, 210-221.

Martin-Castellanos, C., Blanco, M.A., de Prada, J.M., and Moreno, S. (2000). The puc1 cyclin regulates the G1 phase of the fission yeast cell cycle in response to cell size. *Molecular Biology of the* Cell 11, 543-554.

Martin-Castellanos, C., Labib, K., and Moreno, S. (1996). B-type cyclins regulate G1 progression in fission yeast in opposition to the $p25^{rum1}$ cdk inhibitor. *EMBO Journal*. 15, 839-849.

Martinho, R.G., Lindsay, H.D., Flaggs, G., DeMaggio, A.J., Hoekstra, M.F., Carr, A.M., and Bentley, N.J. (1998). Analysis of Rad3 and Chk1 protein kinases defines different checkpoint responses. *EMBO Journal*. 17, 7239-7249.

Maundrell, K. (1990). *nmt1* of fission yeast. A highly transcribed gene completely repressed by thiamine. *Journal of Biological Chemistry* 265, 10857-10864.

Meir, E., von Dassow, G., Munro, E., and Odell, G.M. (2002). Robustness, flexibility, and the role of lateral inhibition in the neurogenic network. *Current Biology* 12, 778-786.

Millar, J.B., Lenaers, G., and Russell, P. (1992). Pyp3 PTPase acts as a mitotic inducer in fission yeast. *EMBO Journal* 11, 4933-4941.

Mitchison, J.M. (1957). The growth of single cells. I. *Schizosaccharomyces pombe*. *Experimental Cell Research* 13, 244-262.

Mondesert, O., McGowan, C.H., and Russell, P. (1996). Cig2, a B-type cyclin, promotes the onset of S in *Schizosaccharomyces pombe*. *Molecular Biology of the Cell* 16, 1527-1533.

Moreno, S., Klar, A., and Nurse, P. (1991). Molecular genetic-ayalysis of fission yeast *Schizosaccharomyces pombe*. *Methods in Enzymology* 194, 795-823.

Moreno, S., and Nurse, P. (1994). Regulation of progression through the G1 phase of the cell cycle by the *rum1+* gene. *Nature* 367, 236-242.

Moriya, H., Shimizu-Yoshida, Y., and Kitano, H. (2006). *In vivo* robustness analysis of cell division cycle genes in *Saccharomyces cerevisiae*. *Plos Genetics 2*, 1034-1045.

Morohashi, M., Winn, A.E., Borisuk, M.T., Bolouri, H., Doyle, J., and Kitano, H. (2002). Robustness as a measure of plausibility in models of biochemical networks. *Journal of Theoretical Biology* 216, 19-30.

Novak, B., and Tyson, J.J. (1997). Modeling the control of DNA replication in fission yeast. *Proceedings of the National Academy of Sciences of the United States of America* 94, 9147-9152.

Nurse, P. (2002). Cyclin dependent kinases and cell cycle control (Nobel lecture). *Chembiochem* 3, 596.

Nurse, P., and Thuriaux, P. (1980). Regulatory genes controlling mitosis in the fission yeast *Schizosaccharomyces pombe*. *Genetics* 96, 627-637.

Oldenburg, K.R., Vo, K.T., Michaelis, S., and Paddon, C. (1997). Recombination-mediated PCR-directed plasmid construction *in vivo* in yeast. *Nucleic Acids Research* 25, 451-452.

Rigaut, G., Shevchenko, A., Rutz, B., Wilm, M., Mann, M., and Seraphin, B. (1999). A generic protein purification method for protein complex characterization and proteome exploration. *Nature Biotechnology* 17, 1030-1032.

Russell, P., and Nurse, P. (1986). *cdc25+* functions as an inducer in the mitotic control of fission yeast. *Cell* 45, 145-153.

Sheff, M.A., and Thorn, K.S. (2004). Optimized cassettes for fluorescent protein tagging in *Saccharomyces cerevisiae*. *Yeast* 21, 661-670.

Sikorski, R.S., and Hieter, P. (1989). A system shuttle vectors and yeast host strains designated for efficient manipulation of DNA in *Saccharomyces cerevisiae.* *Genetics* 122, 19-27.

Sipiczki, M. (2000). Where does fission yeast sit on the tree of life? *Genome Biology* 1, 1011-1011.4.

Springer, M., Weissman, J.S., and Kirschner, M.W. (2010). A general lack of compensation for gene dosage in yeast. *Molecular Systems Biology* 6, 368.

Sveiczer, A., Csikasz-Nagy, A., Gyorffy, B., Tyson, J.J., and Novak, B. (2000). Modeling the fission yeast cell cycle: quantized cycle times in wee1- cdc25Δ mutant cells. *Proceedings of the National Academy of Sciences of the United States of America* 97, 7865-7870.

Sveiczer, A., Novak, B., and Mitchison, J.M. (1996). The size control of fission yeast revisited. *Journal of Cell Science* 109, 2947-2957.

Trautmann, S., Wolfe, B.A., Jorgensen, P., Tyers, M., Gould, K.L., and McCollum, D. (2001). Fission yeast Clp1p phosphatase regulates G2/M transition and coordination of cytokinesis with cell cycle progression. *Current Biology* 11, 931-940.

von Dassow, G., Meir, E., Munro, E.M., and Odell, G.M. (2000). The segment polarity network is a robust development module. *Nature* 406, 188-192.

Wagner, A. (2005). Energy constraints on the evolution of gene expression. *Molecular Biology and Evolution* 22, 1365-1374.

Wang, L.L., Kao, R., Ivey, F.D., and Hoffman, C.S. (2004). Strategies for gene disruptions and plasmid constructions in fission yeast. *Methods* 33, 199-205.

Wood, V., Gwilliam, R., Rajandream, M.A., Lyne, M., Lyne, R., Stewart, A., Sgouros, J., Peat, N., Hayles, J., Baker, S., Basham, D., Bowman, S., Brooks, K., Brown, D., Brown, S., Chillingworth, T., Churcher, C., Collins, M., Connor, R., Cronin, A., Davis, P., Feltwell, T., Fraser, A., Gentles, S., Goble, A., Hamlin, N.,

Harris, D., Hidalgo, J., Hodgson, G., Holroyd, S., Hornsby, T., Howarth, S., Huckle, E.J., Hunt, S., Jagels, K., James, K., Jones, L., Jones, M., Leather, S., McDonald, S., McLean, J., Mooney, P., Moule, S., Mungall, K., Murphy, L., Niblett, D., Odell, C., Oliver, K., O'Neil, S., Pearson, D., Quail, M.A., Rabbinowitsch, E., Rutherford, K., Rutter, S., Saunders, D., Seeger, K., Sharp, S., Skelton, J., Simmonds, M., Squares, R., Squares, S., Stevens, K., Taylor, K., Taylor, R.G., Tivey, A., Walsh, S., Warren, T., Whitehead, S., Woodward, J., Volckaert, G., Aert, R., Robben, J., Grymonprez, B., Weltjens, I., Vanstreels, E., Rieger, M., Schäfer, M., Müller-Auer, S., Gabel, C., Fuchs, M., Düsterhöft, A., Fritzc, C., Holzer, E., Moestl, D., Hilbert, H., Borzym, K., Langer, I., Beck, A., Lehrach, H., Reinhardt, R., Pohl, T.M., Eger, P., Zimmermann, W., Wedler, H., Wambutt, R., Purnelle, B., Goffeau, A., Cadieu, E., Dréano, S., Gloux, S., Lelaure, V., Mottier, S., Galibert, F., Aves, S.J., Xiang, Z., Hunt, C., Moore, K., Hurst, S.M., Lucas, M., Rochet, M., Gaillardin, C., Tallada, V.A., Garzon, A., Thode, G., Daga, R.R., Cruzado, L., Jimenez, J., Sánchez, M., del Rey, F., Benito, J., Domínguez, A., Revuelta, J.L., Moreno, S., Armstrong, J., Forsburg, S.L., Cerutti, L., Lowe, T., McCombie, W.R., Paulsen, I., Potashkin, J., Shpakovski, G.V., Ussery, D., Barrell, B.G., Nurse, P., and Cerrutti, L. (2002). The genome sequence of *Schizosaccharomyces pombe*. *Nature* 415, 871-880.

Yamaguchi, S., Okayama, H., and Nurse, P. (2000). Fission yeast Fizzy-related protein srw1p is a G(1)-specific promoter of mitotic cyclin B degradation. *EMBO Journal*. 19, 3968-3977.

Yi, T.M., Huang, Y., Simon, M.I., and Doyle, J. (2000). Robust perfect adaptation in bacterial chemotaxis through integral feedback control. *Proceedings of the National Academy of Sciences of the United States of America* 97, 4649-4653.

Zarzov, P., Decottignies, A., Baldacci, G., and Nurse, P. (2002). G(1)/S CDK is inhibited to restrain mitotic onset when DNA replication is blocked in fission yeast. *EMBO Journal*. 21, 3370-3376.

Zaslaver, A., Mayo, A.E., Rosenberg, R., Bashkin, P., Sberro, H., Tsalyuk, M., Surette, M.G., and Alon, U. (2004). Just-in-time transcription program in metabolic pathways. *Nature Genetics* 36, 486-491.

Zhu, H., Bilgin, M., Bangham, R., Hall, D., Casamayor, A., Bertone, P., Lan, N., Jansen, R., Bidlingmaier, S., Houfek, T., Mitchell, T., Miller, P., Dean, R.A., Gerstein, M., and Snyder, M. (2001). Global analysis of protein activities using proteome chips. *Science* 293, 2101-2105.

Zhu, H., Klemic, J.F., Chang, S., Bertone, P., Casamayor, A., Klemic, K.G., Smith, D., Gerstein, M., Reed, M.A., and Snyder, M. (2000). Analysis of yeast protein kinases using protein chips. *Nature Genetics* 26, 283-289.

List of Publications

Chino, A., Watanabe, K., and Moriya, H. (2010). Plasmid construction using recombination activity in the fission yeast *Schizosaccharomyces pombe*. *PLoS One* 5, e9652.

Moriya, H., Chino, A., Kapuy, O., Csikasz-Nagy, A., and Novak, B. (2011). Overexpression limits of fission yeast cell-cycle regulators *in vivo* and *in silico*. *Molecular Systems Biology* 7, 556.

Moriya, H., Makanae, K., Watanabe, K., Chino, A., and Shimizu-Yoshida, Y. (2012). Robustness analysis of cellular systems using the genetic tug-of-war method. *Molecular Biosystems* 8, 2513-2522.